

# Geochemical mapping of the Qaanaaq region, 77°10' to 78°10' N, North-West Greenland

Agnete Steenfelt, Peter R. Dawes, Johan Ditlev Krebs,  
Else Moberg and Bjørn Thomassen



# **Geochemical mapping of the Qaanaaq region, 77°10' to 78°10' N, North-West Greenland**

Agnete Steenfelt, Peter R. Dawes, Johan Ditlev Krebs,  
Else Moberg and Bjørn Thomassen

# Contents

Abstract.....	3
Introduction .....	4
Geological setting and mineral occurrences .....	5
Precambrian shield .....	5
Thule mixed-gneiss complex .....	5
Smithson Bjerge magmatic association .....	6
Undifferentiated gneiss complex .....	6
Prudhoe Land supracrustal complex.....	7
Thule Basin .....	7
Smith Sound Group .....	7
Nares Strait Group.....	8
Baffin Bay Group .....	8
Dundas Group.....	8
Regional structures.....	9
Sampling and analysis.....	9
Quality of analytical data.....	10
Presentation of results.....	10
Local variation.....	12
Regional geochemical variation .....	13
Chemical variation within the Precambrian shield.....	16
High Al-Th .....	16
High Cu, Zn and Ni .....	17
Categories relating to meta-igneous rocks.....	18
Low La .....	20
Comparison of categories.....	20
Metamorphic grade.....	20
Chemical variation within the Thule Basin.....	22
Discussion .....	23
Conclusions .....	24
Acknowledgments.....	25
References .....	25
Appendix.....	27

## Abstract

Samples of stream sediment or substitute surficial material were collected systematically over the Qaanaaq region as part of *Qaanaaq 2001*, a reconnaissance mineral exploration project conducted by the Geological Survey of Denmark and Greenland and the Bureau of Minerals and Petroleum, Government of Greenland. Chemical analyses of the < 0.1 mm grain size fractions of the samples were conducted using X-ray fluorescence spectrometry, instrumental neutron activation and inductively coupled plasma emission spectrometry. The results are presented as distribution maps for 44 major and trace elements, together with maps of the geology, loss on ignition, gamma radiation measured at each sample locality and an interpretation map.

The Qaanaaq region features a mountainous terrain in the high-arctic part of Greenland fringing the Inland Ice. Geologically, a high-grade Archaean–Palaeoproterozoic crystalline shield is overlain by unmetamorphosed Mesoproterozoic rocks of the intracratonic Thule Basin.

Element distribution patterns can be related to lithological units of the shield and a more detailed examination of the data allows chemical characterisation and interpretation of these units. High concentrations of Sr, Ba and P<sub>2</sub>O<sub>5</sub> in a large group of samples are taken to reflect the occurrence of quartz dioritic, monzonitic and syenitic meta-igneous rocks in most of south-eastern Prudhoe Land, and high Rb/Sr characterising the Thule mixed-gneiss complex in the Nunatarssuaq area reflects predominance of amphibolite facies orthogneiss influenced by granitic magmatism.

In addition, the following kinds of mineral occurrences are indicated by the geochemical data: REE-enriched heavy minerals in the Palaeoproterozoic Prudhoe Land supracrustals, Ni-Cu-Zn-sulphide mineralisation within paragneisses of the Archaean Thule mixed-gneiss complex, with gold mineralisation and barite veins, respectively, associated with volcanic rocks and faults in the Thule Basin.

## Introduction

The geochemical mapping of the Qaanaaq region formed part of the project *Qaanaaq 2001* jointly conducted by the Geological Survey of Denmark and Greenland and the Bureau of Minerals and Petroleum, Government of Greenland. Other geochemical sampling undertaken during *Qaanaaq 2001* in southern Steensby Land, south of the region shown in Fig. 1, is reported on elsewhere (Steenfelt 2002). The acquired geochemical data from both regions contribute to the reconnaissance geochemical mapping programme of Greenland. The objective of the *Qaanaaq 2001* project is to investigate mineral occurrences and assess mineral potential. (Thomassen *et al.* 2002) presents the project together with preliminary results.

The survey area lies within the municipality of Qaanaaq and comprises about 4300 km<sup>2</sup> ice-free land around Kangerlussuaq (Fig. 1). The mountainous terrain with elevations commonly between 500 and 1000 m varies from steep-sided, ice-capped plateaus intersected by fjords and glaciers to more gentle topography in the eastern and south-eastern part. Surficial deposits, mostly till and glacial sediments, are widespread, particularly in the east. The climate is high-arctic and vegetation sparse.

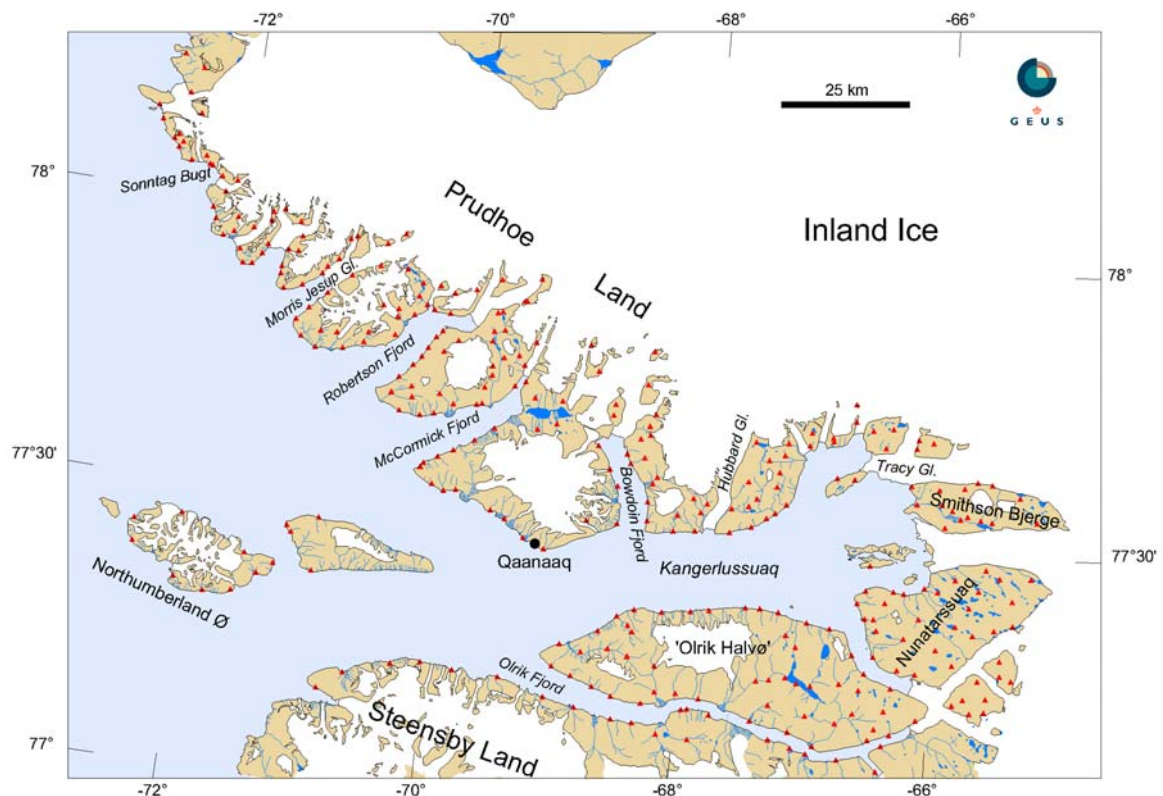


**Figure 1.** Drainage systems in the Qaanaaq region with sample localities. Gl.: Gletscher.

The drainage pattern is dominated by first or second order streams that lead meltwater from the icecaps down the cliffs and steep slopes to the coast. Drainage systems are more evolved in the eastern, topographically less dramatic inland parts of the area (Fig. 1). The streams are frozen during winter, but in the summer months, July and August, they carry water from melting ice and snow as well as from occasional rain.

The samples were collected from July 23 to August 30 by the authors using rubber dinghy and helicopter. A chartered 75-foot vessel, *M/S Kíssavík*, served as a base working from 12 anchorages.

This report presents analytical results for stream sediment samples and substitute surficial material recovered from 327 localities, and it discusses their implications for mineral exploration and geological understanding.

## **Geological setting and mineral occurrences**

The Qaanaaq region is underlain by two bedrock provinces: a high-grade Archaean-Palaeoproterozoic crystalline shield overlain by rocks of the unmetamorphosed Mesoproterozoic intracratonic Thule Basin (Map 1). The profound unconformity between these units is well preserved. The western part of the Thule Basin outcrops in Canada, across Baffin Bay (inset of Map 1).

The Qaanaaq region was mapped by the Survey between 1971 and 1980, mainly by shoreline investigations with limited helicopter traversing inland. The western part exposing the Thule Basin is mapped at 1:100 000; the area at the head of Kangerlussuaq, composed entirely of the Precambrian shield, is depicted at 1:200 000 (Dawes 1988). The only detailed mapping undertaken is of Smithson Bjerger (Nutman 1984). The Survey's 1:500 000 map sheet (Dawes 1991) has a northern border at 78°N; the northernmost part of the project region around Kap Alexander is featured in Dawes (1997) and Dawes *et al.* (2000). Unless otherwise stated, rock unit names in this report are taken from the Survey's 1:500 000 map sheet.

Mineral exploration in the Qaanaaq region has been limited, and significant mineral deposits have not been located. In this report known mineralisation is only briefly described. More information may be obtained from Thomassen *et al.* (2002b), which summarises the results of previous exploration and describes observations and data on mineral occurrences obtained during *Qaanaaq 2001*.

### **Precambrian shield**

#### **Thule mixed-gneiss complex**

This Archaean complex of highly deformed amphibolite- to granulite-facies gneisses forms the shield in the southern part of the study area (Map 1). It is composed of quartzofeldspathic to pelitic paragneisses, multiphase orthogneisses with genetically related grani-

tic rocks, and minor mafic and ultramafic bodies. The paragneisses and multiphase orthogneisses are structurally complex and intricately associated on all scales, so that some intermixed packages can only be unravelled by future detailed mapping. In many places the gneisses show pronounced compositional layering.

Oxide facies banded iron-formation (quartz, magnetite, amphibole, garnet) to near massive magnetite-silicate rocks without any obvious macrostructure have been observed in paragneiss blocks and outcrops over the whole area underlain by the mixed gneisses. The occurrences are interpreted as the northward extension of an Archaean magnetite province stretching for 350 km along the coast of Melville Bugt and into the Pituffik (Thule Air Base) area south of the Qaanaaq region (Dawes 1976, 1991; Dawes & Frisch 1981). Analyses of 19 samples conducted within *Qaanaaq 2001* showed high Fe and Mn values, but no enrichment in other metals.

In 2001, several previously mapped amphibolite bodies were found to grade into ultramafic rocks and new ultramafic bodies were discovered, the largest being a boudin (c. 500 × 150 m) within orthogneiss at the head of Academy Bugt (Map 1). Faint malachite coatings caused by minor disseminated pyrite and chalcopyrite were observed on the amphibolitic and ultramafic lenses and pods in the gneisses. Samples of mineralised rocks returned up to 31 ppb Au, 8 ppb Pt, 19 ppb Pd, 1748 ppm Cu and 1298 ppm Ni.

Faint malachite staining, caused by oxidation of minor disseminated pyrite and chalcopyrite, was observed over a distance of 3–4 km in steep coastal cliffs of banded gneisses east of the snout of Hubbard Gletscher.

### **Smithson Bjerge magmatic association**

This Archaean meta-igneous association is composed of the major Qaqujârssuaq anorthosite and various basic, dioritic and granitic intrusions (Nutman 1984). The main anorthosite mass is predominantly anorthosite *senso stricto* with minor leucogabbro and gabbro. The rocks of the magmatic association that were intruded into the Thule mixed-gneiss complex have been affected by granulite-facies metamorphism.

### **Undifferentiated gneiss complex**

The gneisses of this unit are deemed to be mainly of Palaeoproterozoic age but it cannot be excluded that Archaean gneisses, corresponding to those of the Thule mixed-gneiss complex, do occur. The unit contains the Prudhoe Land granulite complex of Dawes (as named on the 1:500 000 map sheet), and the Etah Group, Etah meta-igneous complex and Palaeoproterozoic gneisses of Inglefield Land to the north (Map 1; Dawes *et al.* 2000). In the study area, the main rocks are high-grade, polydeformed and polymetamorphosed orthogneisses with thin units of quartzo-feldspathic to pelitic paragneiss. The pelitic gneisses are commonly graphitic and they are made conspicuous by their rusty weathering. The paragneisses are considered to be correlatives of the larger tracts of supracrustal rocks that make up the next map unit.

### **Prudhoe Land supracrustal complex**

These supracrustal rocks of supposed Palaeoproterozoic age comprise a thick succession of pelitic, semi-pelitic and quartzitic rocks (including pure quartz rocks) with mafic units (amphibolite and pyrobitite) that form large, rusty-weathering outcrops in two main areas: around Morris Jesup Gletscher and from Bowdoin Fjord to Josephine Peary Ø (Map 1). In 2001, new outcrops of supracrustal rocks were noted in Bowdoin Fjord, between this fjord and McCormick Fjord and in Robertson Fjord. Units of marble, not hitherto known in the succession, were discovered at Bowdoin Fjord and Morris Jesup Gletscher. This strengthens the view that the supracrustal rocks are a correlative of the Etah Group of Inglefield Land in which marble units are common.

The supracrustal rocks have been folded by large recumbent isoclinal folds so that they now occur as shallow-dipping units that can be flanked both below and above by gneiss. The contacts examined between supracrustal rocks and the gneisses are tectonised but structural considerations suggest that the supracrustal rocks represent a cover sequence to the Thule mixed-gneiss complex.

Field work east of Bowdoin Fjord revealed units of highly graphitic and pyritic schist several tens of metres thick with intense argillic alteration. Remobilisation of pyrite into veinlets in quartz-rich pinch-and swell layers is interpreted as due to a hydrothermal overprint. The intense rust coloration is reflected by distinct anomalies in images based on Landsat satellite data (Thomassen *et al.* 2002a). No convincing signs of economic mineral concentrations were found in the pyritic schists. Analyses of chip and grab samples show no significant concentrations of economic metals.

### **Thule Basin**

The Thule Basin developed on the peneplained surface of the Precambrian shield. The basin fill – the Thule Supergroup – is a thick (possibly up to 8 km thick), multicoloured, continental, littoral to shallow marine sedimentary succession with one main interval of basaltic volcanic rocks. Basic sills are common at several levels. Five groups are recognised (Dawes 1997). The lower four groups are Mesoproterozoic in age (basal volcanics c. 1270 Ma). The upper strata (Narssârssuk Group) outcrop outside the study area; their age is uncertain thus explaining the Mesoproterozoic–?Neoproterozoic age assignment attributed to the Thule Supergroup. In Inglefield Land, north of the study area (Map 1), the Supergroup is overlain by Lower Palaeozoic deposits of the Franklinian Basin.

### **Smith Sound Group**

This group directly overlies the crystalline shield; it represents the northern basin margin equivalent of the Nares Strait Group and the overlying Baffin Bay Group of the south. It is composed of varicoloured sandstones and shales, including red beds, with subordinate stromatolitic carbonates. No mineral prospecting was carried out in 2001 in this unit.

### **Nares Strait Group**

This group, up to 1200 m thick and representing the oldest strata of the central basin, is dominated by sandstones (both red beds and clean white quartz arenites), with a formation of basaltic volcanics including flows, sills and volcanoclastic deposits (Cape Combermere Formation). Siltstone/shale- and carbonate-dominated intervals also occur. Stromatolites occur in the carbonates. The succession is taken to represent deposition in alluvial plain, littoral and offshore environments. In 2001, one important revision was made concerning the distribution of the group that has relevance to mineralisation. At the north coast of 'Olrik Halvø' the group was previously deemed absent (Dawes 1997). In 2001, a greenish basaltic unit, at least 20 m thick and in places veined and brecciated was located within a red bed section directly overlying the shield: a succession now referred to the Cape Combermere Formation. Similar basaltic rocks are also present at Bowdoin Fjord, and in 2001 were also identified farther to the east at Hubbard Gletscher. This formation has its maximum thickness in Greenland on Northumberland Ø (c. 200 m; reaches 340 m in Canada); it thins eastwards towards the basin margin.

Malachite staining reveals copper mineralisation in a volcanic breccia of the Cape Combermere Formation on Northumberland Ø (Gowen & Sheppard 1994). The mineralisation resembles a 'volcanic redbed copper' deposit type (Kirkham 1996), and is possibly associated with the NW–SE-trending fault crossing the island (Map 1). Samples of this type of mineralisation collected during *Qaanaaq 2001* returned up to 1% Cu, 11 ppm Ag and 0.9 % Ba.

### **Baffin Bay Group**

The group represents the most widespread strata of the Thule Basin with a composite thickness of at least 1300 m. It is subdivided into five formations, four of which are present in Greenland. In the central part of the basin (western part of the study area) the group conformably overlies the Nares Strait Group; in the east it overlaps onto the crystalline shield. The group consists of shallow water, multicoloured siliciclastic rocks: sandstones, quartz grits and quartz-pebble conglomerates, with important intervals of shales and siltstones, representing mixed continental to marine shoreline environments, with syn-depositional faulting. The sandstones vary from highly ferruginous red beds to clean sands. The uppermost strata (Qaanaaq Formation) indicate a gradually deepening depositional regime from predominantly alluvial plain to shallow-shelf, tide-dominated deposition that is part of a regional regression of the shoreline that continues into the more basinal sequence of the Dundas Group.

The sandstones have disseminated Fe-Cu sulphides giving occasional malachite staining. The highest recorded concentrations of chalcopyrite occur at Red Cliffs where 1.5% Cu and 0.8% Ba were determined in a composite of grab samples.

### **Dundas Group**

This group conformably overlies the previous one along a gradational contact. Its upper limit is marked by Quaternary deposits and the present erosion surface. The group has a dark weathering, monotonous lithology without conspicuous markers and regional correlation of sections is not obvious; its estimated thickness is between 2000 and 3000 m. It is

composed of sandstones, siltstones and shales with lesser amounts of carbonate and evaporite. Deposition was in an overall deltaic to offshore environment. In the study area, two formations are recognised. In Prudhoe Land, the sediments are characterised by coarsening- and thickening-upwards shale-sandstone cycles thought to represent progradation delta front sequences, while the outcrops south of Olrik Fjord are dominated by fissile, multicoloured shale packages with laminated silts and fine-grained sandstones that are interpreted to represent prodelta muds and delta plain deposits. Sporadic basic sills are present; these are very conspicuous in the Dundas Group south of the study area.

Minor sphalerite mineralisation has been located at the base of a limestone unit within the Dundas Group on Northumberland Ø. A composite sample has returned 2.1% Zn and 0.01% Pb. Dark shales within this group commonly contain stratiform pyrite, however with negligible base metal concentrations.

## **Regional structures**

The regional structure is dominated by down-faulted blocks of Thule Basin deposits forming islands and outer coastal areas bordered inland by generally higher areas of the Precambrian shield. Over much of its extent, the Thule Basin has preserved sedimentary contacts with the shield; while in some places, for example in northern Prudhoe Land and in Olrik Fjord, faults delimit the basin deposits. Where the Dundas Group is downthrown against the shield, as in the Olrik Fjord graben (Map 1), displacement of several kilometres has taken place.

Compared to the crystalline shield the Thule Supergroup is little disturbed: main structures are fault blocks, grabens, large-scale flexures, as well as some local folds associated with faults. Prominent faults vary from NW-trending, as the fault blocks of Prudhoe Land, to ESE-WNW-trending like the Olrik Fjord graben mentioned above. These latter faults are parallel to the most conspicuous basic dyke swarm of the region that is Neoproterozoic in age cutting all strata of the Thule Basin. In 2001, new faults of both directions were located. Of these, a steep fault on the southern shore of McCormick Fjord (Map 1) has appreciable downthrow juxtaposing the Baffin Bay Group against the shield.

## **Sampling and analysis**

Prior to the field work preferred sample localities were selected and marked on aerial photographs. It was attempted to obtain an even distribution of localities in first or second order streams with drainage basins not larger than 10 km<sup>2</sup>.

At each locality stream sediment material from 3 to 15 different sites along c. 50 m of the stream course were combined to a bulk sample of c. 500 g contained in a paper sample bag. Additionally, the total gamma-radiation from rock exposures or predominant boulders was measured, using a scintillometer. Duplicate samples were collected at 16 localities with the purpose of estimating the local variation in sample composition.

Suitable sample sites were difficult to find in the flat lying areas in the eastern and south-eastern part of the region. In such places (c. 5 % of all localities) soil samples were collected from small depressions in the terrain. Streams were also scarce on the steep slopes along glaciers in the north-western areas where samples of fine-grained scree were collected instead (c. 3% of all localities).

The sample bags were provisionally dried onboard *M/S Kissavik* and then packed and shipped to Denmark. Here the bags were dried at 60°C and the samples sieved into three fractions. The fine fractions (< 0.1 mm) were sent for analysis, the 0.1 to 1 mm fractions have been archived and the fraction above 1 mm discarded. All samples were analysed at Activation Laboratories Ltd., Canada. Major elements were determined by X-ray fluorescence spectrometry (XRF) using fused samples, trace elements were determined by a combination of instrumental neutron activation analysis (INAA) and inductively coupled plasma emission spectrometry (ICP) using a 'near total' digestion with four acids (HF, HClO<sub>4</sub>, HNO<sub>3</sub>, HCl). Some samples did not contain enough fine fractions to permit all three kinds of analysis hence fewer samples were analysed by XRF than by ICP and INAA. The samples were analysed in two batches, and both were accompanied by a set of three internal stream sediment standards plus one sample of international reference material.

#### **Quality of analytical data**

The precision of the analytical data is documented by means of duplicate analyses, carried out by the laboratory. In total, 20 ICP analyses and 13 XRF were duplicated. No duplicate analyses were performed in the procedure for INAA. The precision is high for major elements, and for trace elements except Y and Pb, as shown by the diagrams in the Appendix, Figs A1 and A2. Differences in analytical values for the standards from each of the two batches are also small (Table A1 in the Appendix) and no correction is needed.

The accuracy is estimated using international reference material, in this case CANMET stream sediment standard STSD-2 (Bowman 1994). A high accuracy is documented by the small differences between the measured and recommended values of STSD-2 (Table A1).

#### **Presentation of results**

In this report results are shown for all elements for which a significant number of samples gave concentrations above the lower detection limit. Concentrations for Cd and Tb are very rarely above the detection limit and maps of these elements are not shown. Only one data set (the one regarded the most reliable) is presented for each of those elements which have been measured by more than one method. The element selection is shown in Table 1 together with analytical method, lower detection limits and statistical parameters. For the major elements, results are given as concentration of oxides calculated on volatile-free basis. The amount of volatiles (determined as loss on ignition) varies with the amount of carbonate, organic matter and hydrous minerals.

Map no.	Unit	Method	L.D.L.	Minimum	Median	98th percentile	Maximum	
2	SiO <sub>2</sub>	%		43.24	65.32	86.56	93.38	
3	TiO <sub>2</sub>	%		0.28	0.97	2.25	4.70	
4	Al <sub>2</sub> O <sub>3</sub>	%		2.44	14.64	26.85	33.09	
5	Fe <sub>2</sub> O <sub>3</sub>	%		0.55	6.93	14.19	16.50	
6	MnO	%		0.00	0.09	0.21	0.77	
7	MgO	%		0.17	2.69	6.59	8.34	
8	CaO	%		0.05	2.10	4.82	7.23	
9	Na <sub>2</sub> O	%		0.01	1.35	3.53	3.89	
10	K <sub>2</sub> O	%		0.77	2.80	5.39	8.25	
11	P <sub>2</sub> O <sub>5</sub>	%		0.03	0.19	0.68	1.26	
12	S	%	ICP-ES	0.001	0.001	0.03	0.21	0.80
13	Ag	ppm	ICP-ES	0.3	0.3	0.84	2.6	3.4
14	As	ppm	INAA	0.5	0.5	1.50	8.8	48
15	Au	ppb	INAA	2	< 2	< 2	8	55
16	Ba	ppm	INAA	50	170	690	1400	5400
17	Be	ppm	ICP-ES	1	< 1	1.44	2.8	3.3
18	Bi	ppm	ICP-ES	2	< 2	< 2	2.5	3.7
19	Br	ppm	INAA	0.5	< 0.5	3.50	72	197
	Cd	ppm	ICP-ES	0.3	< 0.3	0	1.4	2.4
20	Co	ppm	INAA	1	3	20	43	56
21	Cr	ppm	INAA	2	21	109	280	350
22	Cs	ppm	INAA	1	< 1	< 1	7.0	9
23	Cu	ppm	ICP-ES	1	6.1	33	115	151
24	Hf	ppm	INAA	1	2	16	56	85
25	Mo	ppm	ICP-ES	1	< 1	2.3	7	15
26	Ni	ppm	ICP-ES	1	4.5	36	141	245
27	Pb	ppm	ICP-ES	1	< 1	19	48	77
28	Rb	ppm	INAA	15	10.0	86	198	240
29	Sb	ppm	INAA	0.1	< 0.1	0	0.60	1.0
30	Sc	ppm	INAA	0.1	4.1	16	32	42
31	Sr	ppm	ICP-ES	2	15.9	187	450	578
32	Ta	ppm	INAA	0.5	< 0.5	0	3.8	5.7
33	Th	ppm	INAA	0.2	3.8	17.3	116	240
34	U	ppm	INAA	0.5	< 0.5	3.2	14	18
35	V	ppm	ICP-ES	2	10	111	213	269
36	W	ppm	INAA	1	< 1	< 1	3.5	19
37	Y	ppm	ICP-ES	1	7.3	23	48	69
38	Zn	ppm	ICP-ES	1	4.1	69	194	225
39	La	ppm	INAA	0.5	12.8	53	348	661
40	Ce	ppm	INAA	3	28	112	671	1200
41	Nd	ppm	INAA	5	10	46	255	470
42	Sm	ppm	INAA	0.1	2.5	7.6	34	63
43	Eu	ppm	INAA	0.2	< 0.2	1.6	3.5	5.1
	Tb	ppm	INAA	0.5	< 0.5	< 0.5	1.8	4.8
44	Yb	ppm	INAA	0.2	1.1	2.7	5.6	8.8
45	Lu	ppm	INAA	0.05	0.2	0.41	0.8	1.42
46	L.O.I.	%	Fusion		0.09	3.80	17.15	36.05

**Table 1.** Elements determined, analytical methods, lower detection limits (L.D.L) and statistical parameters for concentrations in the < 0.1 mm grain size fraction of 327 stream sediment and substitute samples from the Qaanaaq region. Major element oxides are given as volatile-free percentages. L.O.I.: loss on ignition. ppb: parts per billion, ppm: parts per million. XRF: X-ray fluorescence spectrometry; INAA: Instrumental neutron activation analysis; ICP-ES: Inductively coupled plasma emission spectrometry (4-acid digestion).

The geochemical variation is illustrated by 44 element distribution maps at the scale of c. 1:1 000 000 (Maps 2 to 45), one map of loss on ignition (Map 46) and one map of scintillometer readings (Map 47), the latter reflecting the variation in natural gamma radiation. The division of the colour scale is made separately for each element upon examination of the frequency distribution. The aim is to select colour scales that enhance the chemical variation tied to lithological changes, in addition to highlighting locations of anomalously high values. Software by Geosoft Inc. (the Chimera™ system) was used to produce the maps.

### Local variation

The compositional variation at a sampling locality is illustrated in Fig. 2. The diagrams comprise selected element data from sample pairs from seven out of the sixteen localities where duplicates were collected. The diagrams show that the variation in concentration for most elements is considerably greater *between* the localities than *within* a sample locality. In other words, the regional variation is statistically significant. The poorest reproducibility is found in the concentrations of Pb and Hf.

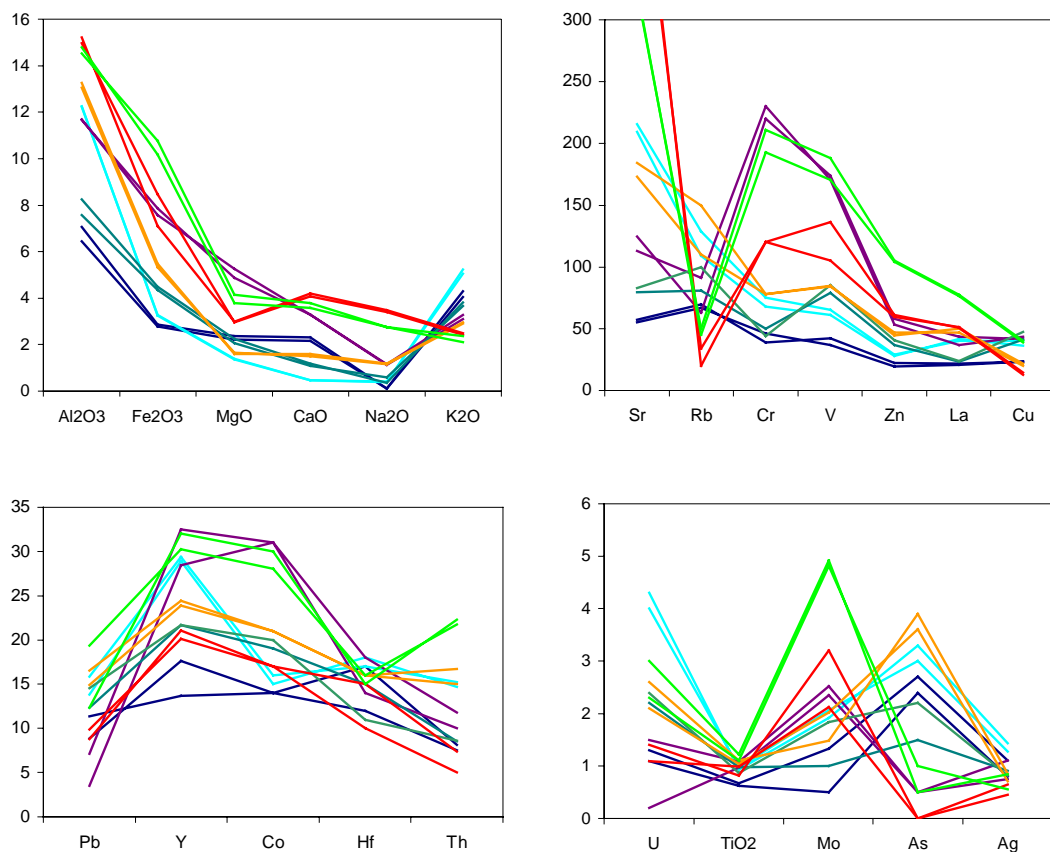


**Figure 2.** Compositional variability within a sampling locality and between localities shown for selected elements. Sample pairs are depicted in the same colour.

## Regional geochemical variation

Many element maps show, as might be expected, a pronounced difference in concentrations between the Precambrian crystalline shield and the Thule Basin. The line drawn on the geochemical maps roughly follows the edge of the Thule Basin and has been used to divide the data into two groups according to the main geology of the catchment area of the sampled streams. The division is not absolutely stringent because a number of streams drain shield outcrops overlain by rocks of the Thule Basin, but the majority of the samples within each group determines the classification. The summary statistics of each group are shown Table 2. A graphical representation of the differences is shown in Fig. 3. Regarded in bulk, as expressed by the medians, samples from the Thule Basin have significantly more SiO<sub>2</sub>, K<sub>2</sub>O, Ag, As and Rb than those from the shield, while almost all other elements have lower concentrations. Median concentrations of U, Yb and Lu are almost the same in the two groups. The natural gamma radiation emitted from the surface (Map 47) is generally higher over the shield.

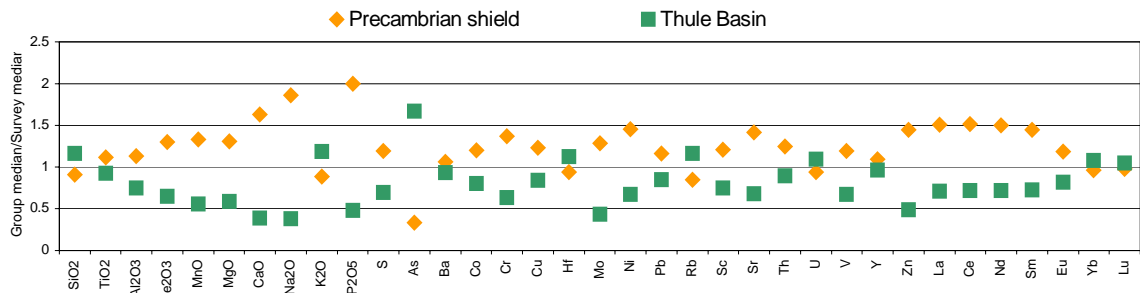


**Figure 3.** Illustration of the compositional difference between stream sediment samples from the shield and from the Thule Basin (cf. Table 2).

The median composition of samples from the crystalline shield in adjacent Precambrian regions, Inglefield Land to the north and Upernavik to the south, is listed for comparison in Table 2. The two datasets are extracted from results of earlier stream sediment surveys (see Steenfelt & Dam 1996; Steenfelt *et al.* 1998, 1999). The Qaanaaq region resembles Inglefield Land more than the Upernavik region, although the differences between the three regions are small. Of note are the higher values of P<sub>2</sub>O<sub>5</sub>, Ba, Sr and LREE (La, Ce, Nd, Sm and Eu) in the Qaanaaq region as discussed below.

		Qaanaaq Thule Basin	Qaanaaq Shield	Inglefield Land Shield	Upernavik Shield
N		154	173	173	363
SiO <sub>2</sub>	%	76.00	59.50	61.44	65.59
TiO <sub>2</sub>	%	0.89	1.08	0.89	0.69
Al <sub>2</sub> O <sub>3</sub>	%	11.00	16.51	16.27	14.59
Fe <sub>2</sub> O <sub>3</sub>	%	4.41	9.05	9.28	7.49
MnO	%	0.05	0.12	0.10	0.08
MgO	%	1.59	3.54	3.00	2.59
CaO	%	0.81	3.46	2.24	2.18
Na <sub>2</sub> O	%	0.50	2.51	2.13	2.52
K <sub>2</sub> O	%	3.32	2.48	2.60	2.70
P <sub>2</sub> O <sub>5</sub>	%	0.09	0.38	0.21	0.19
S	%	0.025	0.038		
As	ppm	2.5	0.5	4.6	5.5
Ba	ppm	640	730	600	560
Co	ppm	16	24	22	19
Cr	ppm	69	149	170	120
Cs	ppm	2	< 1	1	4
Cu	ppm	28	42	46	64
Hf	ppm	18	15	10	11
Mo	ppm	1	3	< 1	4
Ni	ppm	24	52	55	59
Pb	ppm	16	22	17	
Rb	ppm	100	73	71	100
Sb	ppm	0.2	< 0.1	< 0.1	< 0.1
Sc	ppm	12	19	20	16
Sr	ppm	127	263	192	167
Th	ppm	16	22	19	19
U	ppm	3.5	2.8	2.8	6.1
V	ppm	70	133	88	104
Y	ppm	22	25	23	27
Zn	ppm	33	98	93	95
La	ppm	38	82	57	72
Ce	ppm	80	170	120	124
Nd	ppm	33	71	47	48
Sm	ppm	5.5	11.2	7.7	7.9
Eu	ppm	1.3	1.9	1.4	1.4
Yb	ppm	2.9	2.6	3.1	3.5
Lu	ppm	0.43	0.39	0.43	0.47

**Table 2.** Medians of element concentrations of stream sediment samples from the Qaanaaq region and two adjacent areas. Cf. Table 1 for analytical methods.

Significant chemical variation is also observed within the two main geological provinces, and many element distribution patterns in each can be related to individual lithological units.

In a quantitative approach the samples have been screened using the chemical criteria listed in Table 3. As a result eleven sample selections were made. Map 48 shows the location of samples within each category. About 40 samples were not selected, and their locations are not shown on the map. Some of the samples qualify in more than one category, which is indicated by overlapping symbols in Map 48. The map demonstrates a clear spatial relationship between the chemically classified samples, which is further discussed for each category.

**Precambrian shield**

Name	First criteria	Additional criteria, comments
High Al-Th	Al <sub>2</sub> O <sub>3</sub> /SiO <sub>2</sub> > 0.35	Th > 50 ppm. Sr < 200 ppm
High Pb	Pb > 62 ppm	
High Cu-Zn	Cu > 80 while Zn > 110 ppm	
High Ni	Ni ppm/MgO % > 30	
High Sr-Ba	Sr > 300 while Ba > 840 ppm	
High Rb/Sr	Rb/Sr > 0.3	Rb > 75 ppm
High Rb-U	Rb > 140 while U > 6 ppm	
High MgO, low SiO <sub>2</sub>	MgO > 5.4 while SiO <sub>2</sub> < 60%	This category only comprises samples from Nunatarssuaq and 'Olrik Halvø'
Low La	La < 55 ppm	All REE (rare earth elements) have low concentrations

**Thule Basin**

High Cs	Cs > 4 ppm	Rb is > 100 ppm and K <sub>2</sub> O is > 2.8 % in this category
High K <sub>2</sub> O-MgO	K <sub>2</sub> O > 3.6 while MgO > 2.35 %	MgO < 5 %

**Table 3.** Chemical criteria applied to screen stream sediment samples into eleven categories relating to lithology and mineralisation.

	High Al-Th	High Cu-Zn	High Sr-Ba	High Sr, I. L.	High Rb/Sr	TMGmafic	Low La
N	15	18	35	13	50	12	16
SiO <sub>2</sub> %	55.24	57.12	59.10	61.38	61.10	55.93	59.95
TiO <sub>2</sub> %	1.32	0.82	1.12	0.89	0.93	1.19	0.81
Al <sub>2</sub> O <sub>3</sub> %	26.69	17.76	16.40	15.15	15.73	16.76	17.27
Fe <sub>2</sub> O <sub>3</sub> %	9.29	11.35	8.81	7.89	8.97	10.66	8.11
MnO %	0.16	0.11	0.11	0.10	0.13	0.17	0.10
MgO %	2.20	4.43	3.40	3.66	3.96	6.11	3.08
CaO %	1.04	2.34	4.13	4.45	2.96	3.01	3.61
Na <sub>2</sub> O %	0.67	1.91	2.73	3.05	2.49	2.42	2.52
K <sub>2</sub> O %	1.75	2.77	2.39	2.38	2.90	2.73	1.96
P <sub>2</sub> O <sub>5</sub> %	0.19	0.24	0.47	0.46	0.36	0.45	0.17
S %	0.089	0.054	0.032		0.047	0.055	0.028
Ba ppm	470	650	1000	690	730	720	565
Co ppm	18	37	24	20	29	33	22
Cr ppm	238	180	110	160	150	176	180
Cu ppm	43	113	32	18	46	66	56
Hf ppm	19	9	17	12	12	9	7
Ni ppm	33	121	40	54	67	93	86
Pb ppm	23	33	18	9	28	24	26
Rb ppm	91	91	52	63	113	157	58
Sc ppm	23	19	21	19	18	18	15
Sr ppm	50	189	394	461	226	188	261
Th ppm	107	25	17	14	35	30	13
U ppm	9.3	3.5	2.2	1.9	3.8	4.4	2.2
V ppm	140	142	143	83	126	139	111
Y ppm	19	21	29	23	27	32	17
Zn ppm	82	179	100	77	109	120	89
La ppm	261	72	78	70	103	94	44
Ce ppm	551	147	160	150	202	178	88
Nd ppm	213	54	72	64	76	75	31
Sm ppm	28.7	9.4	11.4	11.0	12.2	11.9	5.6
Eu ppm	2.3	1.4	2.4	2.0	1.8	1.9	1.3
Yb ppm	3.1	2.2	2.3	2.9	2.4	2.4	1.7
Lu ppm	0.46	0.32	0.35	0.38	0.37	0.37	0.26

**Table 4.** Medians of element concentrations for the six main categories of stream sediment samples selected by chemical criteria (see Table 3) together with medians of samples with high Sr from Inglefield Land (I.L.). N: number of samples in each category.

## Chemical variation within the Precambrian shield

### High Al-Th

This category embraces samples with high  $\text{Al}_2\text{O}_3$  (alumina, Map 4) relative to  $\text{SiO}_2$  (Fig. 4a). These samples also have very high REE (Fig. 4b) and Th concentrations, as well as elevated  $\text{TiO}_2$ ,  $\text{Fe}_2\text{O}_3$ , U, Cr and Hf (Table 4). They are all located within the Prudhoe Land supracrustals (cf. Map 48 and Map 1) and the high alumina agrees with the described predominance of metapelites. At the present high metamorphic grade the Al-rich components are minerals like sillimanite and garnet. Relatively high  $\text{Fe}_2\text{O}_3$  and MnO concentrations of the samples probably reflect the pyritiferous parts of the supracrustals. In addition, the high concentrations of Hf, Th, U, REE,  $\text{TiO}_2$  and Cr indicate that the metasedimentary sequences are rich in minerals like zircon, allanite, monazite, ilmenite and chromite. It is possible that such heavy minerals occur as concentrates within rocks representing beach or fluvial depositional environments, in which case they may be economically interesting. The samples of this category are also characterised by very low concentrations of  $\text{Na}_2\text{O}$  and Sr (Table 4). One sample with high alumina does not conform to the other high alumina samples regarding concentrations of other elements. It is located in Smithson Bjerge (Map 4), and has combined high Al, Ca, Sr and Na together with low K and LREE suggesting that plagioclase from the anorthosite, instead of garnet or sillimanite, is the major alumina component of this sample.

Stream sediments derived from the Palaeoproterozoic Etah Group metasediments in Inglefield Land, the assumed correlative of the Prudhoe Land supracrustal complex, have equally high concentrations of  $\text{Al}_2\text{O}_3$ , but exhibit no signs of heavy mineral concentrations.

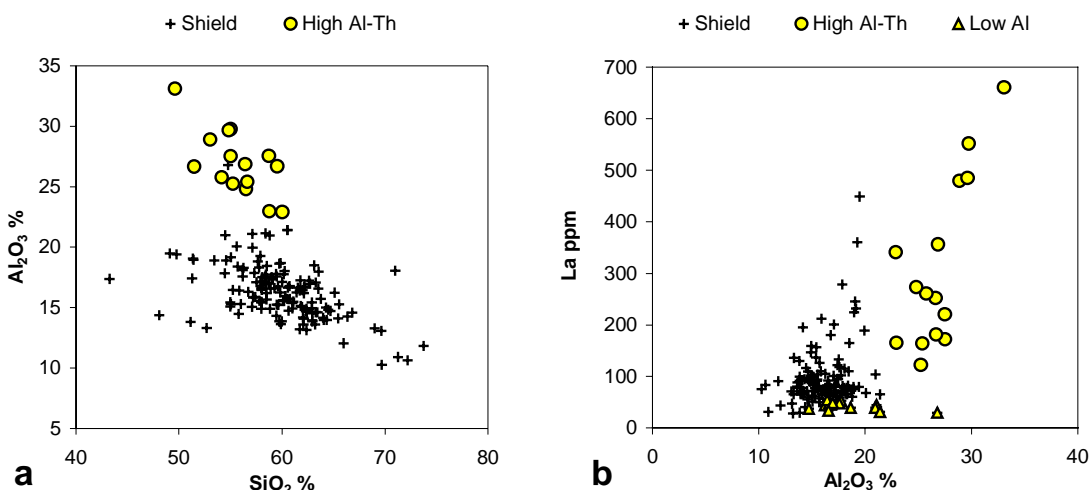


**Figure 4.** Variation in all samples derived from the shield showing the enrichment of  $\text{Al}_2\text{O}_3$  and La in samples derived from the Prudhoe Land supracrustals, as well as the low La in samples from Smithson Bjerge.

Two samples within the High Al-Th category have high concentrations of Pb, and two samples from nunataks at the head of Morris Jesup Gletscher with high alumina and Th (yellow symbols in Map 48) also have high Cu (Map 23).

### High Cu, Zn and Ni

Samples with high Cu and Zn were selected to find possible indications of base metal mineralisation (Fig. 5a). The distribution of the selected samples shows clusters in four areas (Map 48). The Cu-Zn samples from Smithson Bjerge were collected within a series of rusty weathering banded paragneisses south of the anorthosite body, and red garnetiferous rusty paragneisses also occur near the three sample localities at the coast east of Hubbard Gletscher (Thomassen *et al.* 2002b). Ni is generally correlated with MgO, i.e. hosted in olivine and amphiboles, but the Ni in samples from these two areas plot above the correlation trend (Fig. 5b), which suggests that Ni is hosted by sulphides. The two areas are therefore interesting as exploration targets.

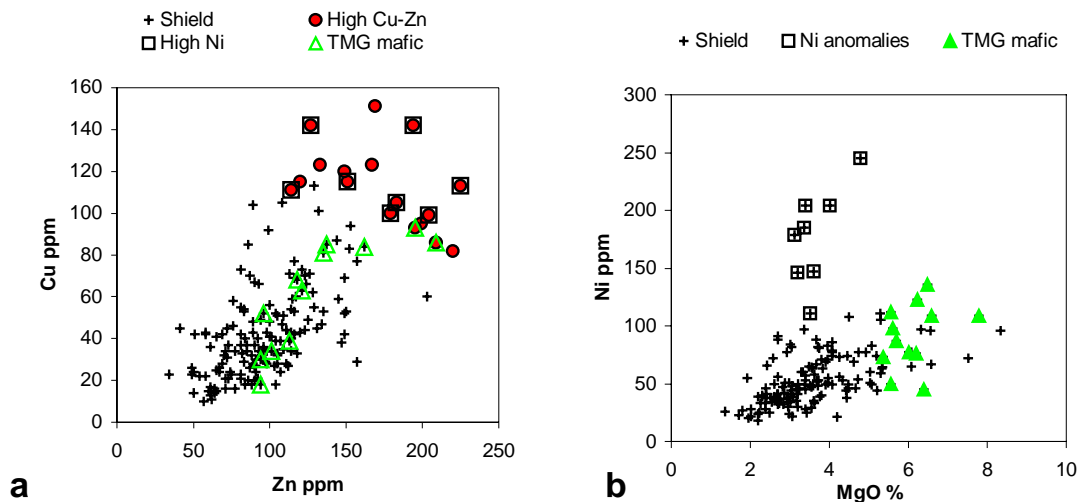


**Figure 5.** Variation in all samples from the shield showing Cu, Zn, Ni and MgO characteristics of samples in the categories High Cu-Zn and High MgO, low SiO<sub>2</sub> (TMG mafic).

Samples with high Zn and Cu, but with lower concentrations of Ni, were collected at Sonntag Bugt, in streams draining mixed para- and orthogneisses of the undifferentiated gneiss complex. In Nunatarssuaq and south-eastern 'Olrik Halvø', the source of elevated Cu and Zn is probably mafic to ultramafic enclaves in the Thule mixed-gneiss complex with small occurrences of with pyrite and chalcopyrite mineralisation like those mentioned in the section on geology.

The Cu-Zn samples from Smithson Bjerge and east of Hubbard Gletscher are similar with regard to Cu, Zn and Ni, but they differ in other ways (Table 4). Smithson Bjerge samples classify together with samples from the anorthosite in having very low REE concentrations, whereas samples east of Hubbard Gletscher have high K<sub>2</sub>O and elevated Rb (Maps 10,

28). The latter reveals pegmatites or granites in the rock assemblage upstream from the sampling site.

The stream sediment data offer no other indications of mineralisation in the shield than those discussed above. The concentrations of Au and As are low and samples with elevated values are scattered.

### Categories relating to meta-igneous rocks

Orthogneisses make up a substantial part of the nunatak zone of Prudhoe Land, as well as Nunatarssuaq and 'Olrik Halvø'. According to previous literature and field observations within *Qaanaq 2001* these rocks are a variety of high-grade gneisses from dioritic to granitic compositions, including K-feldspar porphyritic 'augen'-gneisses.

#### High Sr-Ba

The distribution of Sr (Map 31) delineates a high-Sr province comprising the south-eastern part of the nunatak zone of Prudhoe Land. South of Tracy Gletscher Sr values are generally lower with scattered high values. Many of the samples with high Sr also have high concentrations of Ba (Map 16 and Fig. 6a) and  $P_2O_5$  (Map 11 and Fig. 6b). Samples surrounding the head of Robertson Fjord are additionally rich in  $TiO_2$ , Y, and REE (Maps 3, 37, 39–45). In Inglefield Land samples with such characteristics are collected in syenitic gneisses belonging to the Palaeoproterozoic Etah meta-igneous complex (Steenfelt & Dam 1996; Dawes *et al.* 2000). It is likely, therefore, that similar Palaeoproterozoic intrusions of quartz dioritic, monzonitic or syenitic character also occur throughout Prudhoe Land. Hitherto, such rocks have only been recognised in northern Prudhoe Land forming the Prudhoe Land granulite complex of Dawes (1991).

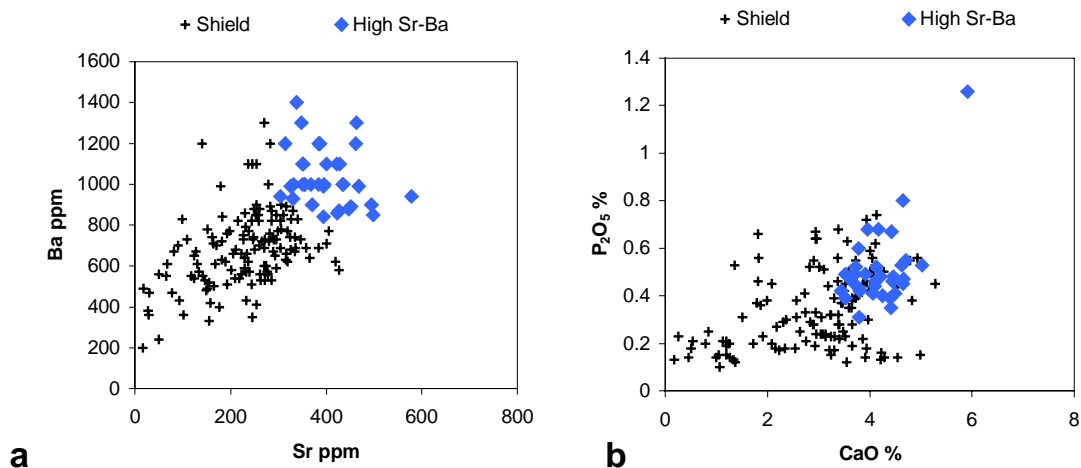


**Figure 6.** Variation of all samples from the shield showing Sr, Ba, CaO and  $P_2O_5$  characteristics of samples within the category High Sr-Ba that is mainly derived from Prudhoe Land.

### High Rb/Sr

The majority of samples with high Rb/Sr ratio ( $> 0.3$ ) and Rb  $> 75$  ppm are derived from the Thule mixed-gneiss complex at Nunatarssuaq and eastern 'Olrik Halvø'. These samples are also characterised by high gamma radiation (Map 47) and  $K_2O$ , medium high  $Na_2O$ , Th and La (Table 6), which indicates the predominance of granodioritic to granitic gneisses. In Fig. 7a this category is shown together with other categories derived from feldspathic gneisses. The categories occupy well-defined fields in both diagrams of Fig. 7.

Samples with the highest Rb and U probably contain material derived from pegmatites. The concentrations of 'gabbroophile' elements,  $Fe_2O_3$ , MgO,  $TiO_2$ , MnO, Co, Cu, Sc, Zn vary considerably in this sample category, irrespective of the general high concentrations of lithophile elements. The median values for the 'gabbroophile' elements are high, reflecting many enclaves of mafic rocks, as well as the magnetite-rich supracrustal units and iron-formations observed in the field. A small cluster of samples with high Rb/Sr ratio is located around Hubbard Gletscher, south of the Prudhoe Land supracrustals.

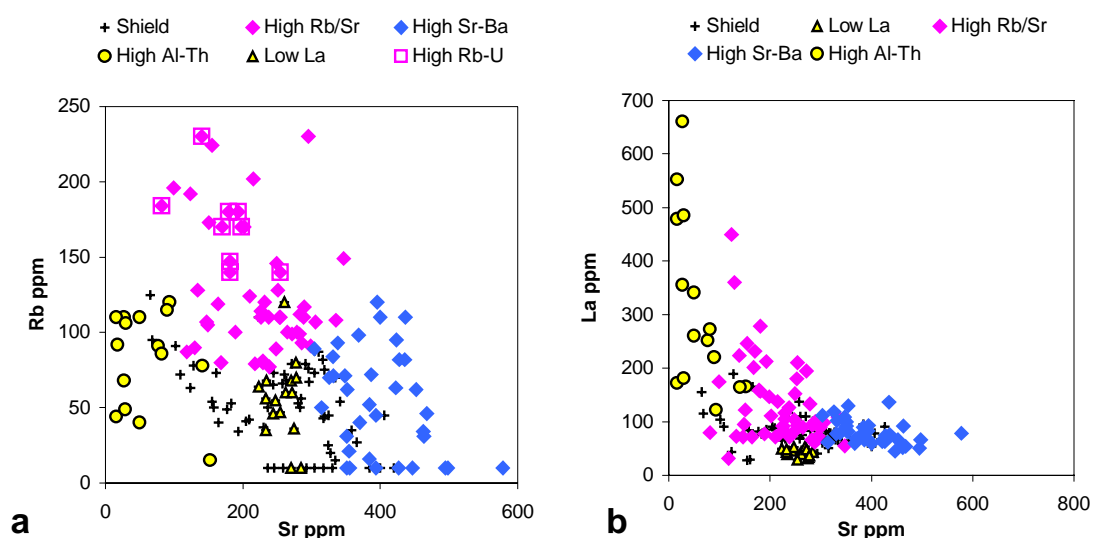


**Figure 7.** Variation of all samples from the shield showing Sr, Rb and La characteristics of samples within five categories (cf. Table 3). High Rb/Sr samples are mainly derived from the Thule mixed-gneiss complex and are differentiated from the other groups.

### High MgO in the Thule mixed-gneiss complex (TMG)

Some of the samples from the region of high Rb, i.e. Nunatarssuaq and 'Olrik Halvø', have high concentrations of 'gabbroophile elements', such as  $Fe_2O_3$ , MgO, MnO, Sc and V. This reflects a contribution from the enclaves of mafic meta-igneous rocks. This category of samples is labelled 'TMG mafic' and their position in the diagrams of Fig. 5 shows that they are variably enriched in Cu and Zn and that their Ni is correlated with MgO as is the case in non-mineralised, mafic to ultramafic igneous suites.

### **Low La**

The samples from the anorthosite body at Smithson Bjerge have very low concentrations of REE. The same applies to samples collected in the paragneisses south of the anorthosite. The position of the samples is shown in Figs 4b, 7a and 7b. The samples collected within the outcrops of the anorthosite body as well as those collected in streams draining the supracrustals are low in elements like  $K_2O$ ,  $P_2O_5$ , Ba, Hf, Rb, Th, and U relative to samples of the other categories (Table 4), and they reflect plagioclase-dominated lithologies.

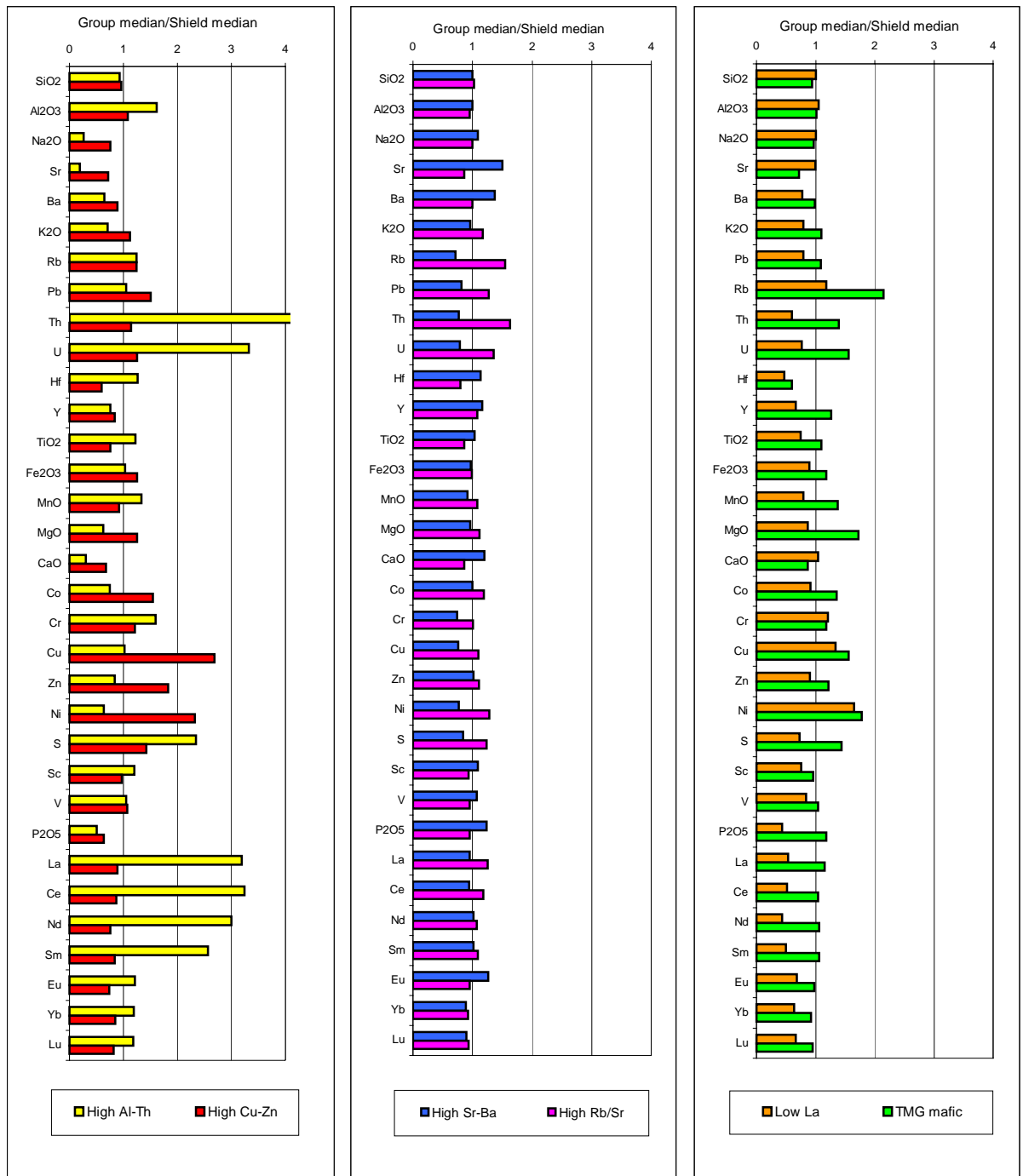
### **Comparison of categories**

Figure 7 shows how categories relating to para- and orthogneisses are differentiated in diagrams of Sr versus Rb and Sr versus La. The Sr-Rb variation relates to the proportion of feldspars and shows the predominance of plagioclase in the orthogneisses of Prudhoe Land and Smithson Bjerge and higher amounts of potassic feldspar in Nunatarssuaq. Along with higher amounts of potassic feldspar, the orthogneisses have higher amounts of Th and light REE (La to Eu).

Figure 8 is a graphical presentation of the data of Table 4, where the main categories are represented by their medians normalised against the medians for all samples of the shield. The elements are sorted according to their affinity to major lithologies of crystalline shields. From the top ( $SiO_2$  to Hf) are the elements associated with felsic, quartzo-feldspathic rocks, then follows elements (Y to  $P_2O_5$ ) typically enriched in mafic metavolcanic and gabbroic rocks, and at the base the rare earth elements (La to Lu). The diagrams emphasise that differences between the categories apply to a wider range of elements than those used to establish the categories and presented in the element variation diagrams.

### **Metamorphic grade**

The distribution patterns of the gamma radiation and lithophile elements such as  $K_2O$ , Rb and U reflect the metamorphic conditions to which the gneiss complexes have been subjected. Low concentrations, i.e. high metamorphic grade (granulite facies), characterise samples from the nunatak zone of Prudhoe Land whereas higher concentrations of lithophile elements are found in samples from Nunatarssuaq. The geochemistry therefore confirms observed amphibolite facies grade of the southern gneisses of the Thule mixed-gneiss complex of Dawes (1991).



**Figure 8.** Medians of element concentrations of stream sediment and substitute samples within the categories selected by chemical criteria and relating to lithologies within the Precambrian shield of the Qaanaaq region (see Tables 3 and 4).

## Chemical variation within the Thule Basin

Samples from streams draining rocks of the Thule Basin are generally high in SiO<sub>2</sub> concentrations reflecting the quartz rich sediments that characterise the Thule Supergroup. Samples with material derived from basic volcanics of the Nares Strait Group are few because of the limited volume of such rocks; the recognition of the chemical characteristics of the volcanics is also hampered by fact that they occupy a low stratigraphic position not far from rocks of the crystalline shield that has similar chemical signatures. The volcanics are thickest in northern Northumberland Ø and the sample from the northern coast does have high Fe<sub>2</sub>O<sub>3</sub>, MnO, and MgO while concentrations of elements like Co, Cu, Cr, Sc and V are lower than expected. Thus, the observed Cu-mineralisation is not recorded in the stream sediment. More interestingly, the sample stands out as an Au-Mo anomaly with 38 ppb Au and 11 ppm Mo. Another sample with high Au (55 ppb) is located immediately west of the snout of Hubbard Gletscher (Map15), where a new occurrence of volcanics of the Cape Combermere Formation has been identified during *Qaanaaq 2001*. The stream sediment results therefore suggest gold potential associated with these volcanic rocks.

High Cs plus high concentrations of other lithophile elements, K<sub>2</sub>O, Rb and Pb, appear to characterise samples collected in streams draining rocks of the Dundas Group (see Maps 1, 48). A small group of samples with elevated MgO and high K<sub>2</sub>O (Maps 7, 10) are from the area between Sonntag Bugt and Robertson Fjord and these can also be related to outcrops of the Dundas Group. The elevated MgO is interpreted to reflect the presence of dolomite in the strata. The chemical characteristics are in accordance with a higher proportion of clay, silt and carbonate relative to the stratigraphically lower Baffin Bay and Nares Strait Groups. Elevated sulphur concentrations are recorded in some of the stream sediment samples from the Dundas Group, in accordance with known occurrences of stratiform pyrite in shales. At Northumberland Ø, elevated Zn concentrations may reflect the observed occurrences of mineralisation with sphalerite.

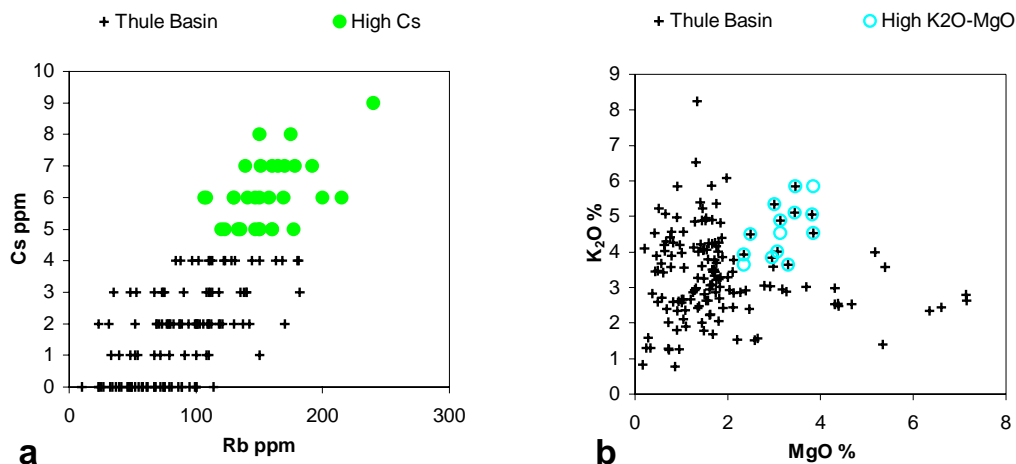


**Figure 9.** Variation diagrams used to select the High-Cs and the High K<sub>2</sub>O-MgO categories of stream sediment samples from the Thule Basin.

The faults developed during and after the evolution of the Thule Basin appear to be the most interesting features with regard to mineralisation of economic potential. High values of As, Ba, Sb, and U at Red Cliffs, south shore of McCormick Fjord (Map 1), reflect the observed barite-sulphide mineralisation. The other unusually high Ba values (above 1500 ppm) in the Thule Basin (Map 16) may well reflect other occurrences of fault-related barite mineralisation.

## Discussion

The geology of the Precambrian shield of the Qaanaaq region has not been mapped or studied in detail and lithogeochemical data are not available, except for meta-igneous rocks at Smithson Bjerger (Nutman 1984). The geochemical data acquired during *Qaanaaq 2001* are therefore a valuable contribution to the understanding of geological setting.

The distribution patterns of many elements as well as of the chemically classified samples agrees well with the division of the shield into four main components (Map 1). However, the geochemical data suggest that meta-igneous rocks similar to the Palaeoproterozoic undifferentiated gneisses are prominent in the entire nunatak zone from McCormick Fjord to Tracy Gletscher. In addition, the geochemical data provide evidence that there are orthogneisses of quartz dioritic, monzonitic and syenitic compositions resembling those recognised in Inglefield Land (Steenfelt & Dam 1996; Dawes *et al.* 2000). Rocks of Palaeoproterozoic age with the same chemical characteristics (high Sr-Ba-P) are also known from the Nagssugtoqidian and Ketilidian orogens farther south in Greenland (see Steenfelt *et al.* 2000; Steenfelt 2001).

The geochemical data confirm that the Prudhoe Land supracrustals are dominated by metasediments and strongly suggest that heavy minerals occur in all of the mapped outcrops of this unit. The provenance of the heavy minerals is likely to be a terrain with granitic (providing zircon, monazite, allanite) and gabbroic rocks (providing ilmenite and chromite). This agrees with the structural consideration that the supracrustals represent a cover sequence formed by erosion of the Thule mixed-gneiss complex.

The high Rb/Sr signature of the Thule mixed-gneiss complex in Nunatarssuaq also applies to samples from around the snout of Hubbard Gletscher and a few samples between Robertson Fjord and Bowdoin Fjord. This can be interpreted as the presence of Archaean gneisses at low structural levels in Prudhoe Land. Alternatively, the signature reflects the occurrence of late granites and pegmatites. Granites with high concentrations of Rb were recognised at Smithson Bjerger intruding the supracrustal sequence that has been correlated with the Thule mixed-gneiss complex (Nutman 1984).

The low La (low REE) signature in samples collected over the anorthosite at Smithson Bjerger agrees with very low concentrations of La and Ce in chemical analyses of anorthosite rock (Nutman 1984). The stream sediment samples from the area of supracrustal rocks south of the anorthosite share this signature and are chemically very similar. The main difference is that the samples from the supracrustals are enriched in Cu, Ni and Zn and have

slightly higher  $K_2O$  and  $MgO$ . Nutman (1984) describes the supracrustal sequence as quartzo-feldspathic with subordinate layers of ferruginous quartzites considering the sequence to be purely of sedimentary origin. If this is true, the base metals and  $K_2O$  may, therefore, have been introduced by hydrothermal activity after deposition of the sediments possibly in connection with the intrusion of ferrodiorites and granites. A source with very low REE concentrations must be assumed for the sediments.

The distribution of Rb and  $K_2O$  outlines a roughly east–west boundary separating granulite and amphibolite facies gneisses between Smithson Bjerge and Nunatarssuaq. This is in agreement with Dawes (1991) and Nutman (1984). The latter provided evidence that all of Smithson Bjerge lithologies, except late, undeformed pegmatites have been metamorphosed under granulite-facies conditions.

## Conclusions

Chemical data for stream sediment or substitute surficial material sampled at 327 localities within the Qaanaaq region provide information of the geochemistry and possible mineralisation of lithologies of the Precambrian shield and Thule Basin. Although the intricate mixing of para- and orthogneisses constrains the use of the stream sediment chemistry to characterise individual units, some regional features are recognised, and groups of samples with distinct chemical characteristics can be related to specific units within para- or orthogneiss assemblages. The main outcomes of the data treatment and interpretation of geochemical signatures of samples are:

1. The Prudhoe Land supracrustals are dominated by pelitic rocks and contain heavy minerals possibly concentrated in littoral or deltaic facies of the sedimentary deposits.
2. Metasedimentary rocks within ?Archaean supracrustal sequences at Smithson Bjerge and east of Hubbard Gletscher contain Ni-Cu-Zn sulphide mineralisation.
3. Palaeoproterozoic intrusive complexes (equivalent of the Etah meta-igneous suite in Inglefield Land) occur throughout Prudhoe Land, i.e. also in areas mapped as Archaean Thule mixed-gneiss complex (Dawes 1991).
4. The Thule mixed-gneiss complex in Nunatarssuaq has been subjected to high level granite magmatism or veining due to anatectic melting.
5. Gold mineralisation is associated with basic volcanic rocks within the Nares Strait Group of the Thule Supergroup.
6. Fault structures within the Thule Basin host barite veins with subordinate associated sulphides (As, Sb).

## Acknowledgments

The authors acknowledge support during the field programme by Jes Burghardt, Nuuk, skipper of *M/S Kissavik* and his crew, Grønlandsfly A/S pilot Glenn Lindström, field assistants Piuaitsoq Petersen and Peter Peary Aleqatsiaq from Qaanaaq, Hans Jensen and company, Hotel Qaanaaq, and Svend Erik Ascaneus, Geophysical Observatory of the Danish Meteorological Institute, Qaanaaq.

## References

- Bowman, W.S. 1994: Catalogue of Certified Reference Materials. CCRMP 94 - 1E, 74 pp. Ottawa: CANMET, Natural Resources of Canada.
- Dawes, P.R. 1976: 1:500 000 mapping of the Thule district, North-West Greenland. Rapport Grønlands Geologiske Undersøgelse **80**, 23–28.
- Dawes, P.R. 1988: Geological map of the Thule district, North-West Greenland, 1:100 000, sheets Siorapaluk, Qaanaaq, Hvalsund, Olrik Fjord and 1:200 000, sheet Inglefield Bredning. Unpublished maps, Geological Survey of Greenland (in archives of Geological Survey of Denmark and Greenland).
- Dawes, P.R. 1991: Geological map of Greenland, 1:500 000, Thule, Sheet 5. Copenhagen: Geological Survey of Greenland.
- Dawes, P.R. 1997: The Proterozoic Thule Supergroup, Greenland and Canada: history, lithostratigraphy and development. *Geology of Greenland Survey Bulletin* **174**, 150 pp.
- Dawes, P.R. & Frisch, T. 1981: Geological reconnaissance of the Greenland Shield in Melville Bugt, North-West Greenland. Rapport Grønlands Geologiske Undersøgelse **105**, 18–26.
- Dawes, P.R., Frisch, T., Garde, A.A., Iannelli, T.R., Ineson, J.R., Jensen, S.M., Piranjo, F., Sønderholm, M., Stemmerik, L., Stouge, S., Thomassen, B. & van Gool, J.A.M. 2000: Kane Basin 1999: mapping, stratigraphic studies and economic assessment of Precambrian and Lower Palaeozoic provinces in north-western Greenland. *Geology of Greenland Survey Bulletin* **186**, 11–28.
- Gowen, J. & Sheppard, B. 1994: Reconnaissance mineral exploration in the Thule area, North West Greenland, 24 pp. Unpublished report, Nunaoil A/S, Nuuk, Greenland (in archives of Geological Survey of Denmark and Greenland, GEUS Report File 21418).
- Kirkham, R.V. 1996: Volcanic redbed copper. In: Eckstrand, O.R., Sinclair, W.D. & Thorpe, R.I. (eds): *Geology of Canadian mineral deposit types*. *Geology of Canada* **8**, 241–252. Ottawa: Geological Survey of Canada.
- Nutman, A.P. 1984: Precambrian gneisses and intrusive anorthosite of Smithson Bjerge, Thule district, North-West Greenland. Rapport Grønlands Geologiske Undersøgelse **119**, 31 pp.
- Steenfelt, A. 2001: Geochemical atlas of Greenland - West and South Greenland. Danmarks og Grønlands Geologiske Undersøgelse Rapport **2001/46**, 39 pp., 1 CD-ROM.
- Steenfelt, A. 2002: Geochemistry of southern Steensby Land. Danmarks og Grønlands Geologiske Undersøgelse Rapport **2002/56**, 25 pp.
- Steenfelt, A. & Dam, E. 1996: Reconnaissance geochemical mapping of Inglefield Land, North-West Greenland. Danmarks og Grønlands Geologiske Undersøgelse Rapport, **1996/12**, 27 pp., 49 maps.

- Steenfelt, A., Dam, E. & Kyed, J. 1998: Geochemical mapping of the Ummannaq region (70°30' to 72°30' N, 50° to 56°W), central West Greenland. Danmarks og Grønlands Geologiske Undersøgelse Rapport **1998/40**, 25 pp., 41 maps.
- Steenfelt, A., Dam, E. & Kyed, J. 1999: Geochemical mapping of the Upernavik - Kap Seddon region North-West Greenland. Danmarks og Grønlands Geologiske Undersøgelse Rapport **1999/43**, 21 pp., 45 maps.
- Steenfelt, A., Nielsen, T.F.D. & Stendal, H. 2000: Mineral resource potential of South Greenland: review of new digital data sets. Danmarks og Grønlands Geologiske Undersøgelse Rapport **2000/50**, 47 pp.
- Thomassen, B., Dawes, P.R., Steenfelt, A. & Krebs, J.D. 2002a: *Qaanaaq 2001*: mineral exploration reconnaissance in North-West Greenland. Geology of Greenland Survey Bulletin **191**.
- Thomassen, B., Krebs, J.D. & Dawes, P.R. 2002b: *Qaanaaq 2001*: Mineral exploration in the Olrik Fjord - Kap Alexander region, North-West Greenland. Danmarks og Grønlands Geologiske Undersøgelse Rapport **2002/xx**.

# Appendix

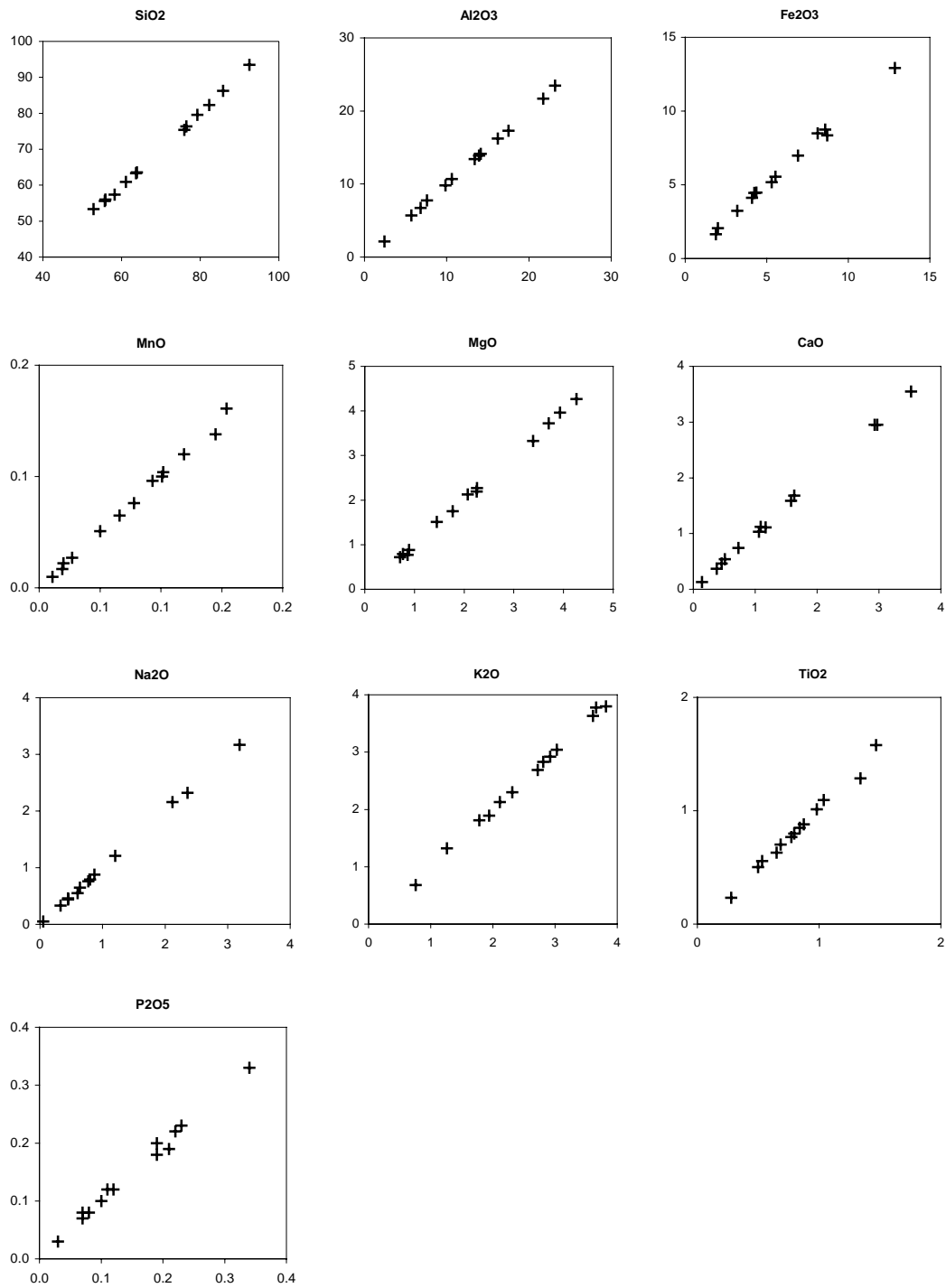


**Figure A1.** Analytical precision of element concentrations determined by X-ray fluorescence spectrometry. Results of repeated analysis of 13 samples.

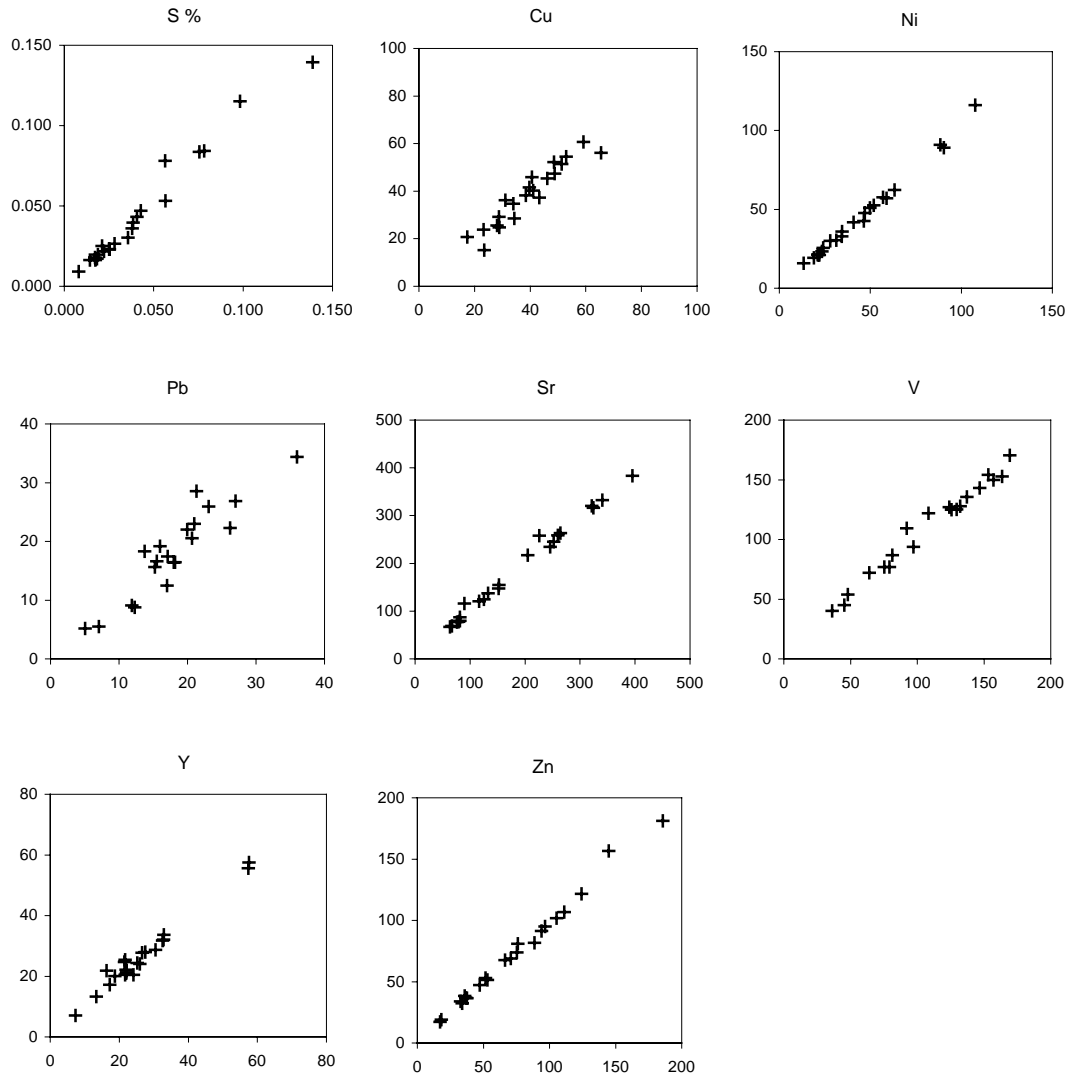


**Figure A2.** Analytical precision of element concentrations determined by inductively coupled plasma emission spectrometry. Results of repeated analysis of 20 samples.

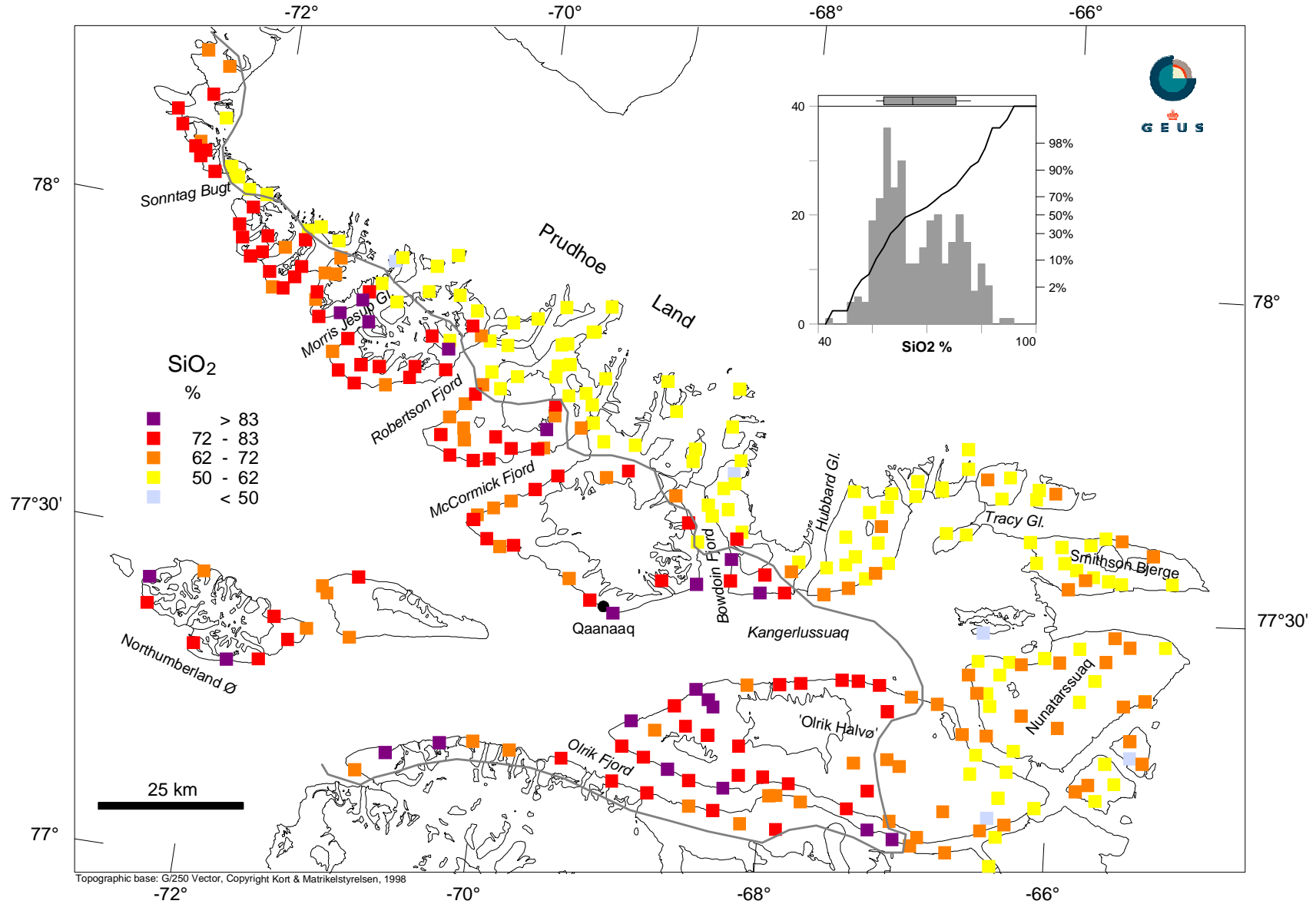
	GEUS2_1	GEUS2_2	GEUS3_1	GEUS3_2	GEUS5_1	GEUS5_2	STSD-2_1	STSD-2_2	STSD2_rec.
<b>XRF</b>									
SiO <sub>2</sub>	65.81	66.65	61.51	62.04	49.84	49.91	53.80	54.26	53.70
TiO <sub>2</sub>	0.412	0.409	0.940	0.947	1.416	1.436	0.737	0.754	0.80
Al <sub>2</sub> O <sub>3</sub>	13.64	13.09	12.84	12.27	13.14	12.81	15.76	15.57	16.1
Fe <sub>2</sub> O <sub>3</sub>	4.44	4.01	6.48	6.81	10.26	10.50	7.27	7.03	7.50
MnO	0.072	0.073	0.089	0.090	0.142	0.144	0.129	0.133	0.1
MgO	3.61	3.56	5.11	5.30	8.00	8.17	3.13	3.10	3.10
CaO	3.24	3.26	5.47	5.66	6.28	6.42	4.17	4.17	4.00
Na <sub>2</sub> O	3.64	3.45	3.14	3.05	1.45	1.45	1.76	1.78	1.70
K <sub>2</sub> O	2.73	2.19	2.49	2.02	0.94	0.93	2.40	2.05	2.10
P <sub>2</sub> O <sub>5</sub>	0.13	0.11	0.20	0.20	0.14	0.14	0.32	0.30	0.30
L.O.I.	1.99	2.15	1.75	1.88	7.33	7.39	9.89	10.00	10.30
TOTAL	99.72	98.95	100.01	100.26	98.94	99.30	99.37	99.12	99.70
<b>ICP-ES</b>									
Ag	-0.3	-0.3	0.8	1.0	0.5	0.7	0.5	0.7	0.5
Be	1.2	1.1	1.0	-1.0	-1.0	-1.0	4.4	3.9	5.2
Bi	-2	-2	-2	-2	-2	-2	-2	2	
Cd	0.6	-0.3	1.2	-0.3	1.9	0.9	1.7	1.4	0.8
Cu	26	28	60	65	95	101	46	49	47
Mo	3	2	4	2	2	4	15	14	13
Ni	138	132	167	173	312	312	58	56	53
Pb	16	18	15	20	6	11	75	73	66
S	0.008	0.004	0.025	0.021	0.034	0.030	0.051	0.045	0.060
Sr	228	248	254	308	170	191	421	419	400
V	55	53	197	206	277	283	102	100	101
Y	14	9	20	16	24	21	30	21	37
Zn	59	53	53	56	85	80	237	212	246
<b>INAA</b>									
Au	-2	-2	-2	-2	71	-2	5	-2	3
Ag	-5	-5	-5	-5	-5	-5	-5	-5	
As	-0.5	-0.5	-0.5	-0.5	2.1	1.6	42.1	41.5	42
Ba	450	640	830	780	50	520	580	600	540
Br	1.6	-0.5	-0.5	-0.5	-0.5	-0.5	4.3	4.5	4
Co	18	21	27	30	52	49	20	19	19
Cr	215	220	675	720	1260	1370	116	118	116
Cs	3	4	-1	-1	-1	-1	12	12	12
Hf	4	5	14	14	6	7	5	5	5
Rb	86	-15	68	-15	76	-15	96	100	104
Sb	-0.1	-0.1	-0.1	0.5	-0.1	-0.1	4.7	4.5	4.8
Sc	9.8	10.6	20.9	22	30.8	32.8	15.4	15.6	16
Ta	-0.5	-0.5	-0.5	-0.5	-0.5	1.5	1.8	1.5	
Th	7.3	8.1	14.6	13.3	4	4.7	17.3	16.2	17.2
U	5.1	5.5	1.3	3.2	-0.5	3.2	18.3	18.4	18.6
W	-1	-1	-1	-1	-1	-1	7	6	
Zn	119	-50	-50	95	-50	140	265	240	246
La	25.7	29.5	41.8	45.4	17.5	19.5	59.8	58	59
Ce	52	51	85	80	47	40	107	95	93
Nd	23	23	37	35	23	15	52	43	43
Sm	3.7	3.9	5.2	5.3	4.4	4.3	8.5	8.2	8
Eu	1	0.8	1.6	1.2	1.2	1.2	2.1	2	2
Tb	-0.5	-0.5	-0.5	-0.5	0.8	-0.5	1.1	-0.5	
Yb	1.5	1.6	1.9	1.8	2.5	2.5	3.6	3.7	3.7
Lu	0.23	0.25	0.28	0.26	0.38	0.37	0.54	0.57	0.7

**Table A1** *Reproducibility between two batches and accuracy of stream sediment analyses. Analytical results of internal standards GEUS2, GEUS3, GEUS5 and international reference material STSD-2 accompanying each of the two samples batches from the Qaanaaq region submitted for analysis. STSD-2\_rec. are recommended values for STSD-2. XRF: X-ray fluorescence spectrometry. ICP-ES: Inductively coupled plasma emission spectrometry. INAA: Instrumental neutron activation analysis. Negative values are below detection limit. Oxides, loss on ignition (L.O.I.) and S in %, Au in ppb, remaining elements in ppm.*



# Stream sediment samples

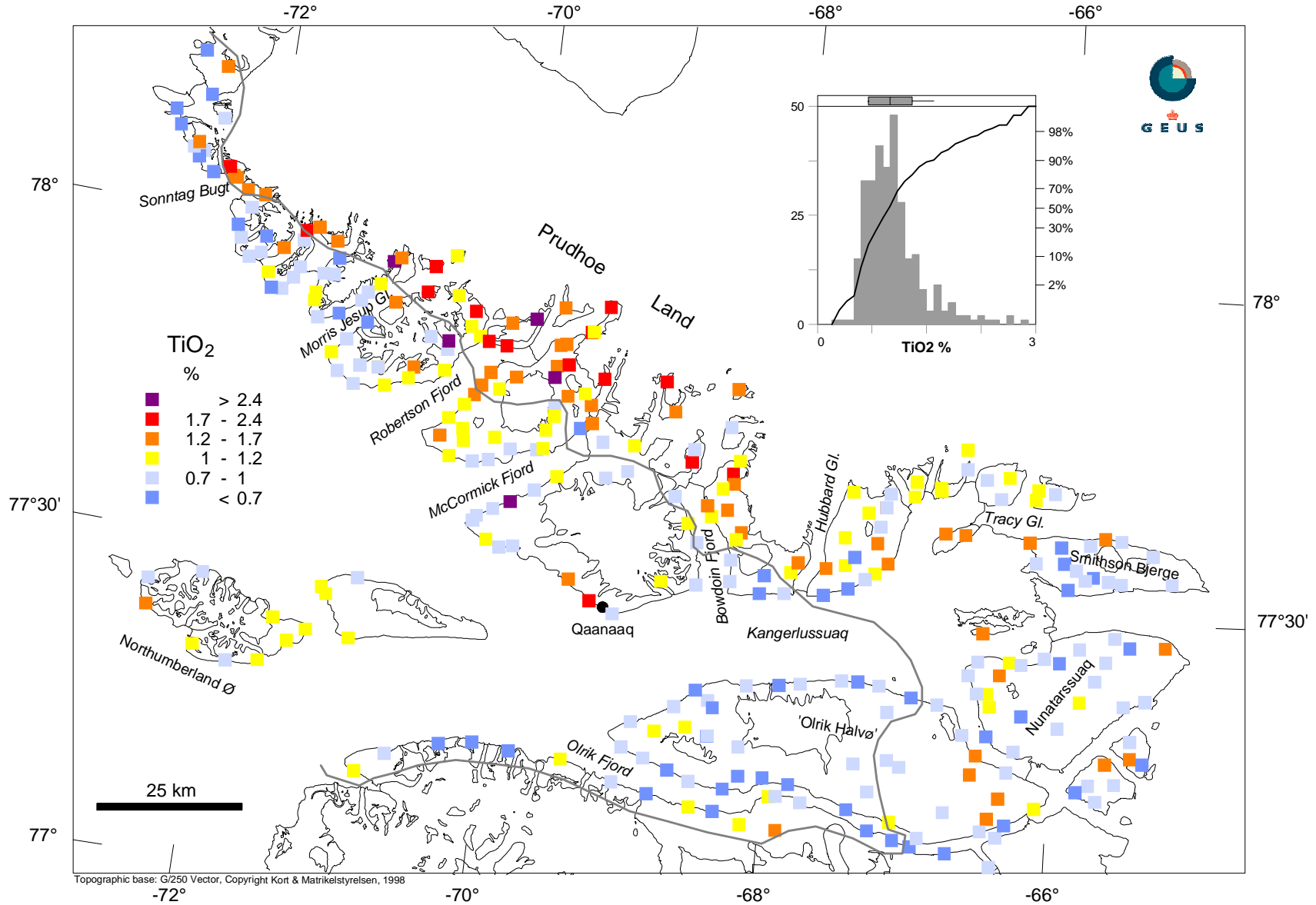
Grain size fraction < 0.1mm analysed by XRF



Map 2

# Stream sediment samples

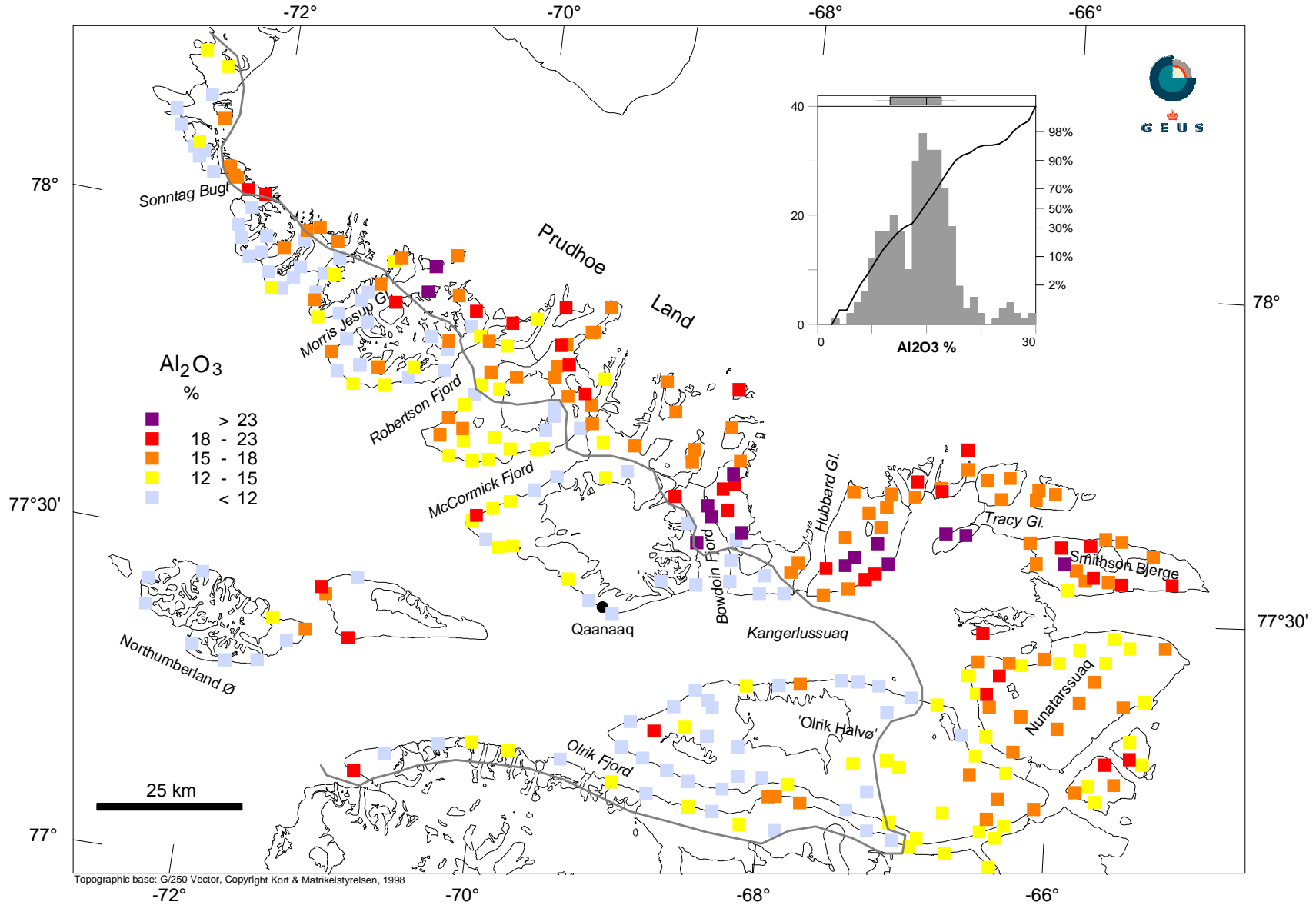
Grain size fraction < 0.1mm analysed by XRF



Map 3

# Stream sediment samples

Grain size fraction < 0.1mm analysed by XRF

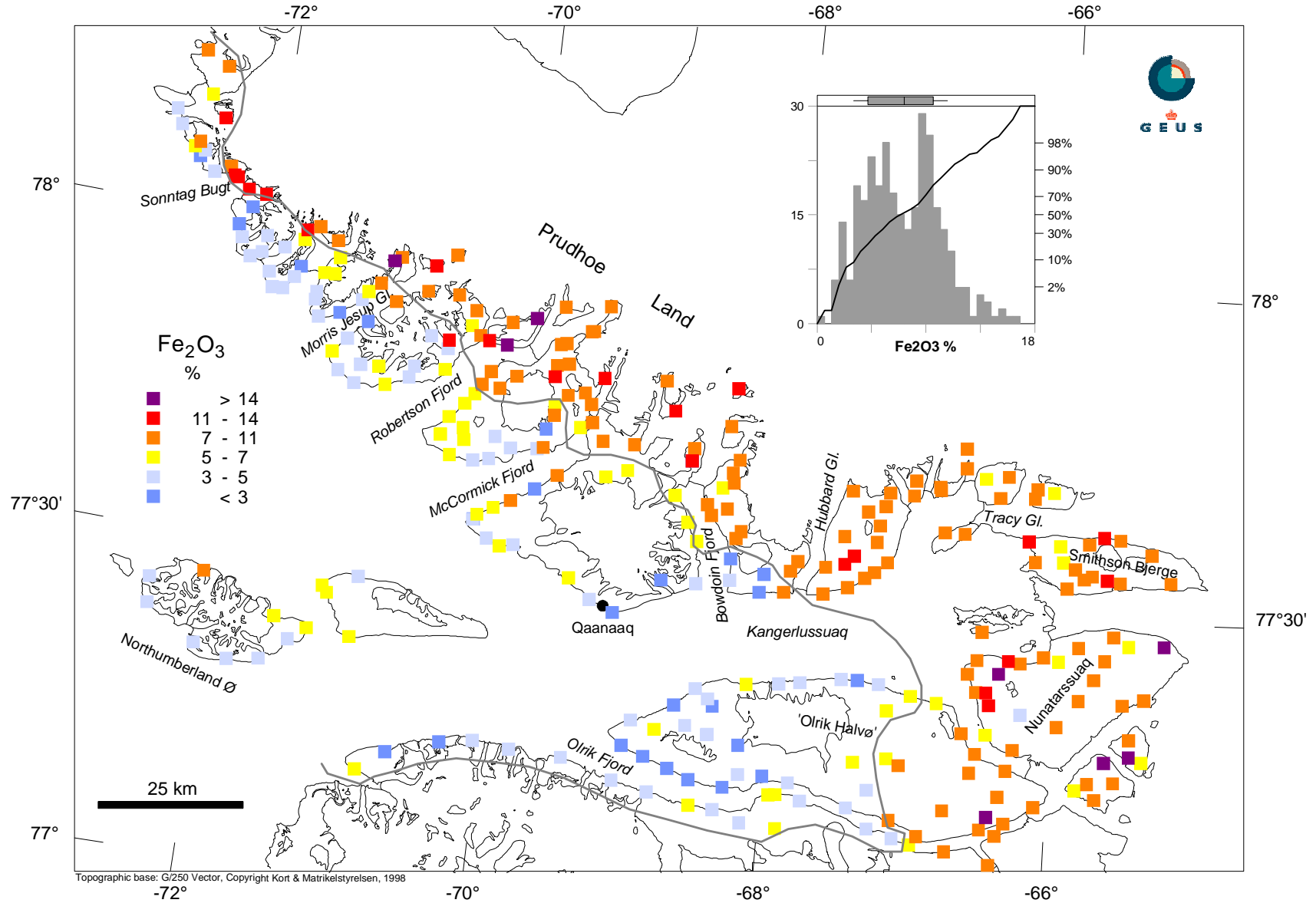


Map 4

Topographic base: G/250 Vector, Copyright Kort & Matrikelstyrelsen, 1998

# Stream sediment samples

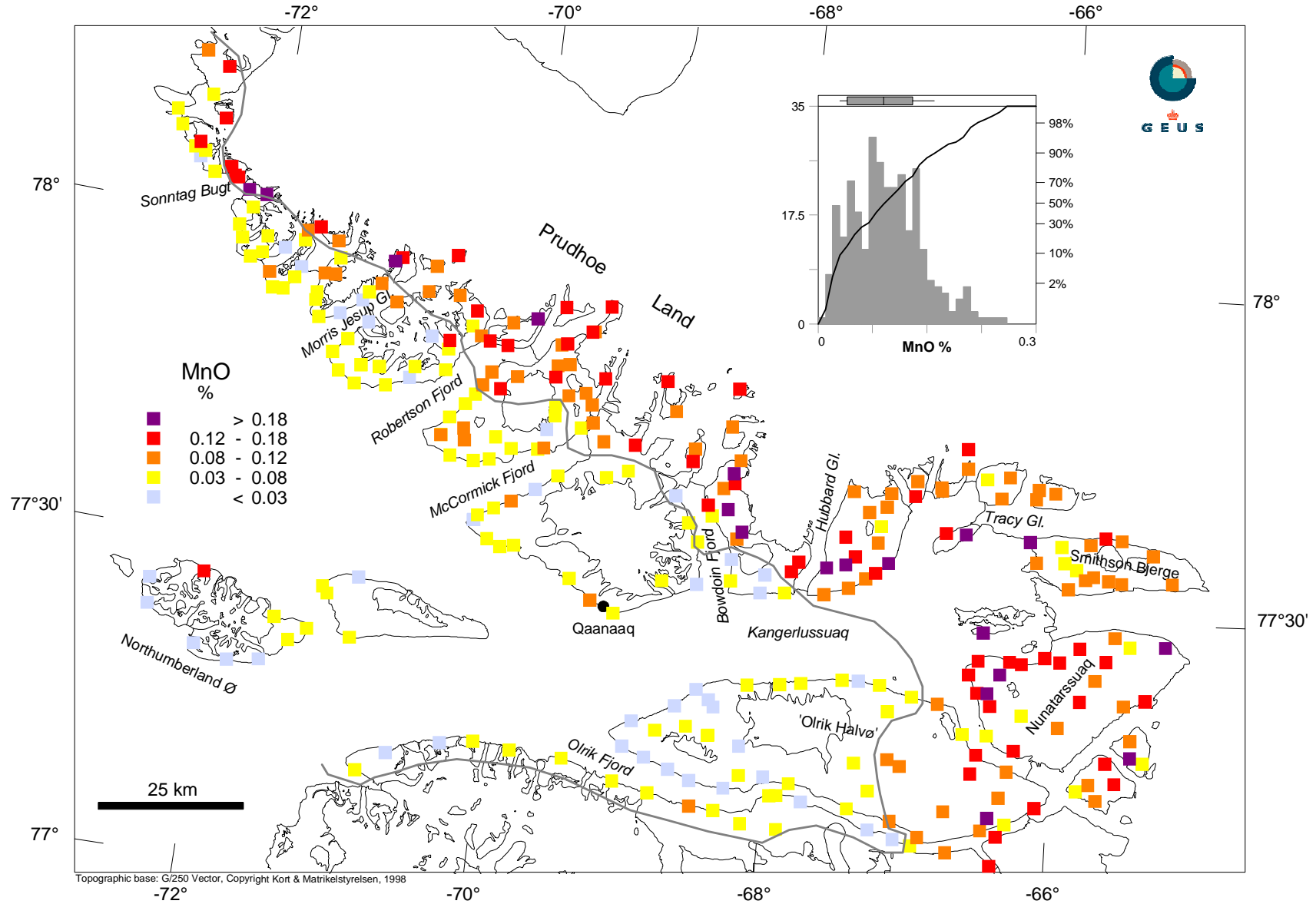
Grain size fraction < 0.1mm analysed by XRF



Map 5

# Stream sediment samples

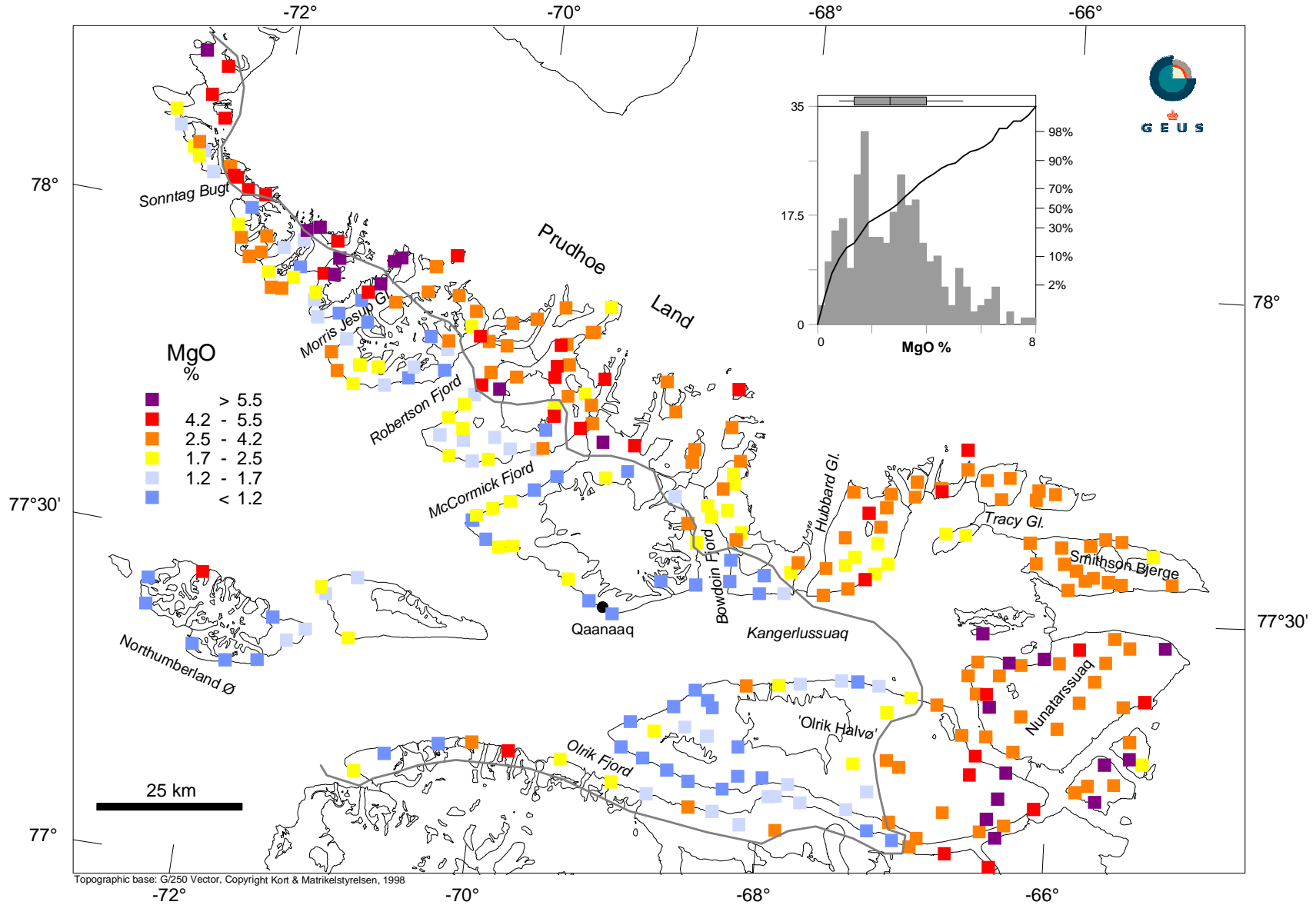
Grain size fraction < 0.1mm analysed by XRF



Map 6

# Stream sediment samples

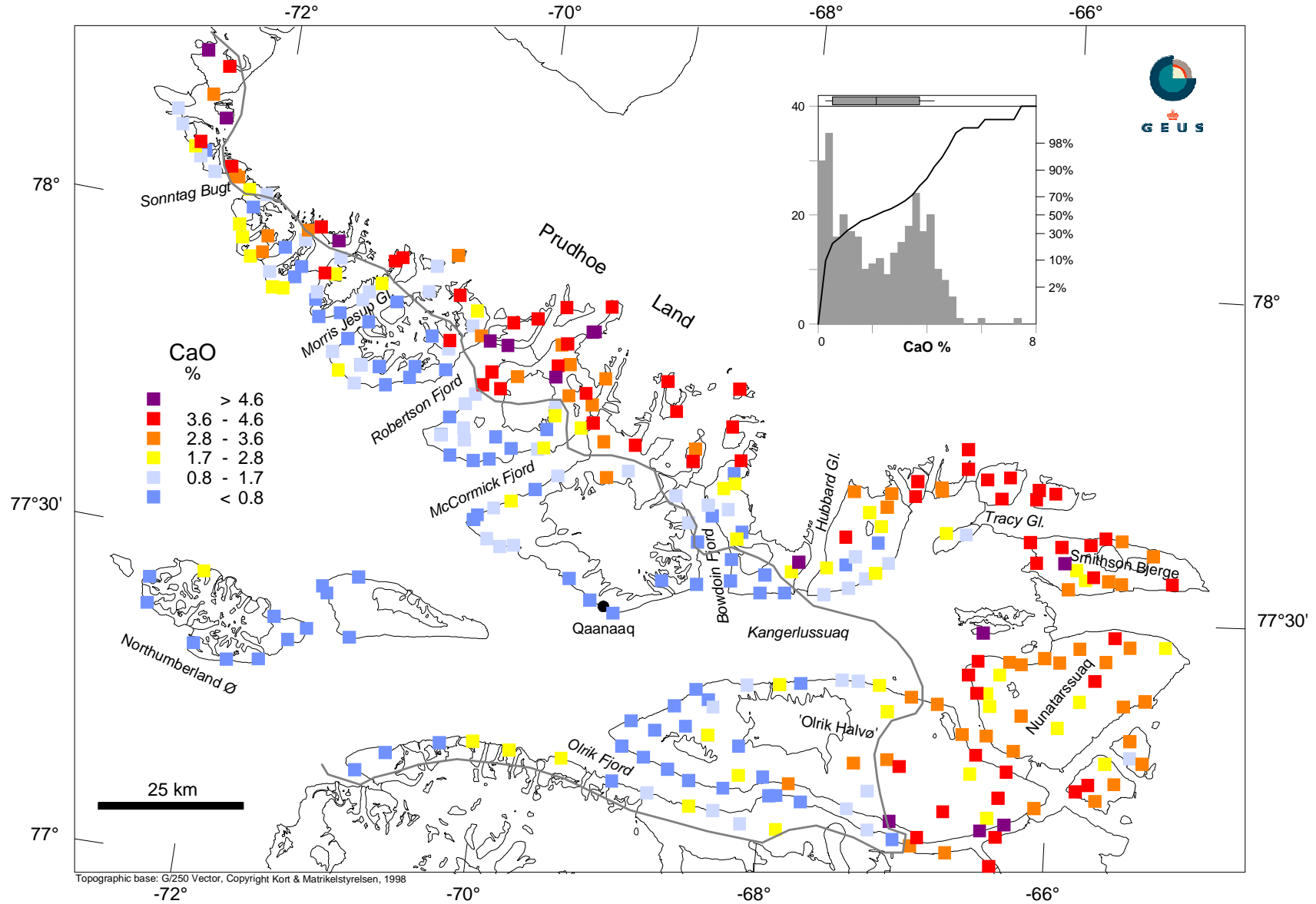
Grain size fraction < 0.1mm analysed by XRF



Map 7

# Stream sediment samples

Grain size fraction < 0.1mm analysed by XRF

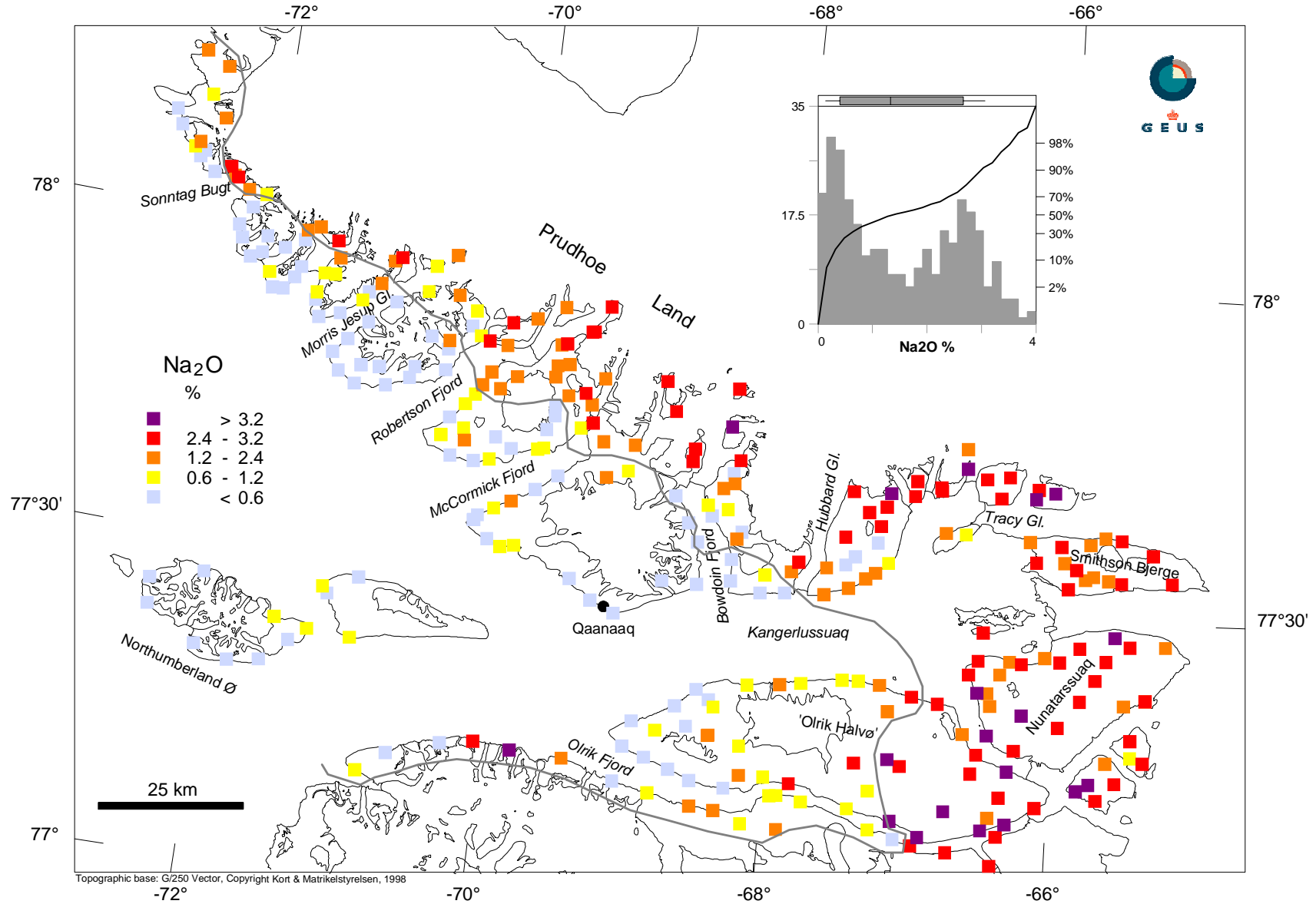


Map 8

Topographic base: G/250 Vector, Copyright Kort & Matrikelstyrelsen, 1998

# Stream sediment samples

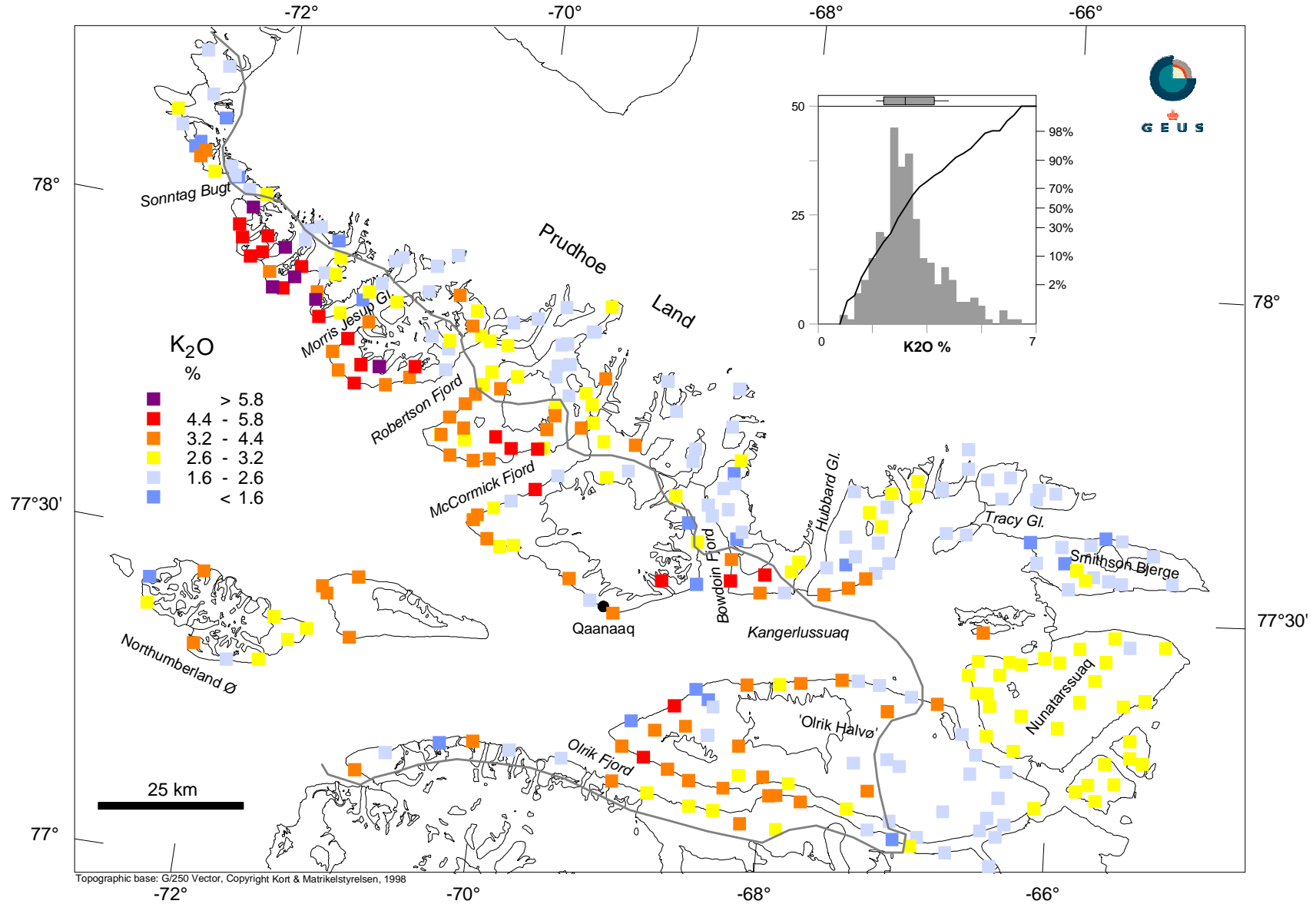
Grain size fraction < 0.1mm analysed by XRF



Map 9

# Stream sediment samples

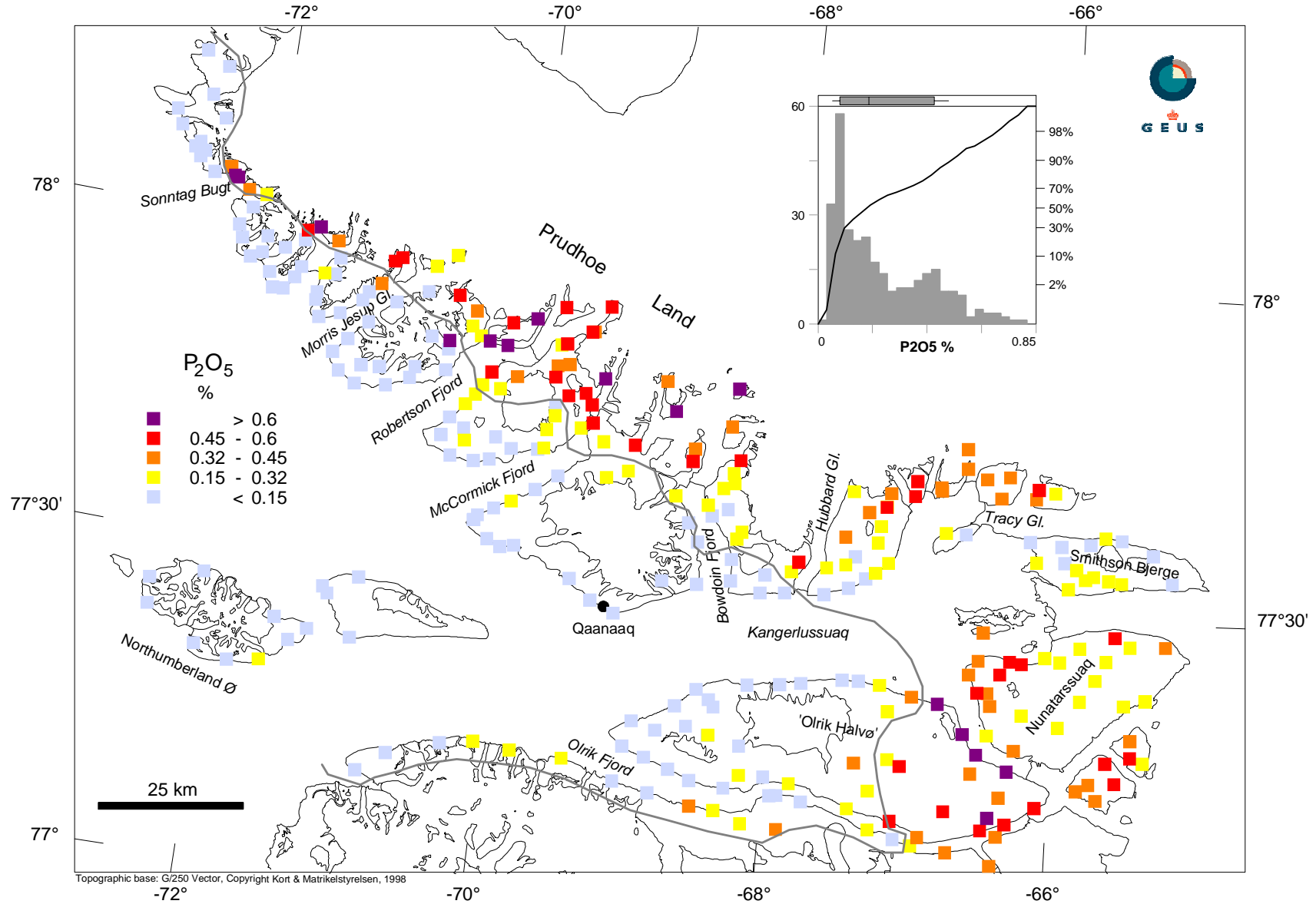
Grain size fraction < 0.1mm analysed by XRF



Topographic base: G/250 Vector, Copyright Kort & Matrikelstyrelsen, 1998

# Stream sediment samples

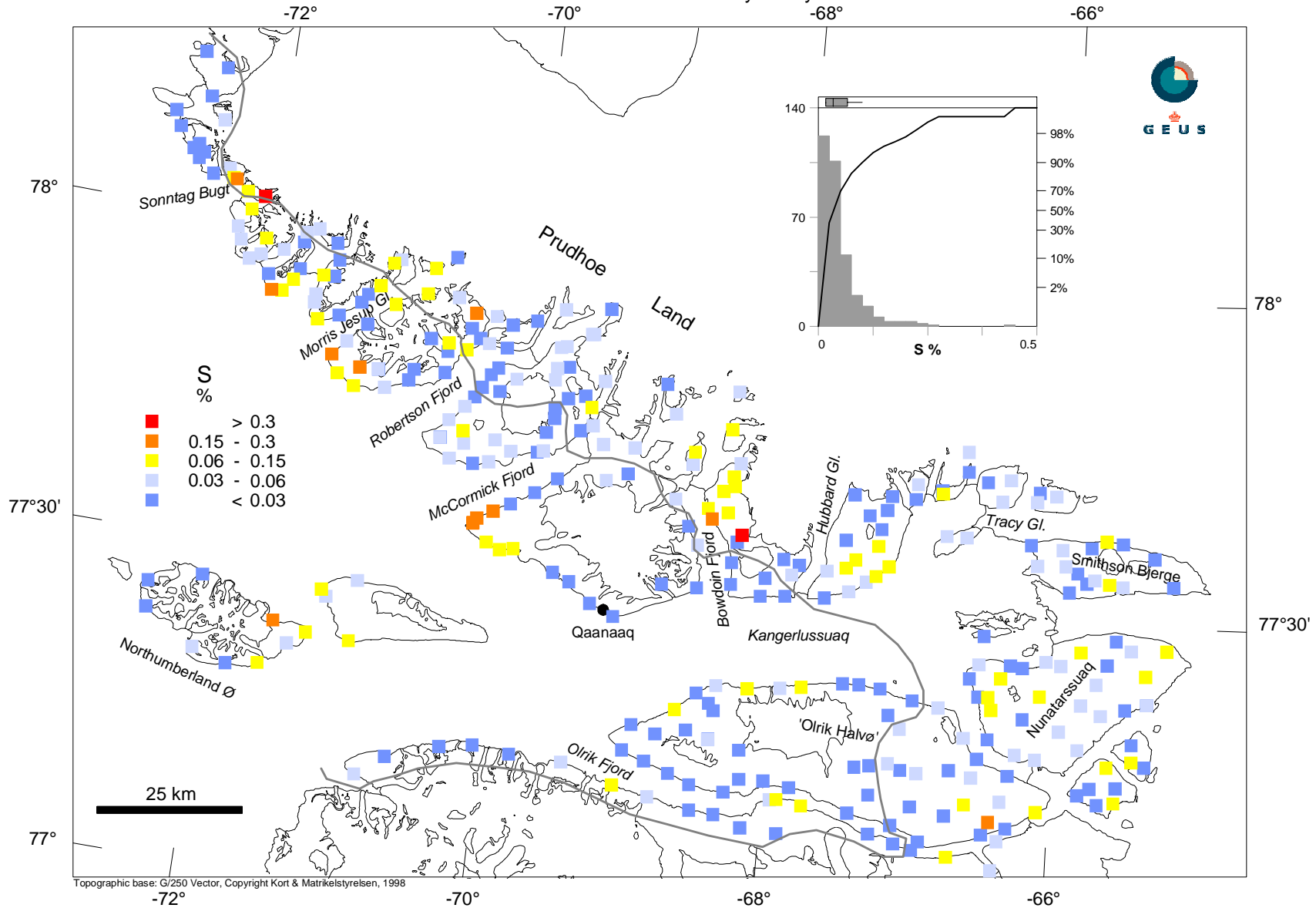
Grain size fraction < 0.1mm analysed by XRF



Map 11

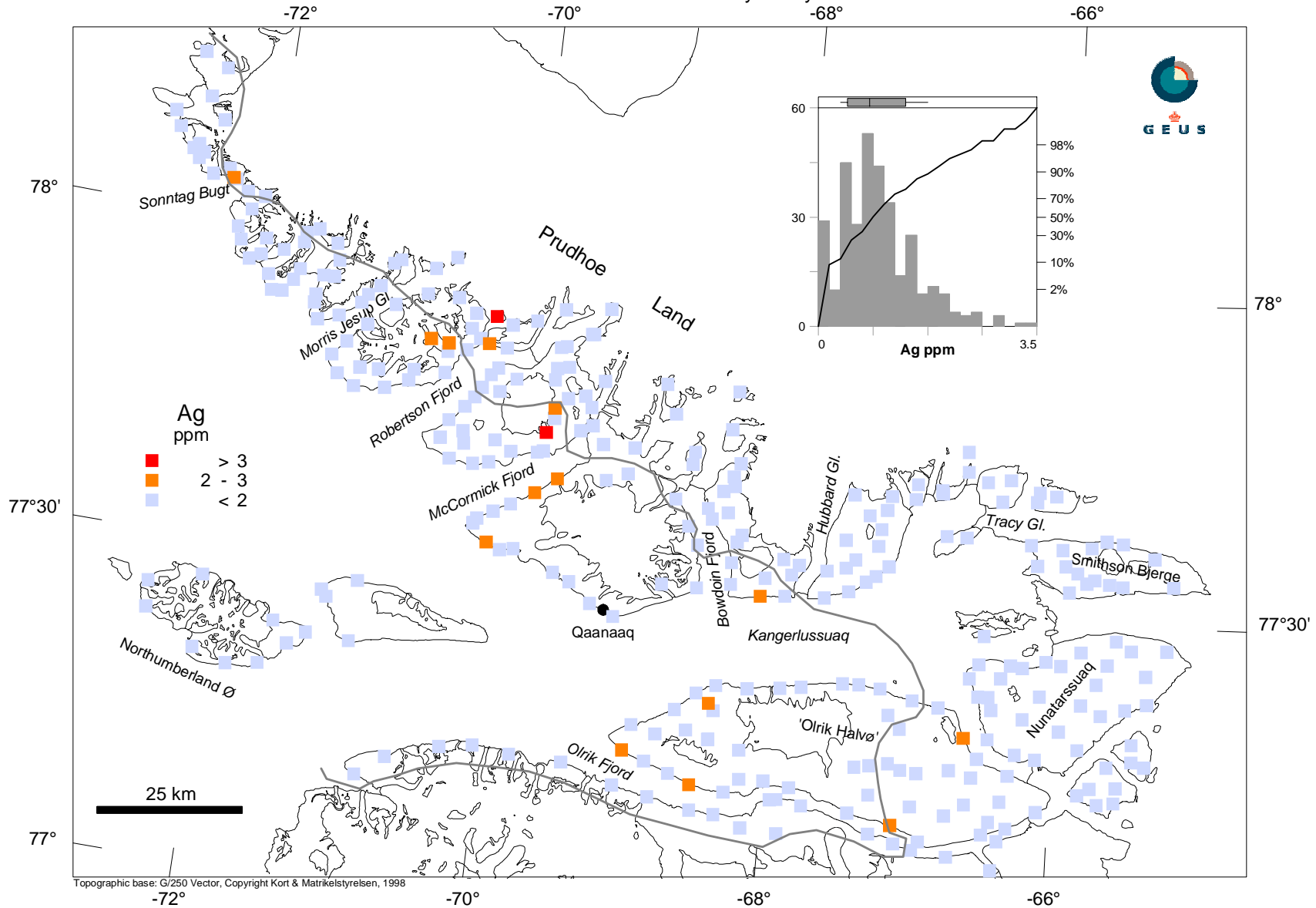
# Stream sediment samples

Grain size fraction < 0.1mm analysed by ICP - ES



# Stream sediment samples

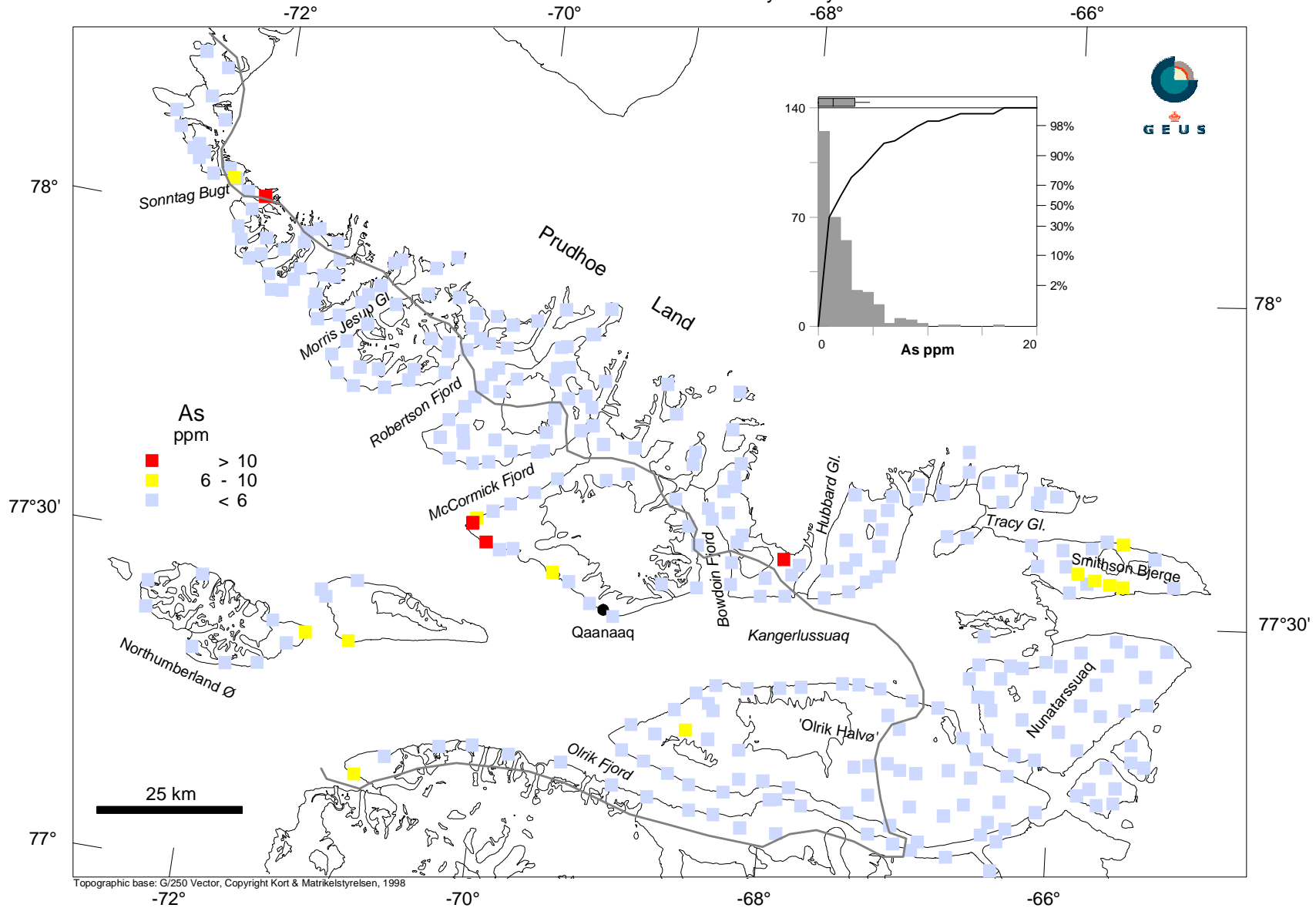
Grain size fraction < 0.1mm analysed by ICP - ES



Map 13

# Stream sediment samples

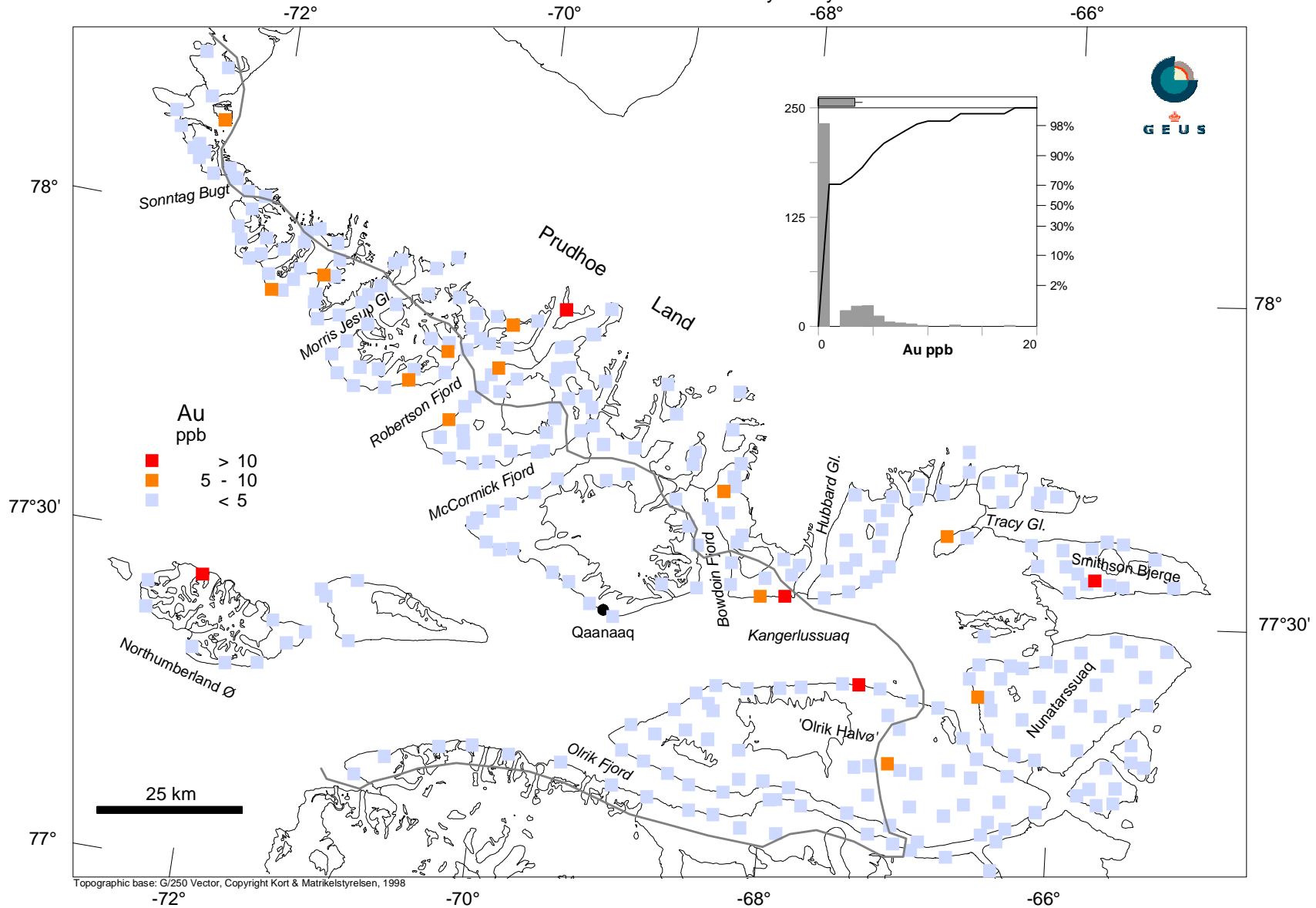
Grain size fraction < 0.1mm analysed by INAA



Map 14

# Stream sediment samples

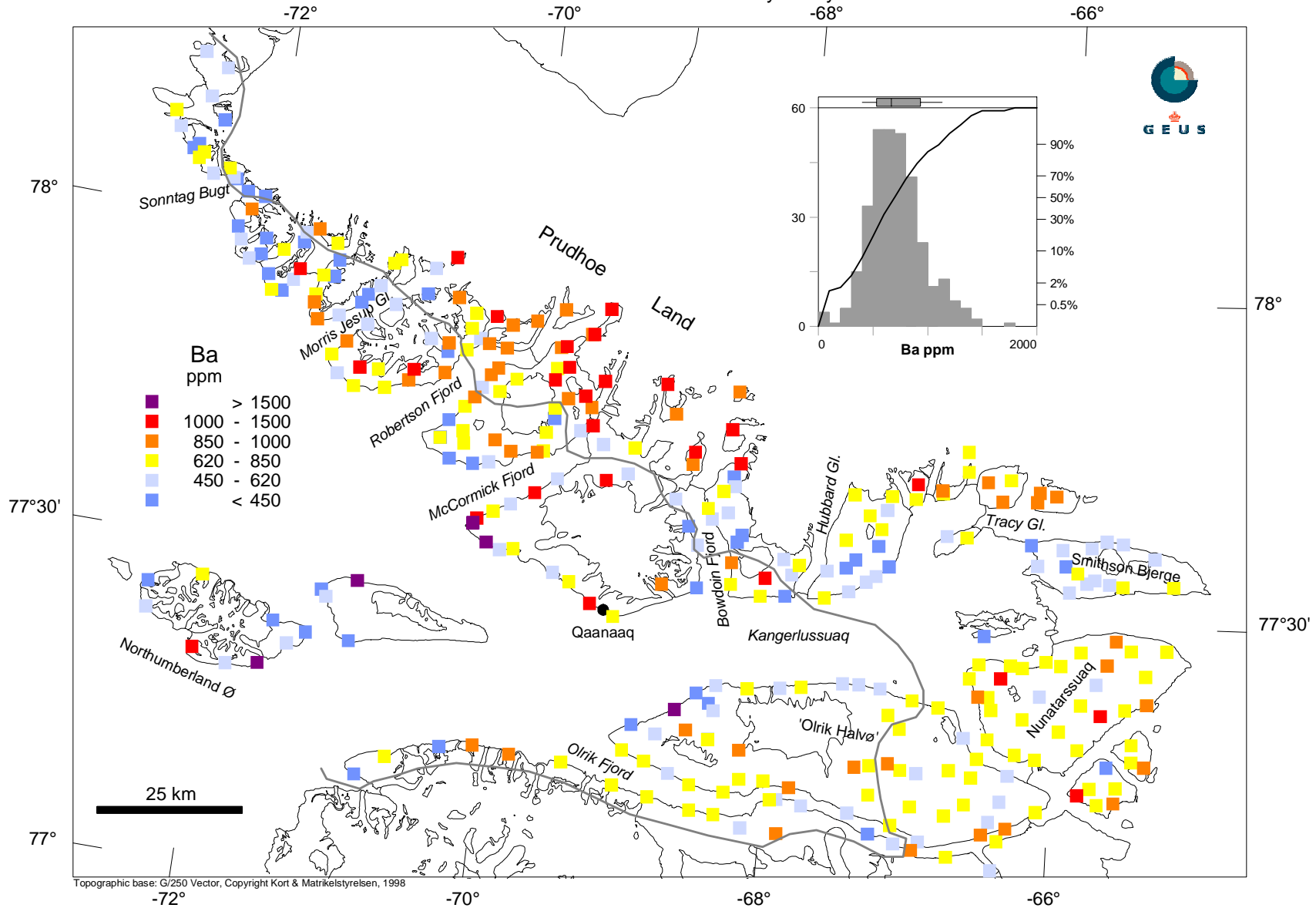
Grain size fraction < 0.1mm analysed by INAA



Map 15

# Stream sediment samples

Grain size fraction < 0.1mm analysed by INAA

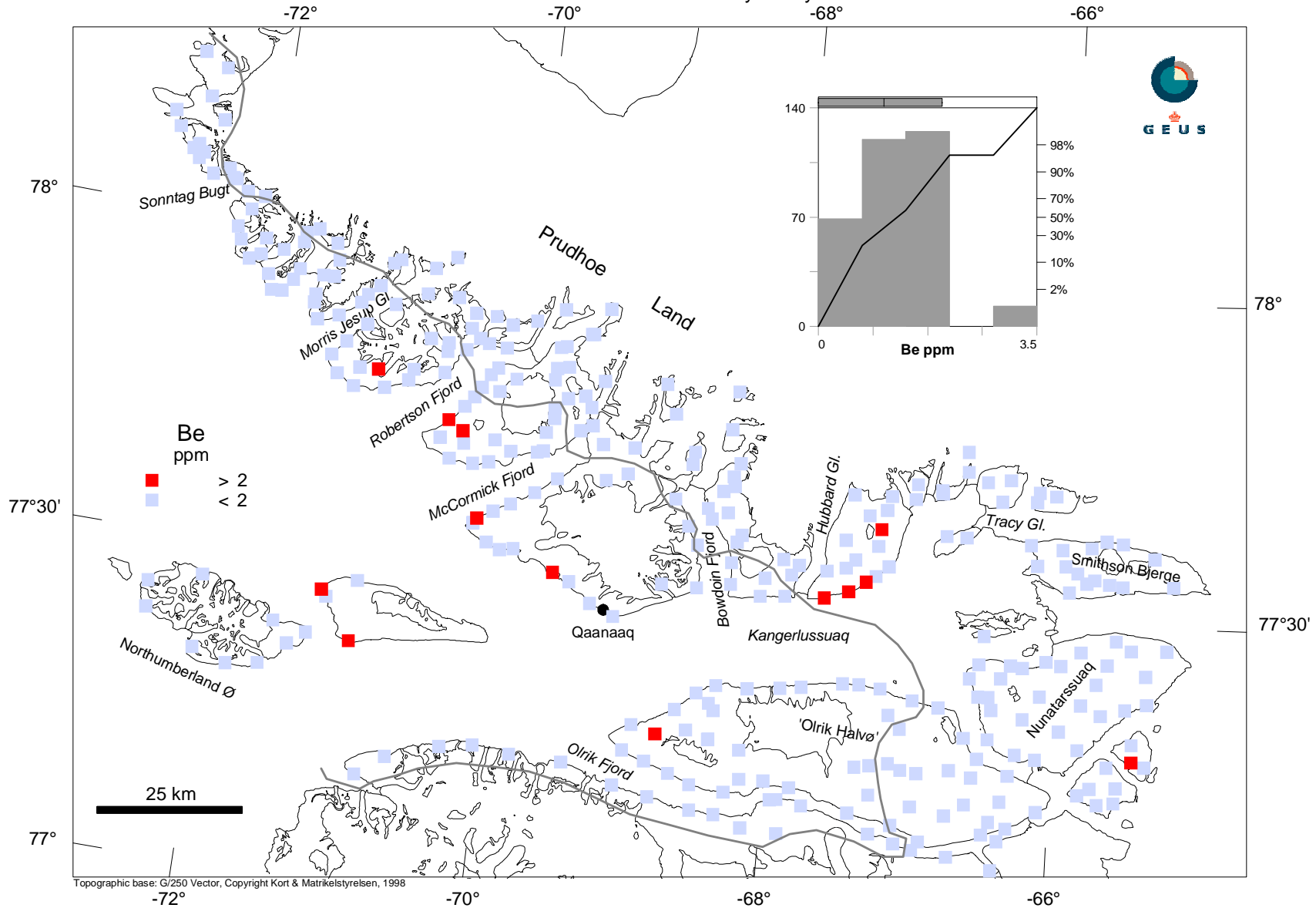


Map 16

Topographic base: G/250 Vector, Copyright Kort & Matrikelstyrelsen, 1998

# Stream sediment samples

Grain size fraction < 0.1mm analysed by ICP - ES

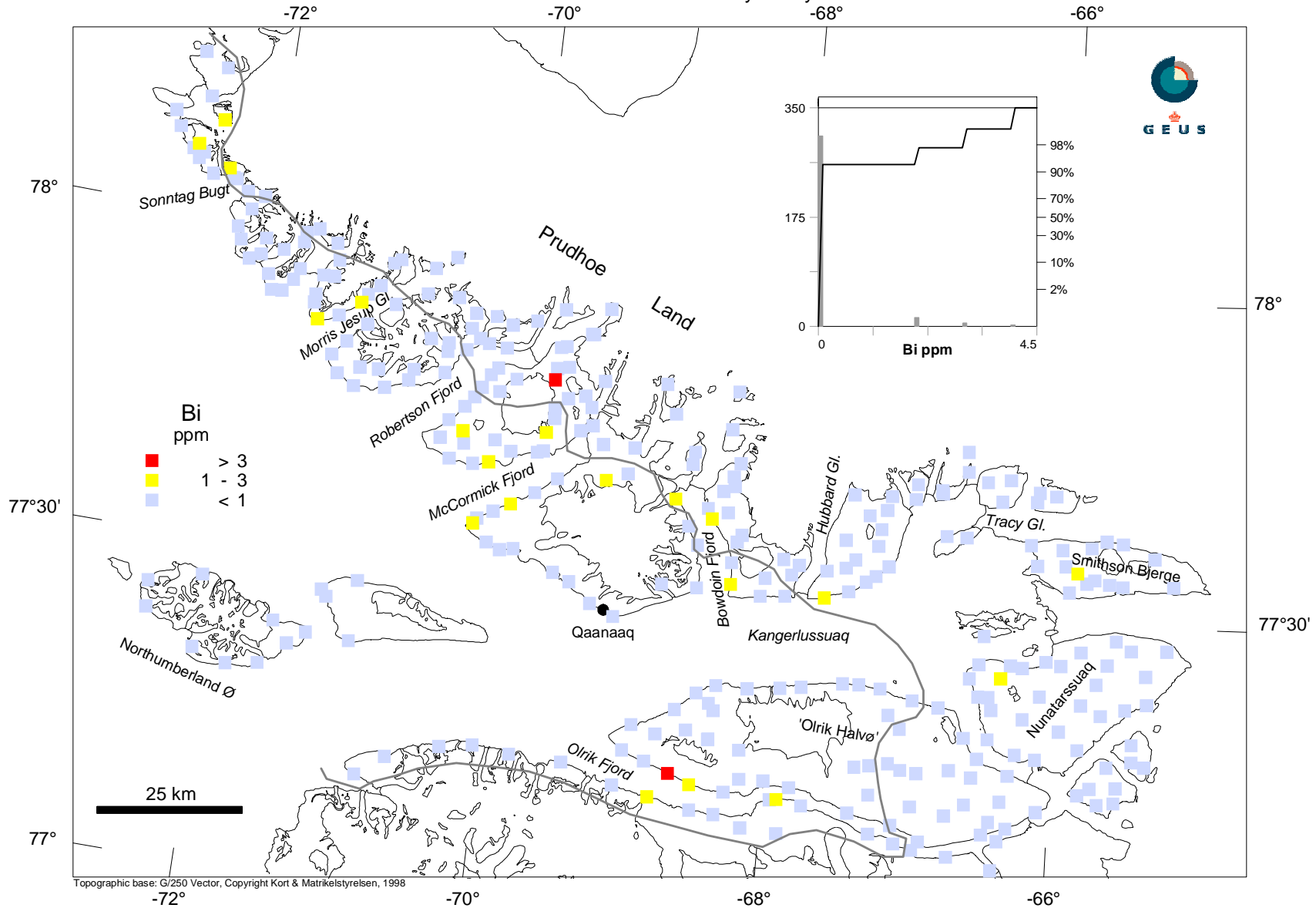


Map 17

Topographic base: G/250 Vector, Copyright Kort & Matrikelstyrelsen, 1998

# Stream sediment samples

Grain size fraction < 0.1mm analysed by ICP - ES

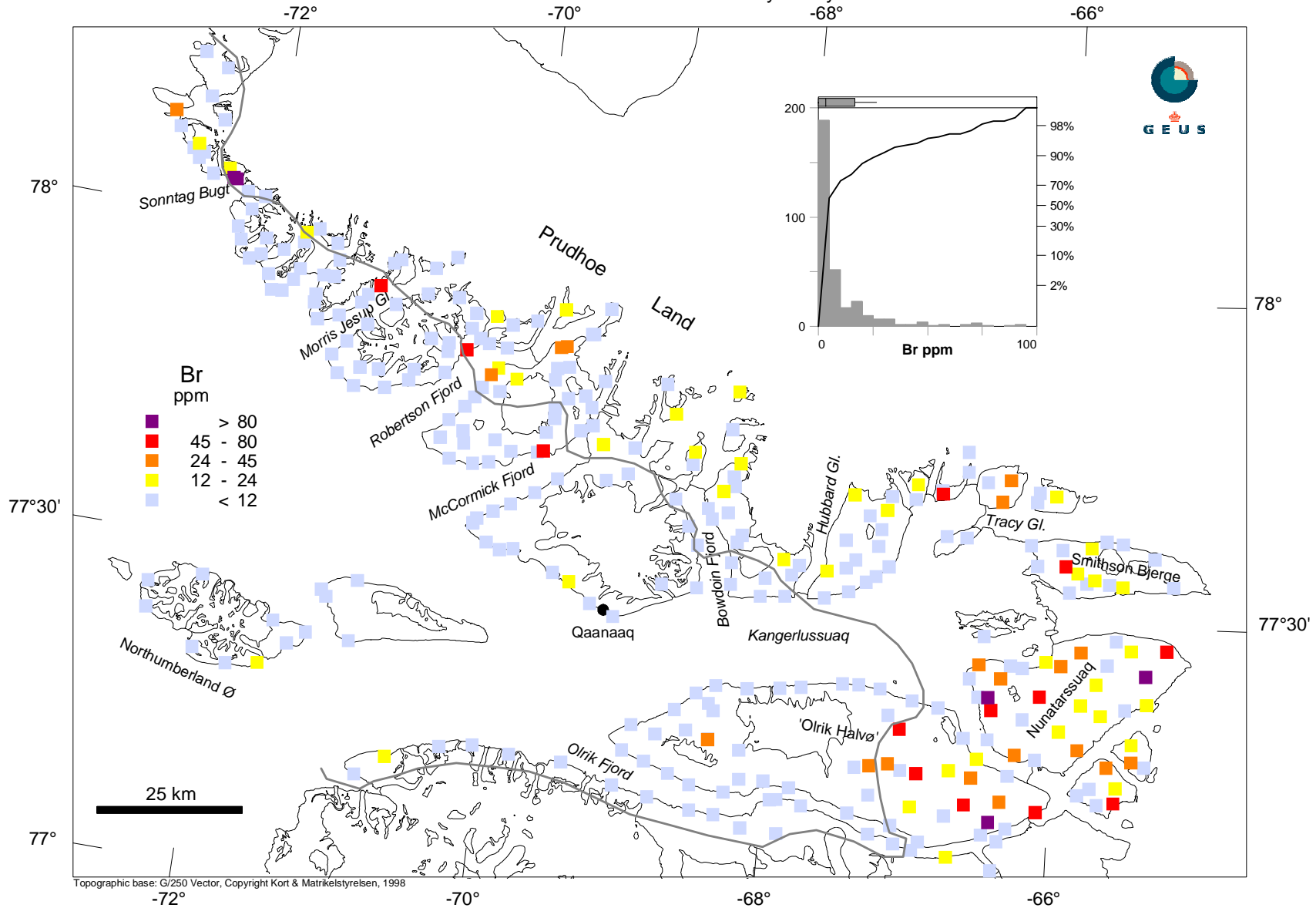


Map 18

Topographic base: G/250 Vector, Copyright Kort & Matrikelstyrelsen, 1998

# Stream sediment samples

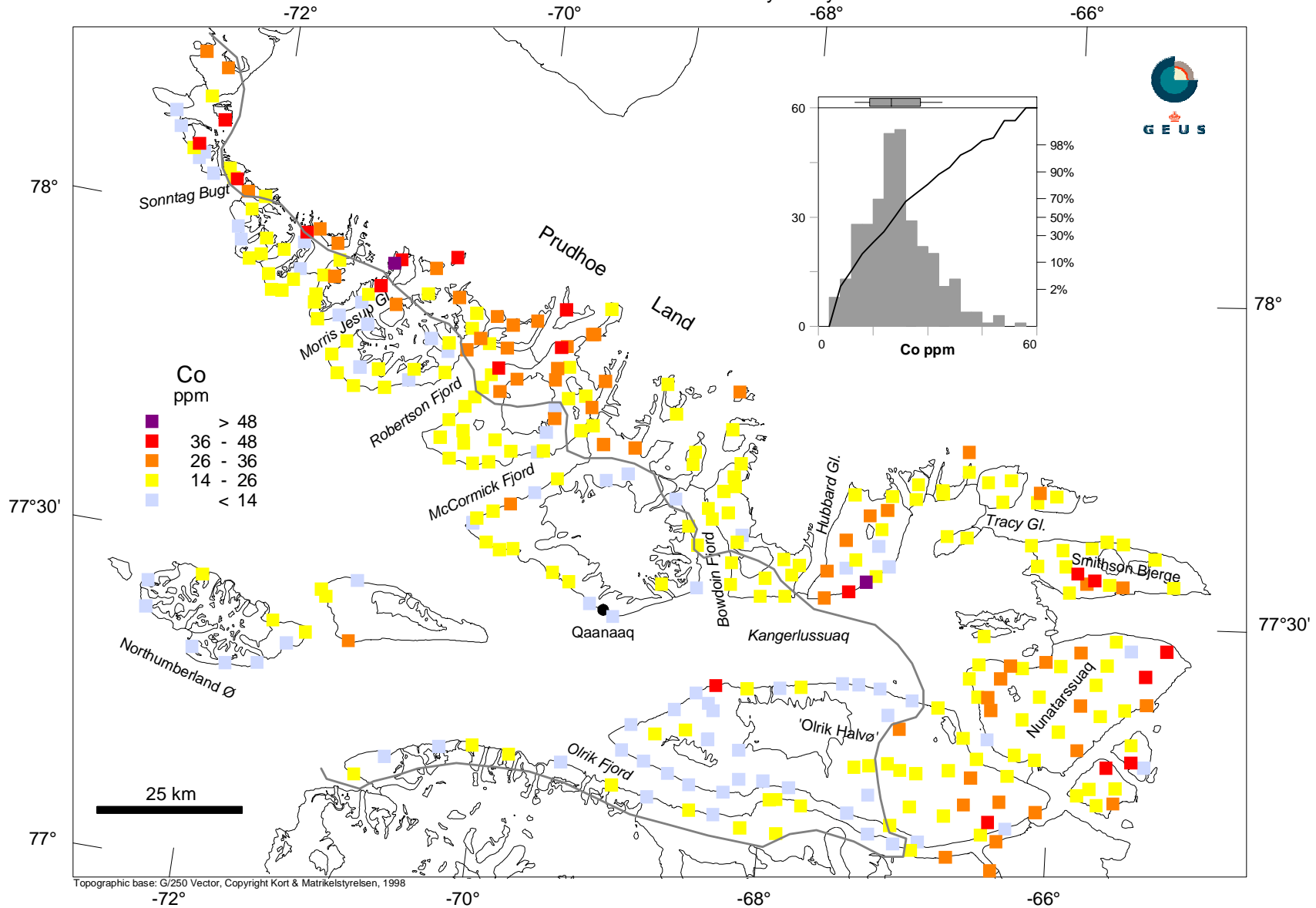
Grain size fraction < 0.1mm analysed by INAA



Map 19

# Stream sediment samples

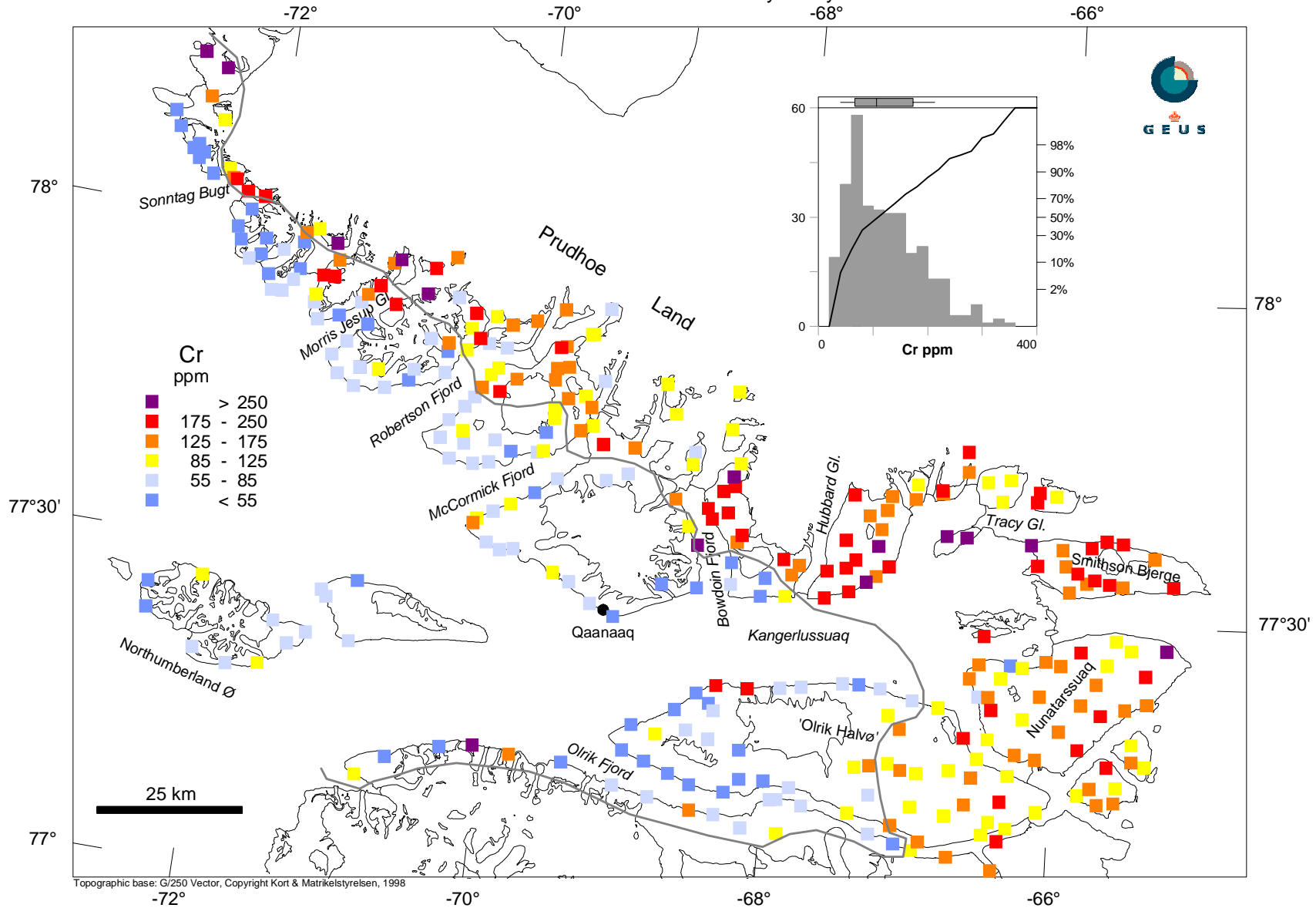
Grain size fraction < 0.1mm analysed by INAA



Map 20

# Stream sediment samples

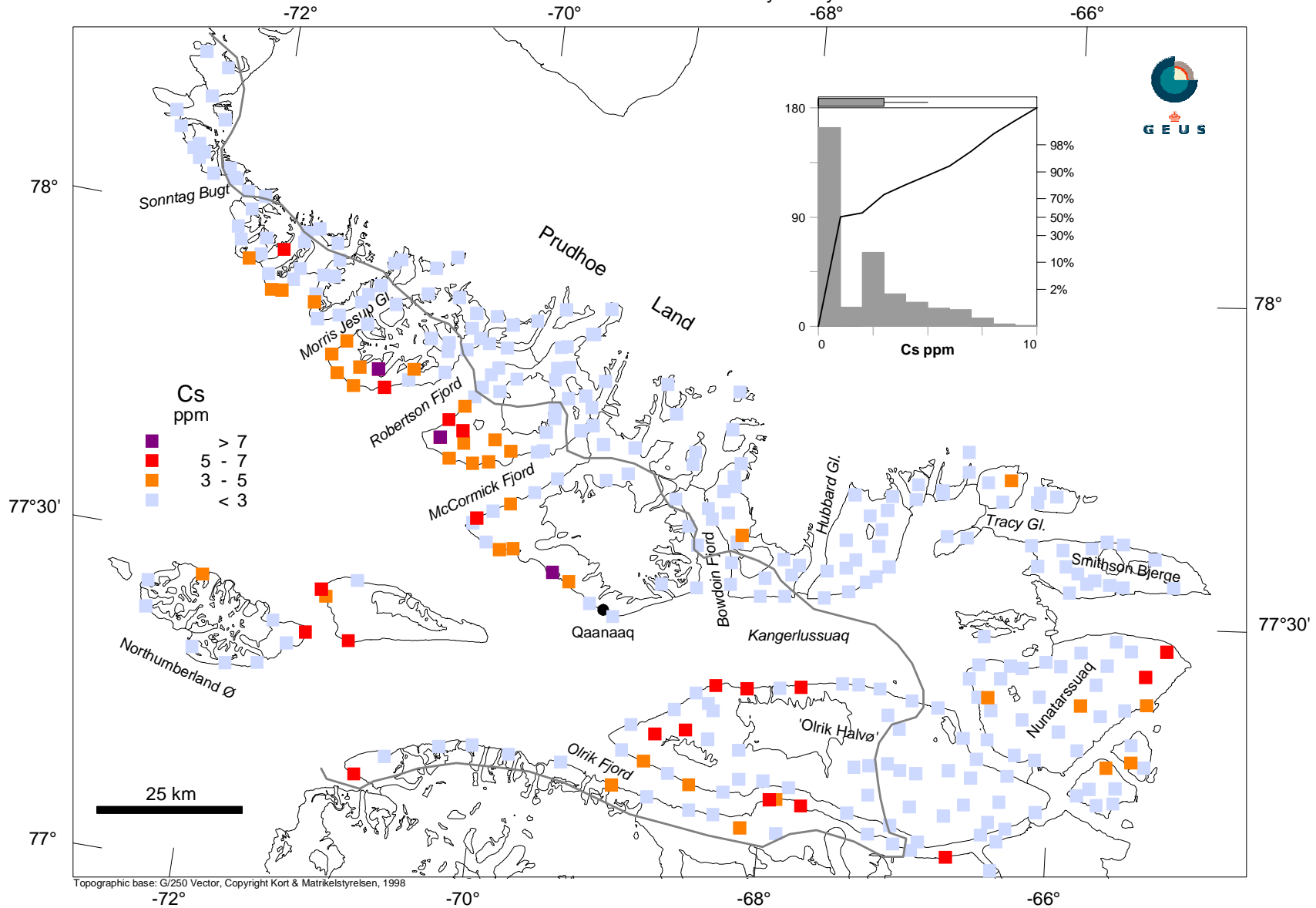
Grain size fraction < 0.1mm analysed by INAA



Topographic base: G/250 Vector, Copyright Kort & Matrikelstyrelsen, 1998

# Stream sediment samples

Grain size fraction < 0.1mm analysed by INAA

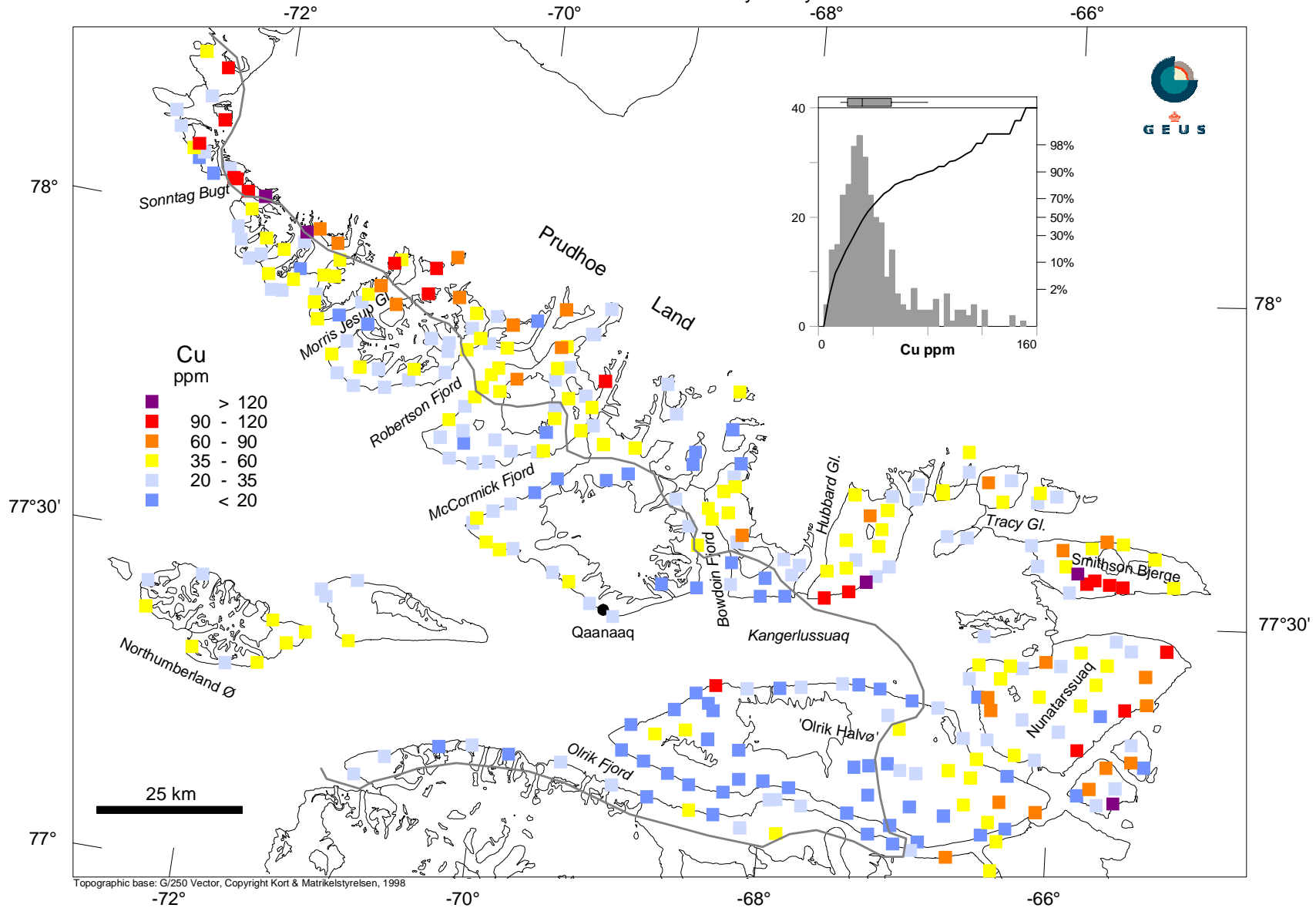


Map 22

Topographic base: G/250 Vector, Copyright Kort & Matrikelstyrelsen, 1998

# Stream sediment samples

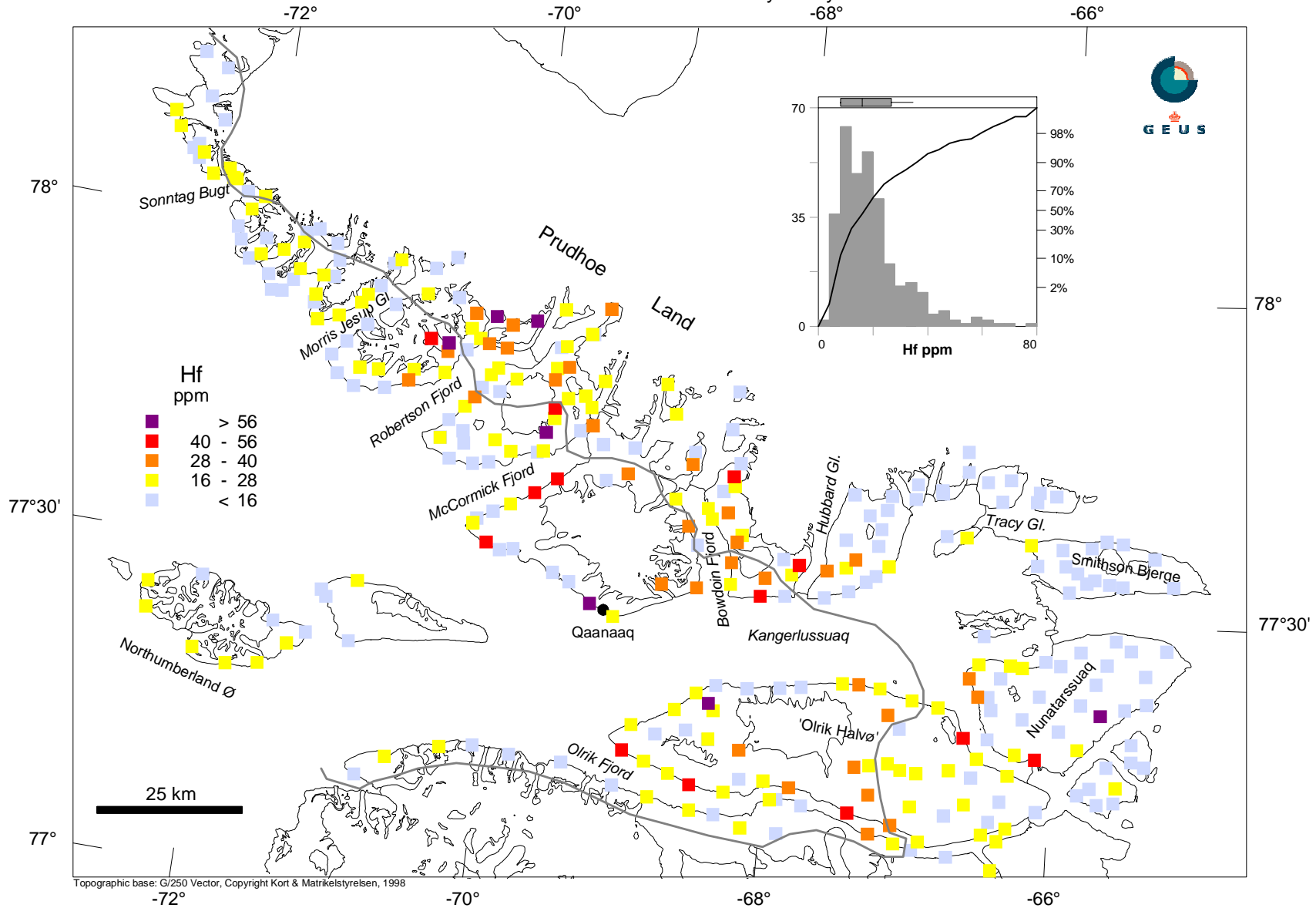
Grain size fraction < 0.1mm analysed by ICP - ES



Topographic base: G/250 Vector, Copyright Kort & Matrikelstyrelsen, 1998

# Stream sediment samples

Grain size fraction < 0.1mm analysed by INAA

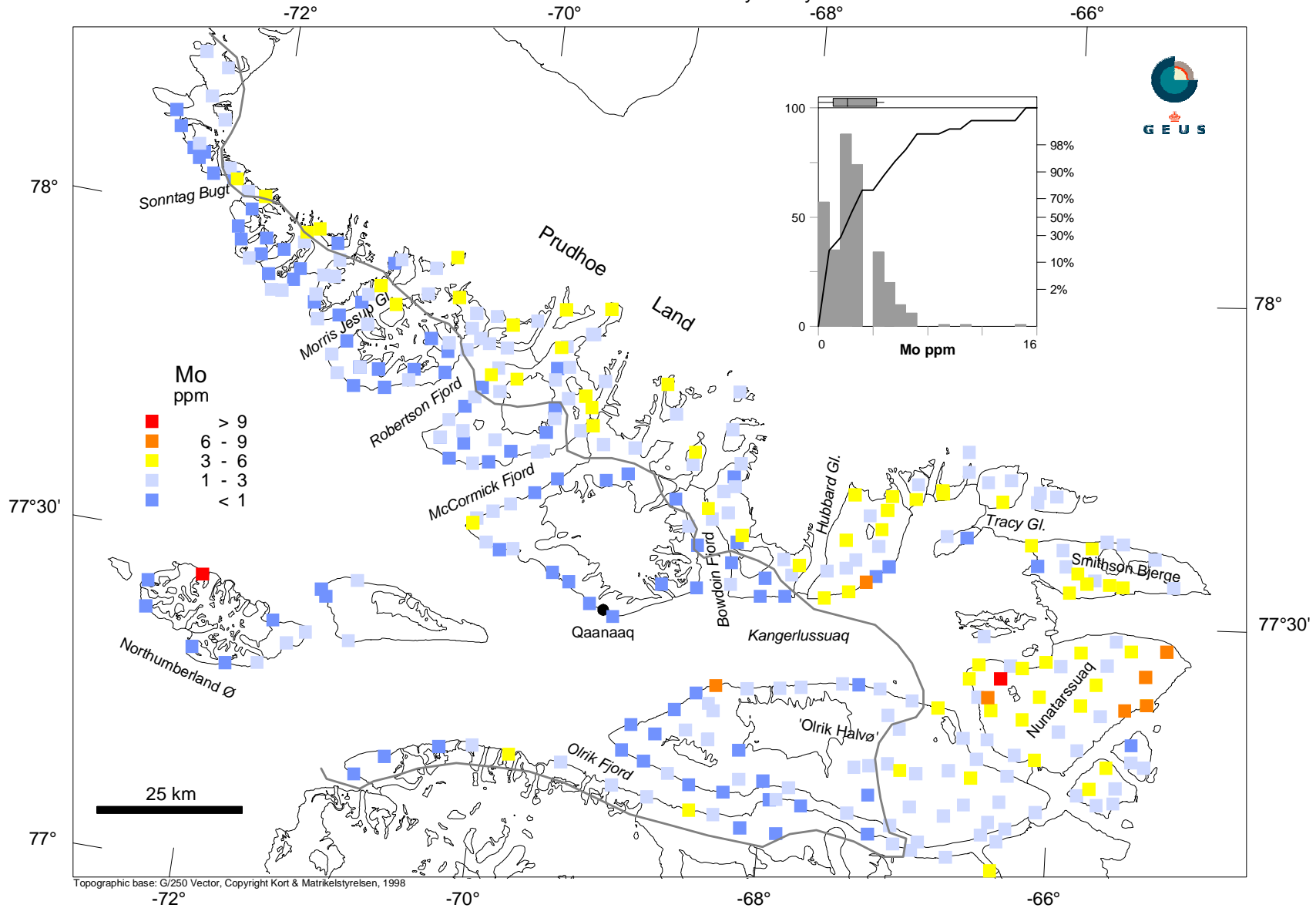


Map 24

Topographic base: G/250 Vector, Copyright Kort & Matrikelstyrelsen, 1998

# Stream sediment samples

Grain size fraction < 0.1mm analysed by ICP - ES

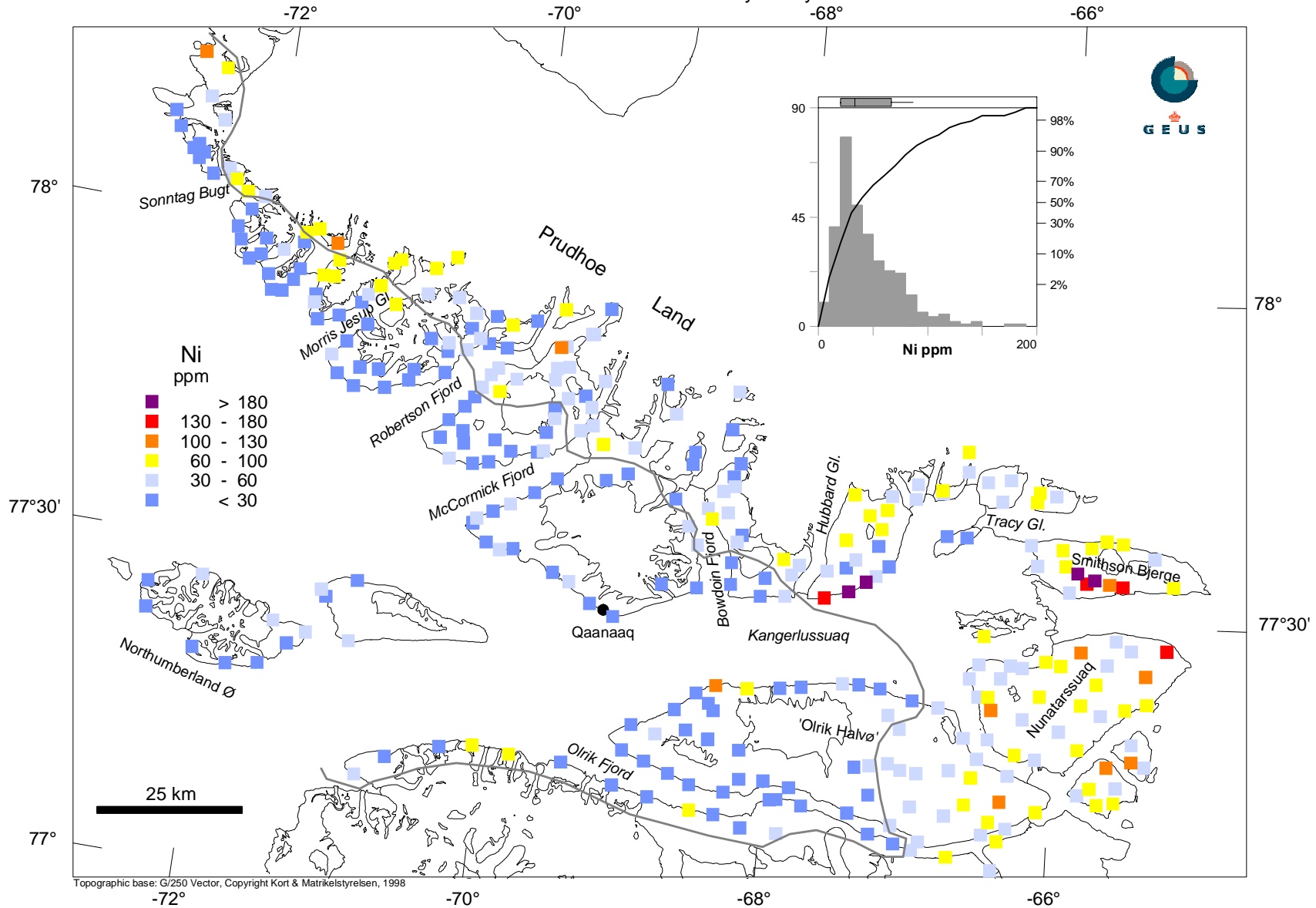


Map 25

Topographic base: G/250 Vector, Copyright Kort & Matrikelstyrelsen, 1998

# Stream sediment samples

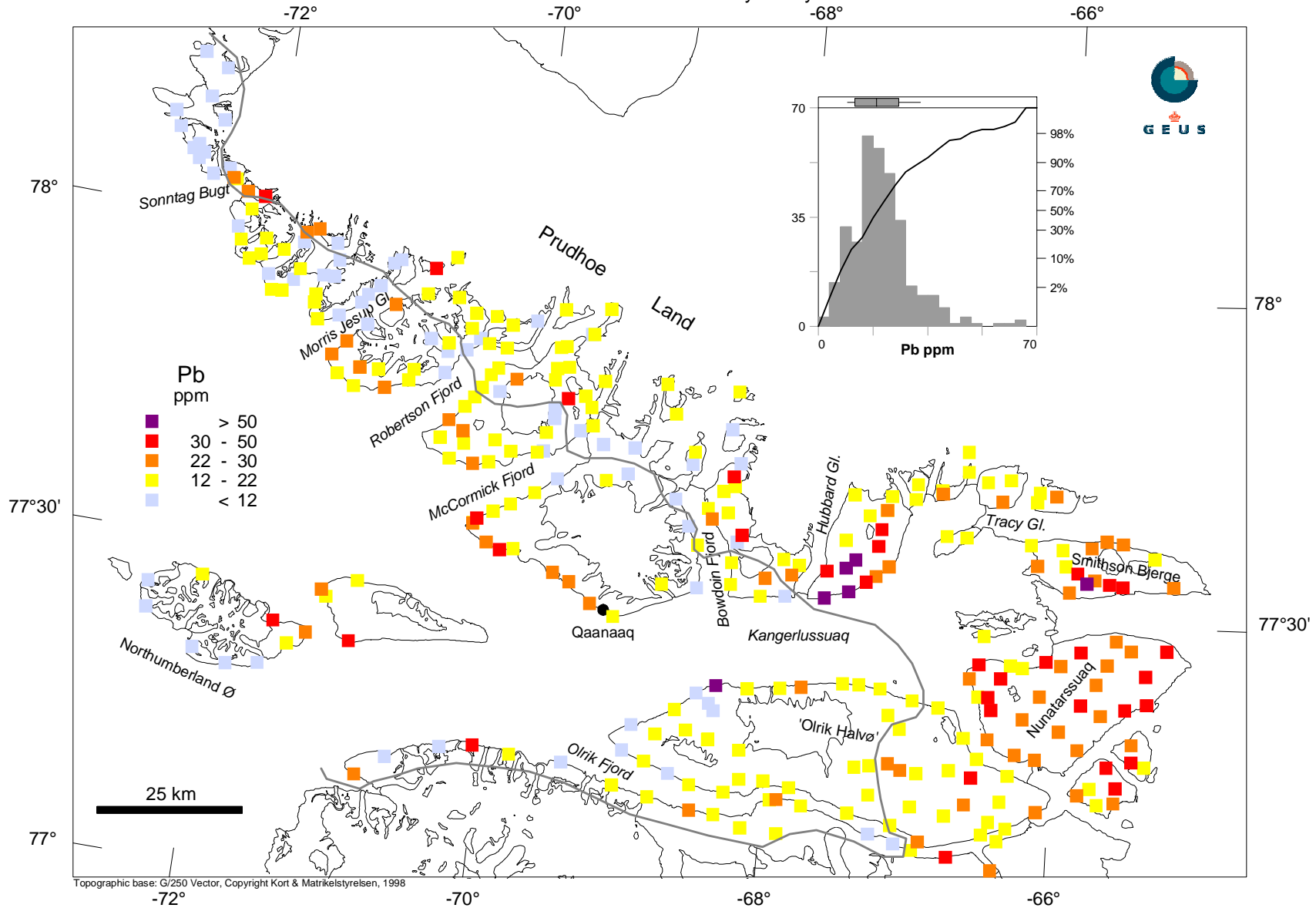
Grain size fraction < 0.1mm analysed by ICP - ES



Topographic base: G/250 Vector, Copyright Kort & Matrikelstyrelsen, 1998

# Stream sediment samples

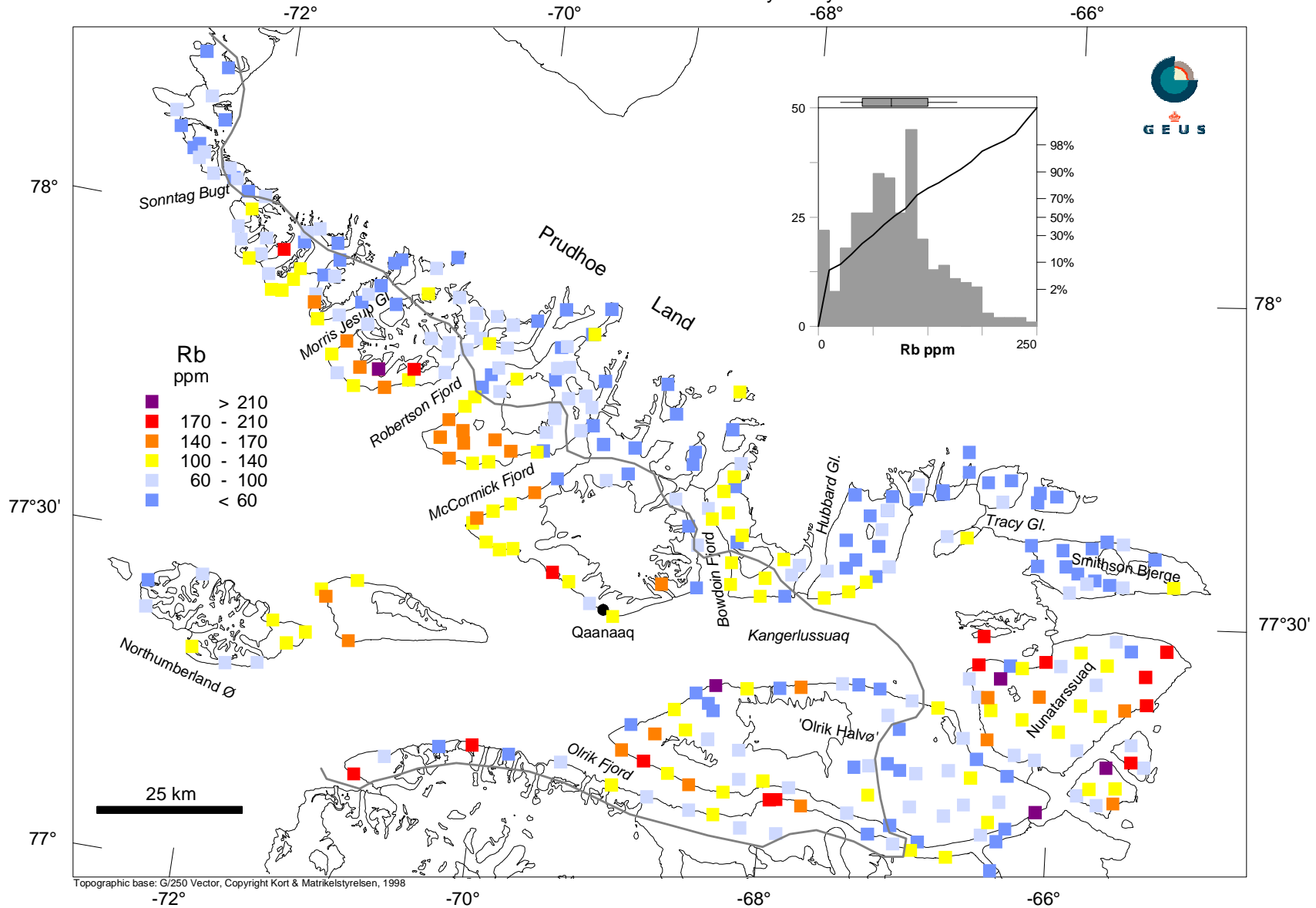
Grain size fraction < 0.1mm analysed by ICP - ES



Map 27

# Stream sediment samples

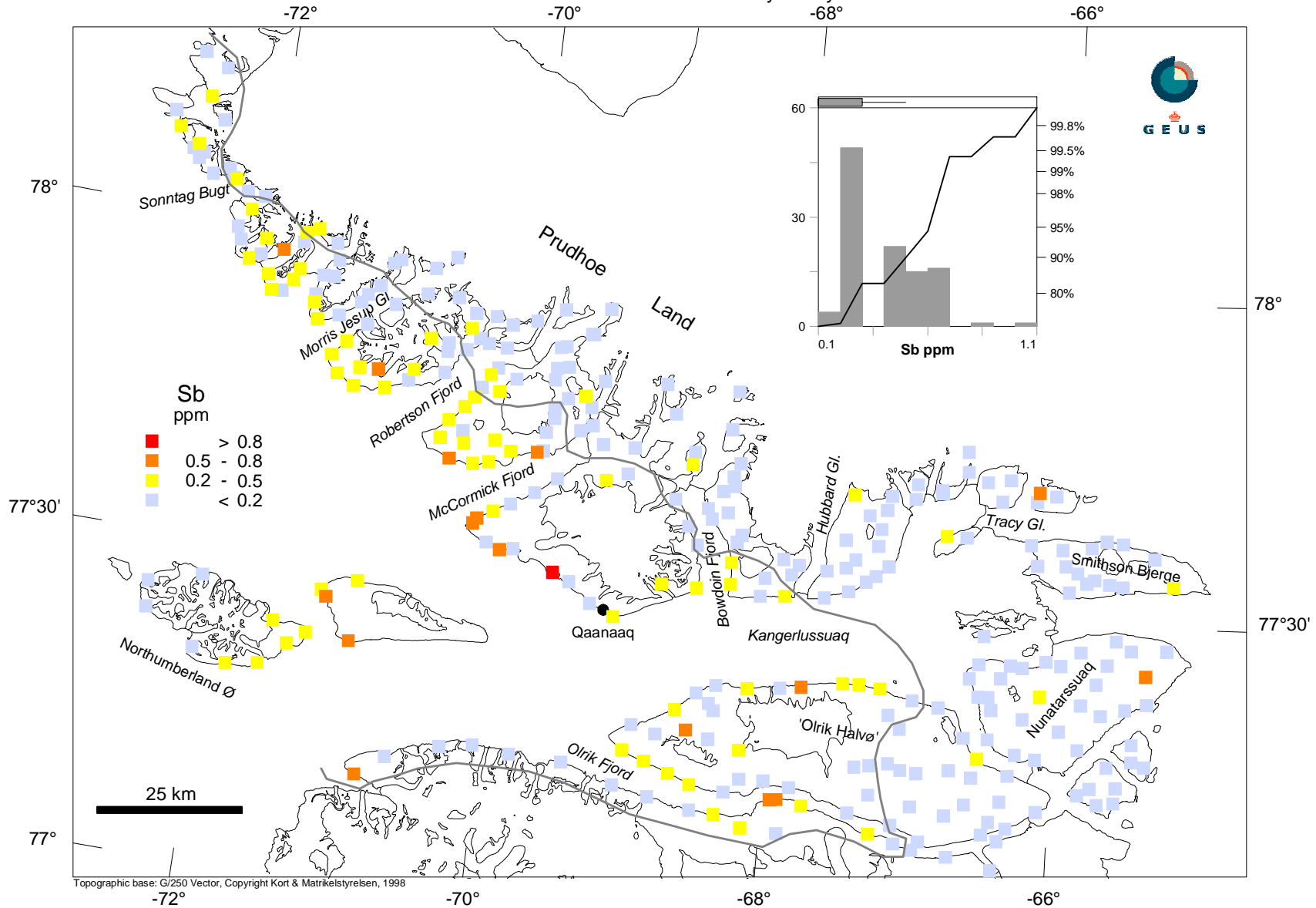
Grain size fraction < 0.1mm analysed by INAA



Map 28

# Stream sediment samples

Grain size fraction < 0.1mm analysed by INAA

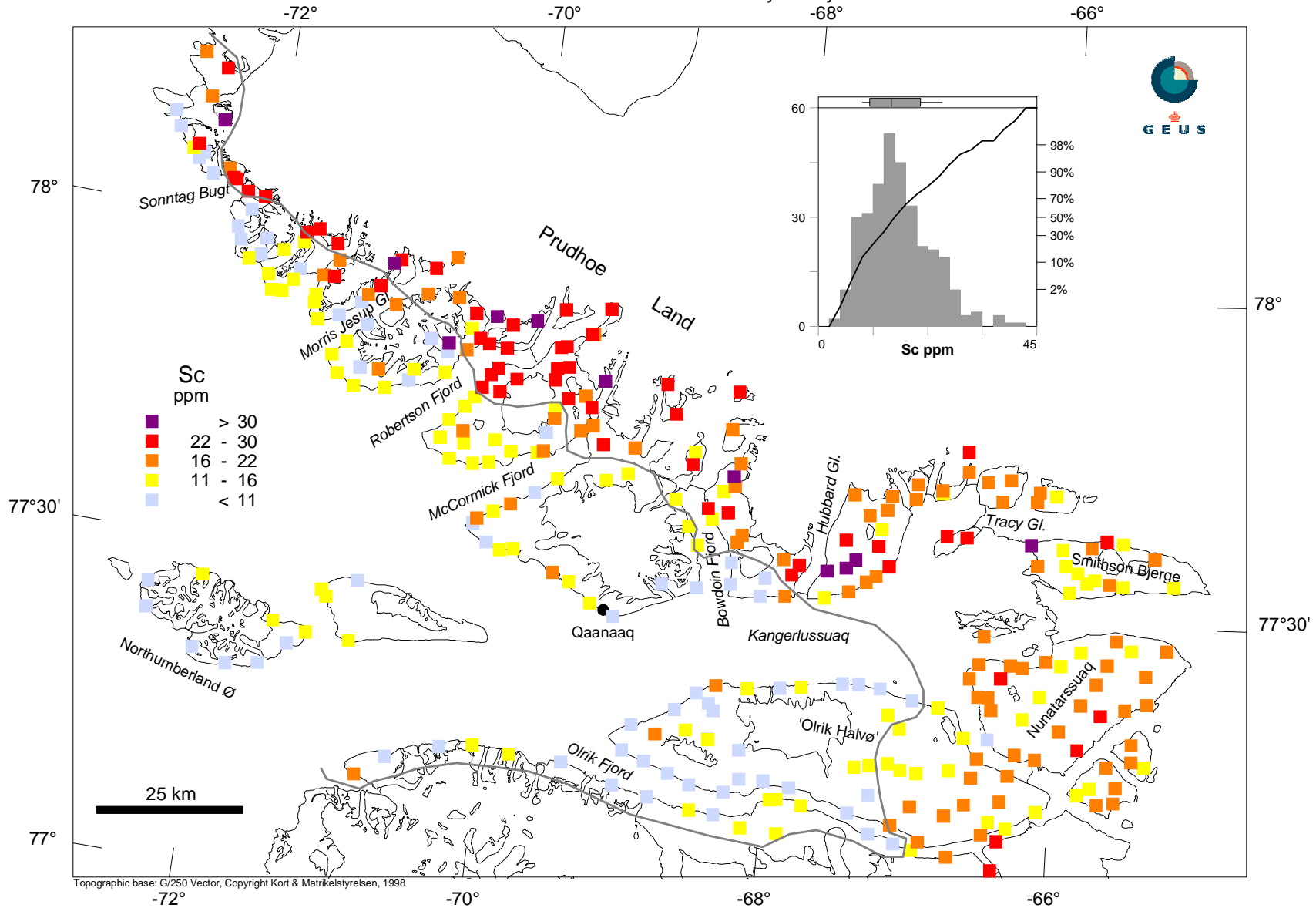


Map 29

Topographic base: G/250 Vector, Copyright Kort & Matrikelstyrelsen, 1998

# Stream sediment samples

Grain size fraction < 0.1mm analysed by INAA

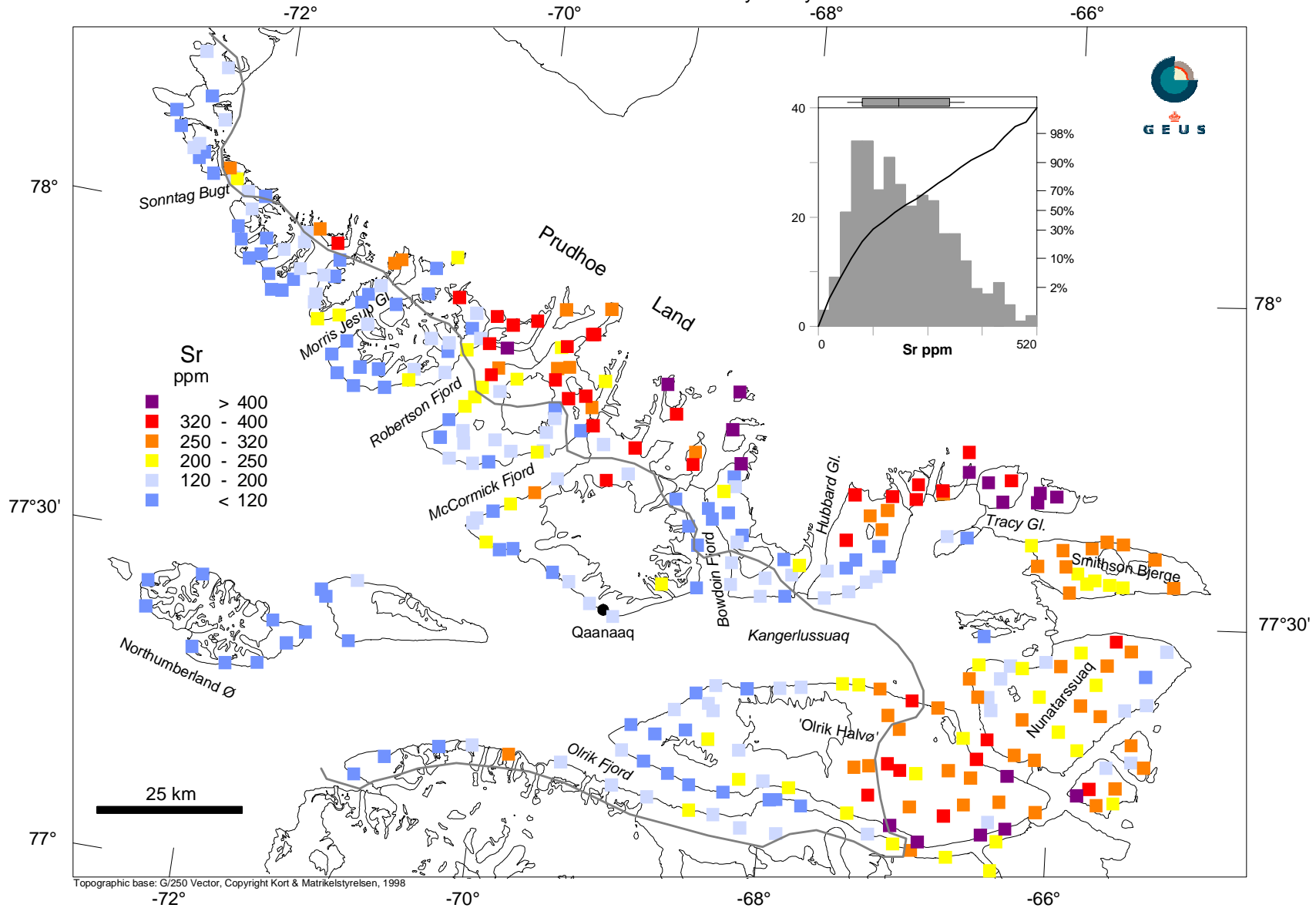


Map 30

Topographic base: G/250 Vector, Copyright Kort & Matrikelstyrelsen, 1998

# Stream sediment samples

Grain size fraction < 0.1mm analysed by ICP - ES

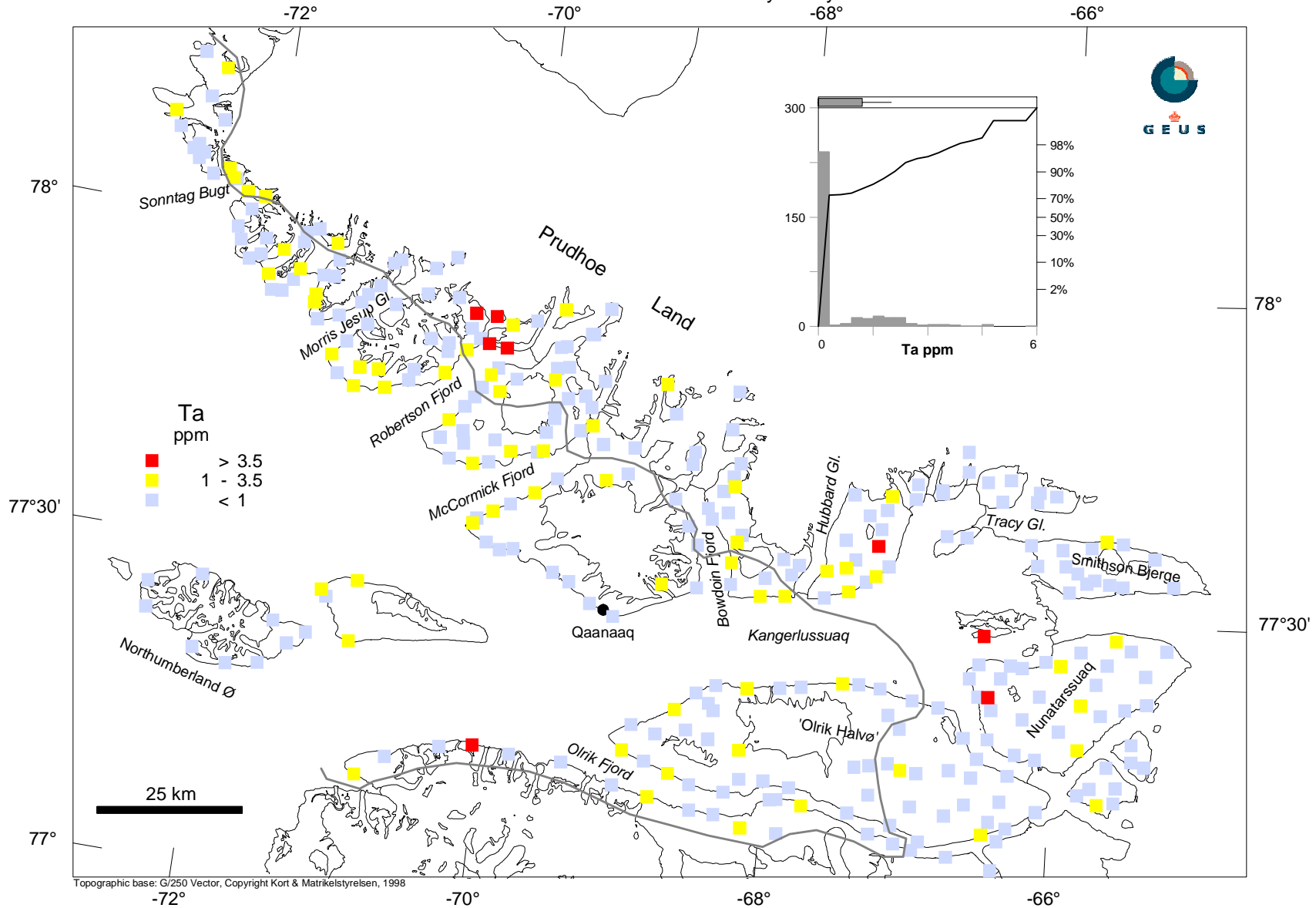


Map 31

Topographic base: G/250 Vector, Copyright Kort & Matrikelstyrelsen, 1998

# Stream sediment samples

Grain size fraction < 0.1mm analysed by INAA

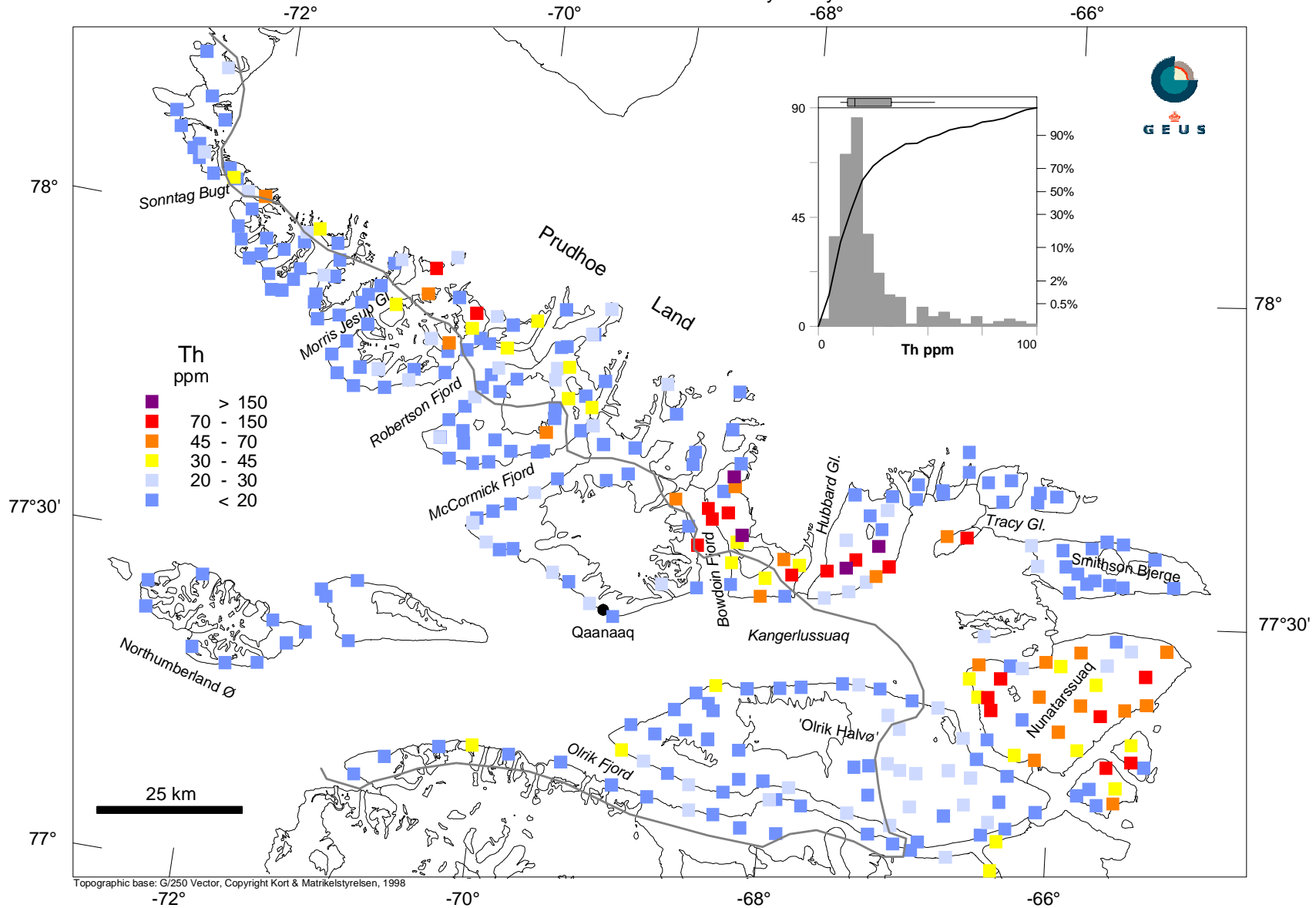


Map 32

Topographic base: G/250 Vector, Copyright Kort & Matrikelstyrelsen, 1998

# Stream sediment samples

Grain size fraction < 0.1mm analysed by INAA

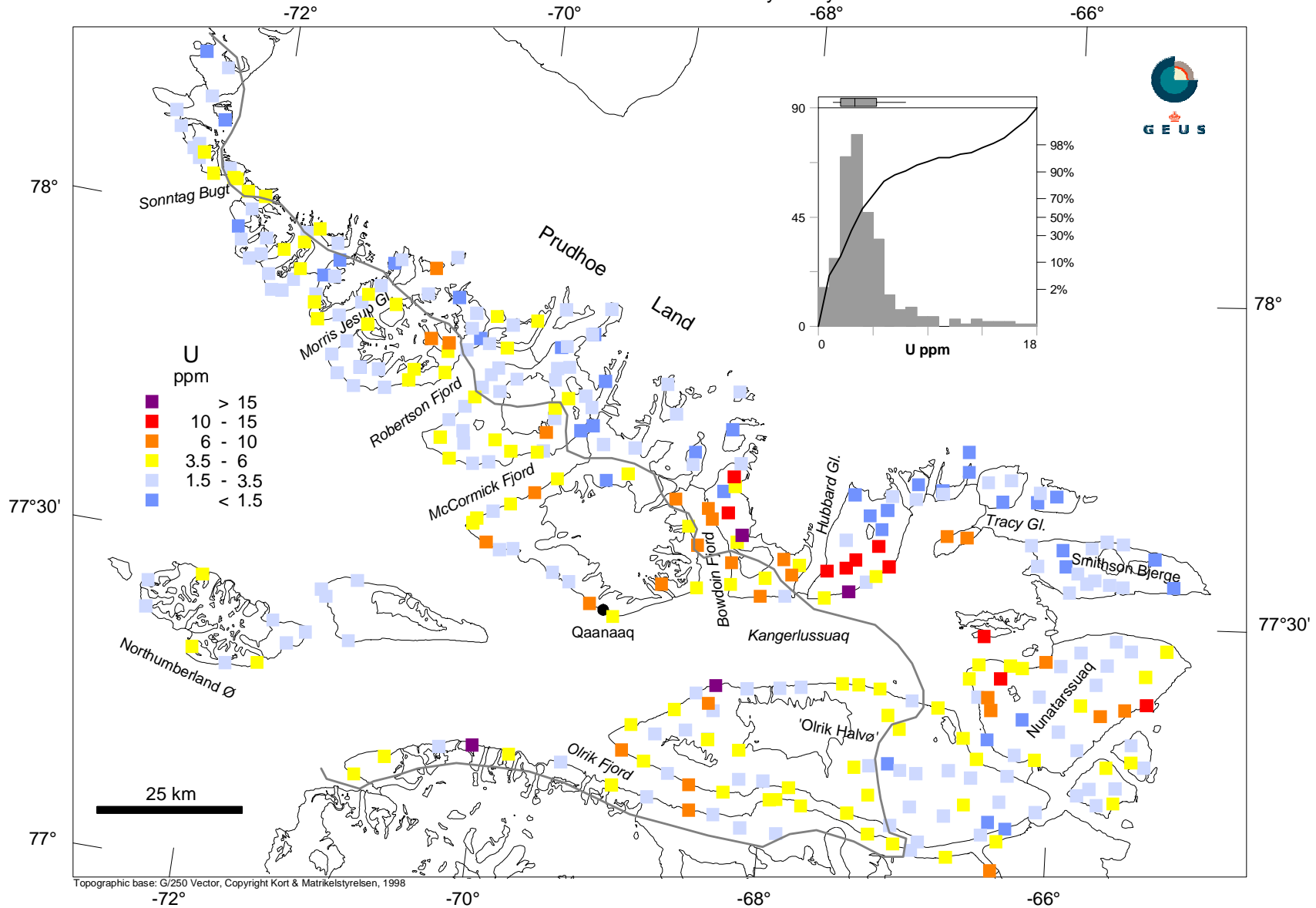


Map 33

Topographic base: G/250 Vector, Copyright Kort & Matrikelstyrelsen, 1998

# Stream sediment samples

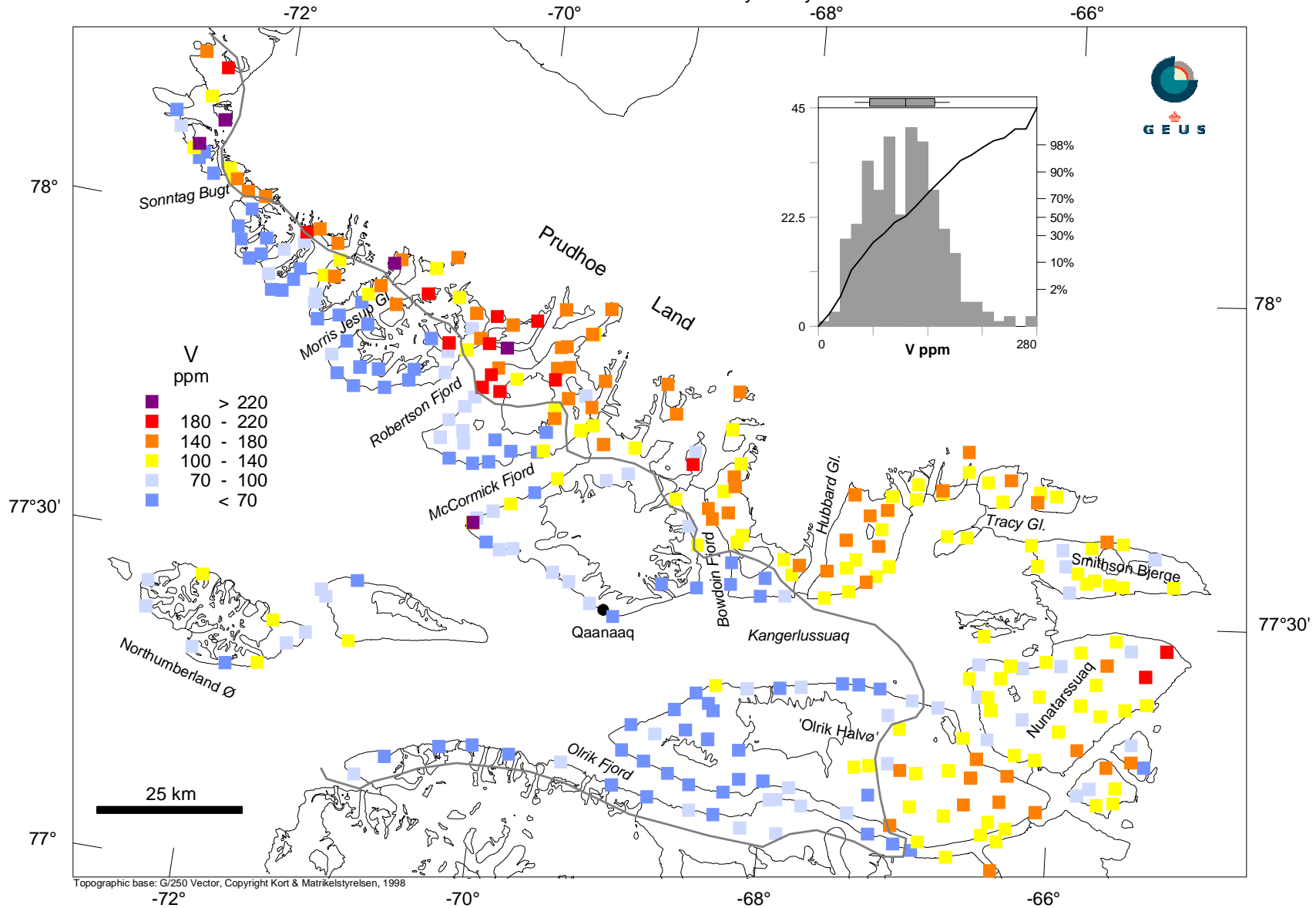
Grain size fraction < 0.1mm analysed by INAA



Map 34

# Stream sediment samples

Grain size fraction < 0.1mm analysed by ICP - ES

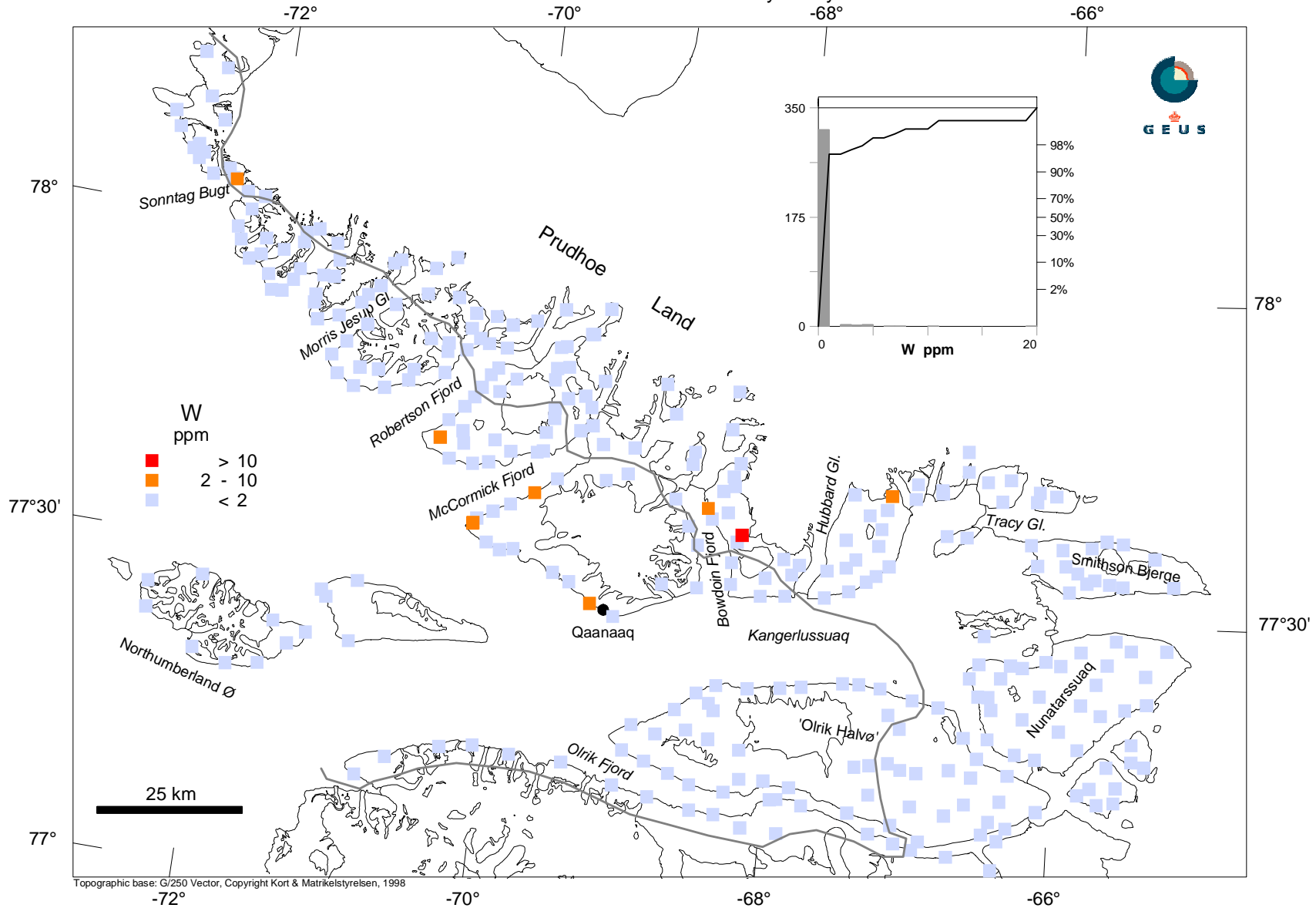


Map 35

Topographic base: G/250 Vector, Copyright Kort & Matrikelstyrelsen, 1998

# Stream sediment samples

Grain size fraction < 0.1mm analysed by INAA

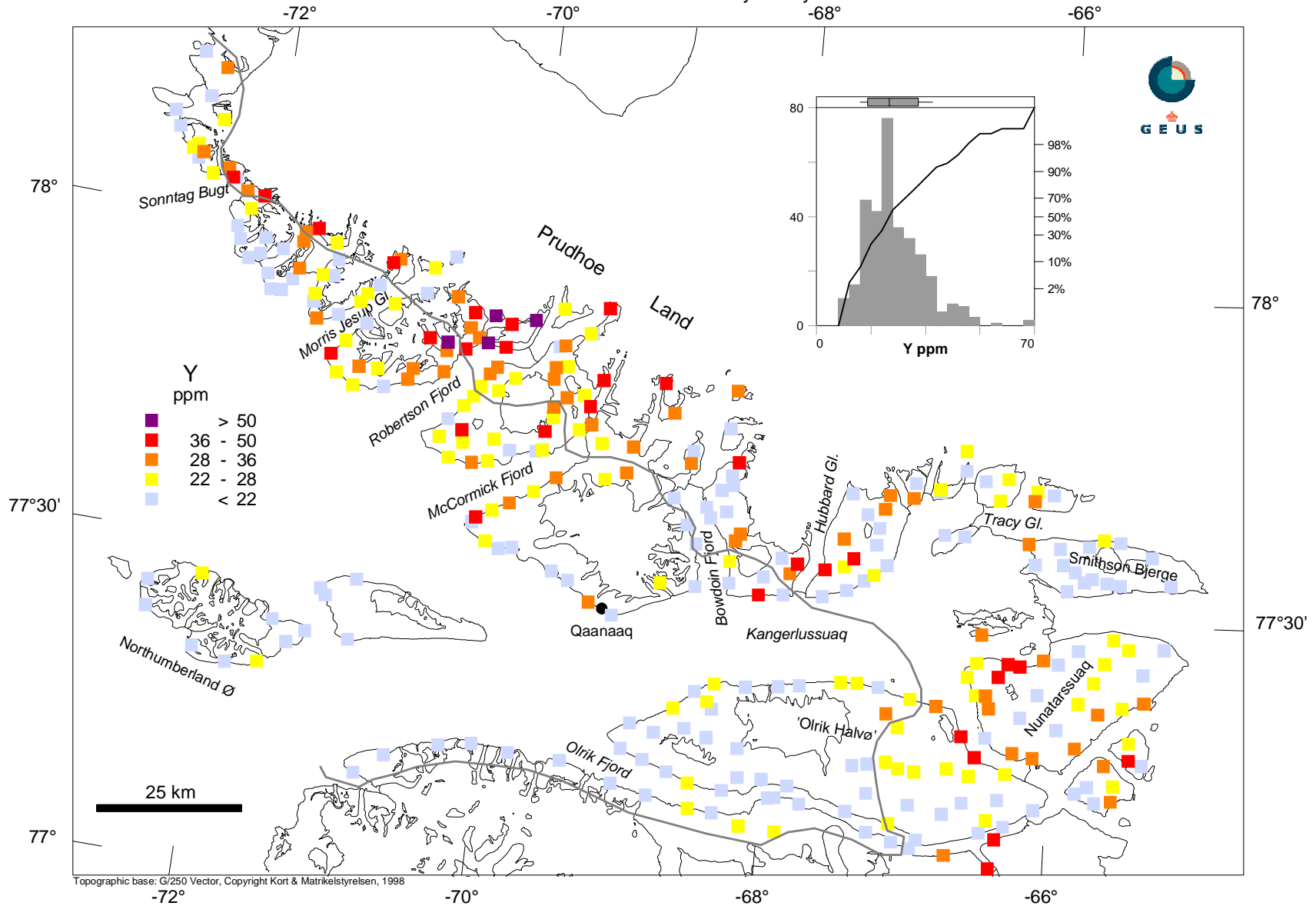


Map 36

Topographic base: G/250 Vector, Copyright Kort & Matrikelstyrelsen, 1998

# Stream sediment samples

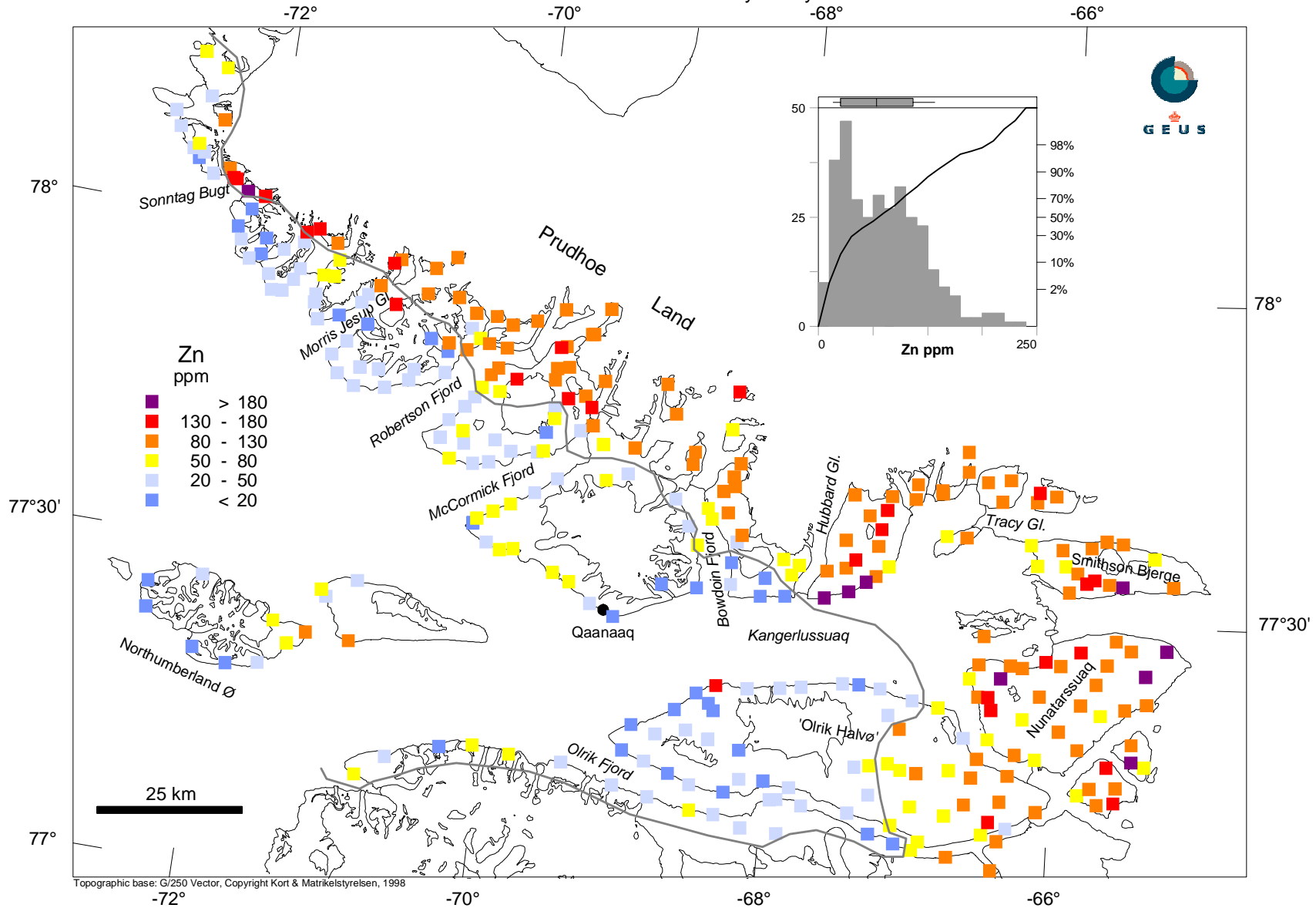
Grain size fraction < 0.1mm analysed by ICP - ES



Topographic base: G/250 Vector, Copyright Kort & Matrikelstyrelsen, 1998

# Stream sediment samples

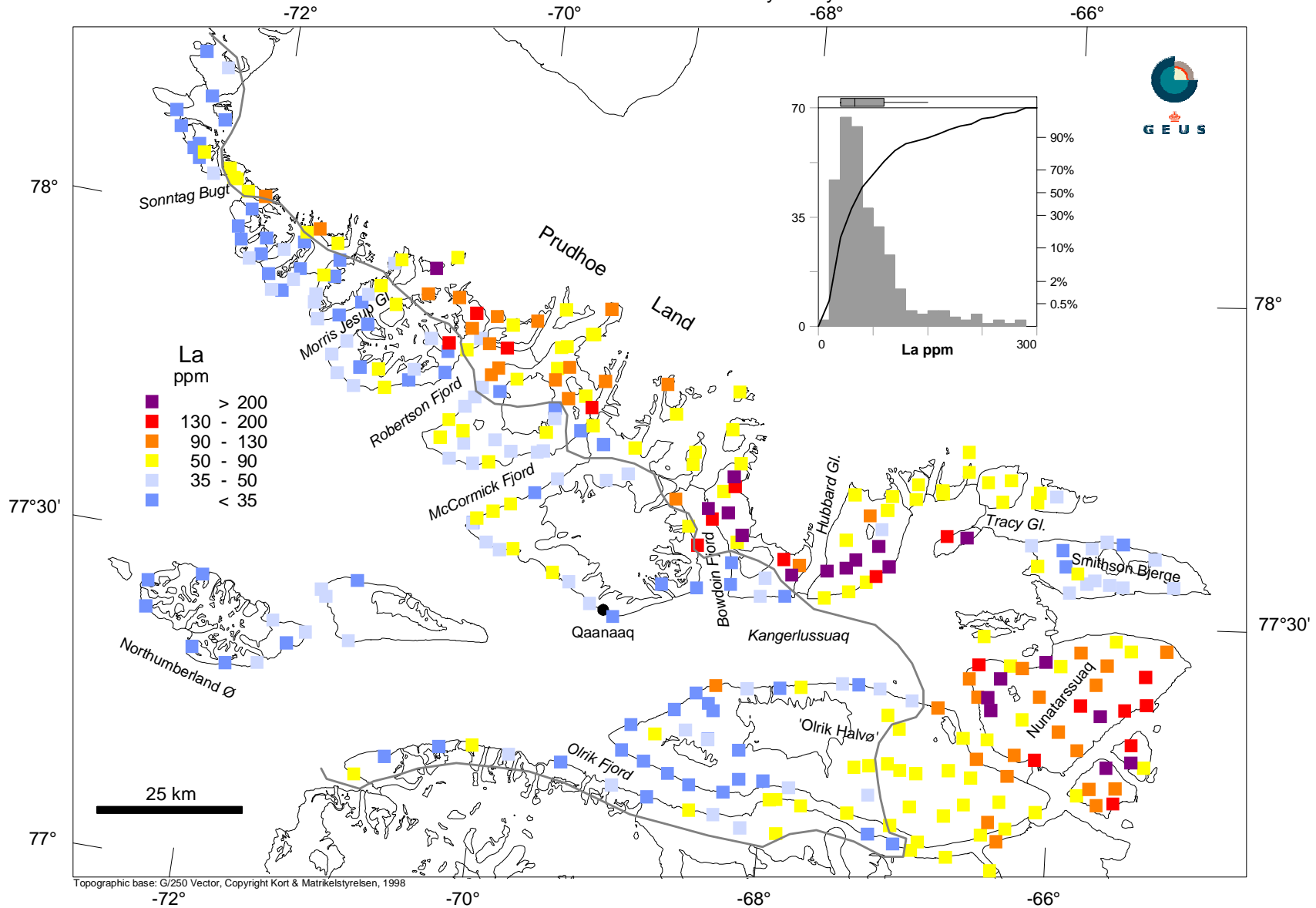
Grain size fraction < 0.1mm analysed by ICP - ES



Topographic base: G/250 Vector, Copyright Kort & Matrikelstyrelsen, 1998

# Stream sediment samples

Grain size fraction < 0.1mm analysed by INAA

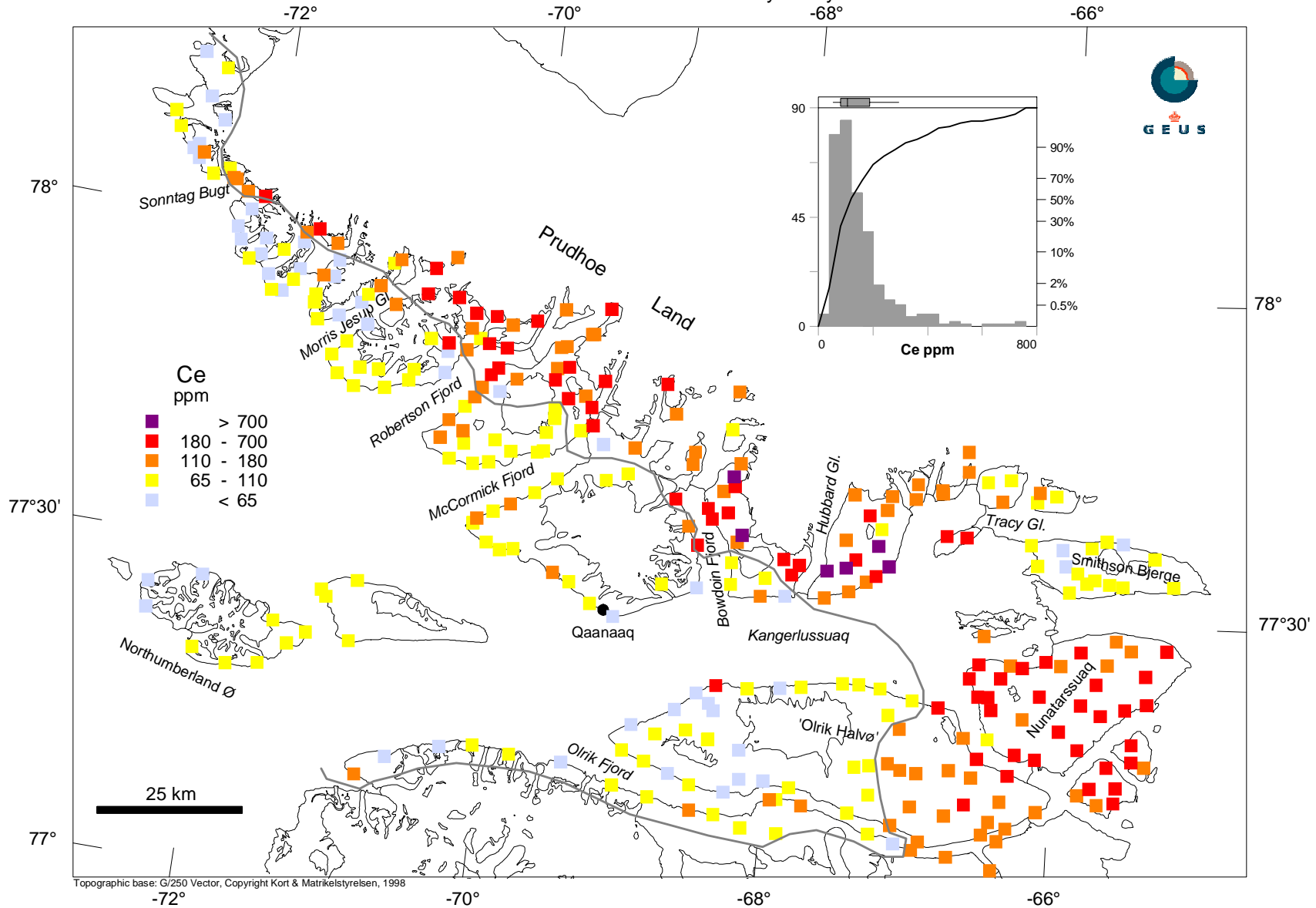


Map 39

Topographic base: G/250 Vector, Copyright Kort & Matrikelstyrelsen, 1998

# Stream sediment samples

Grain size fraction < 0.1mm analysed by INAA

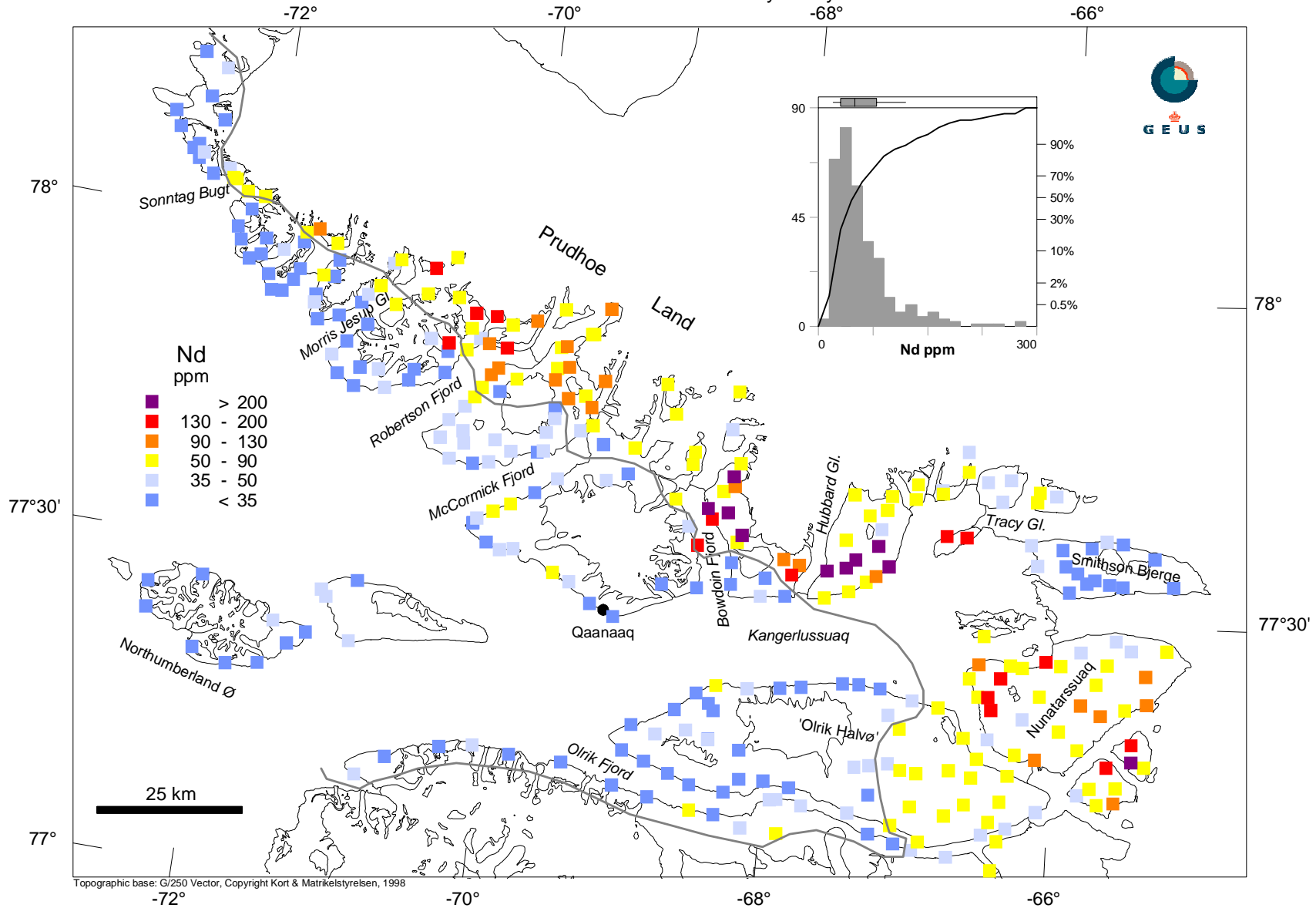


Map 40

Topographic base: G/250 Vector, Copyright Kort & Matrikelstyrelsen, 1998

# Stream sediment samples

Grain size fraction < 0.1mm analysed by INAA

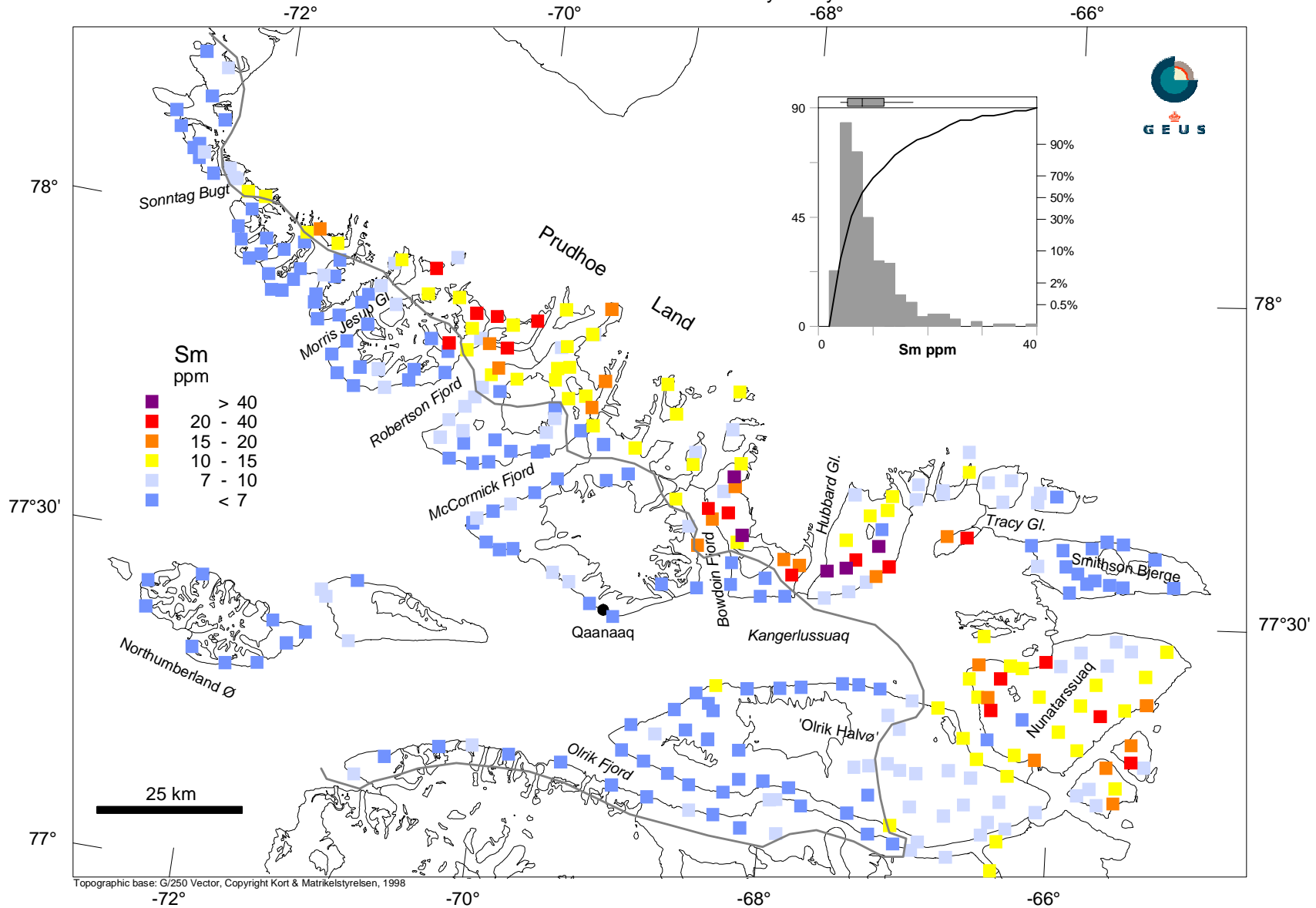


Map 41

Topographic base: G/250 Vector, Copyright Kort & Matrikelstyrelsen, 1998

# Stream sediment samples

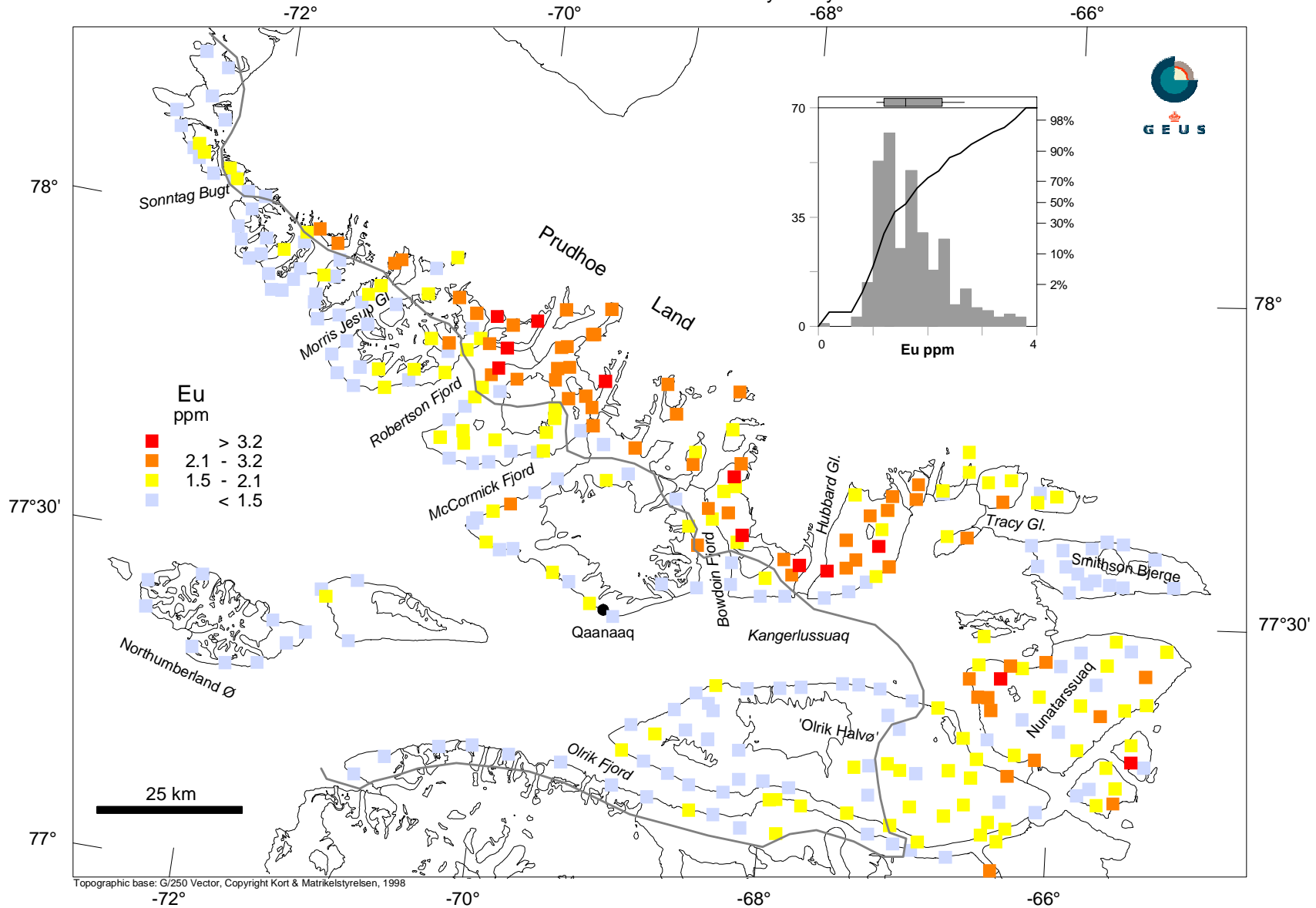
Grain size fraction < 0.1mm analysed by INAA



Topographic base: G/250 Vector, Copyright Kort & Matrikelstyrelsen, 1998

# Stream sediment samples

Grain size fraction < 0.1mm analysed by INAA

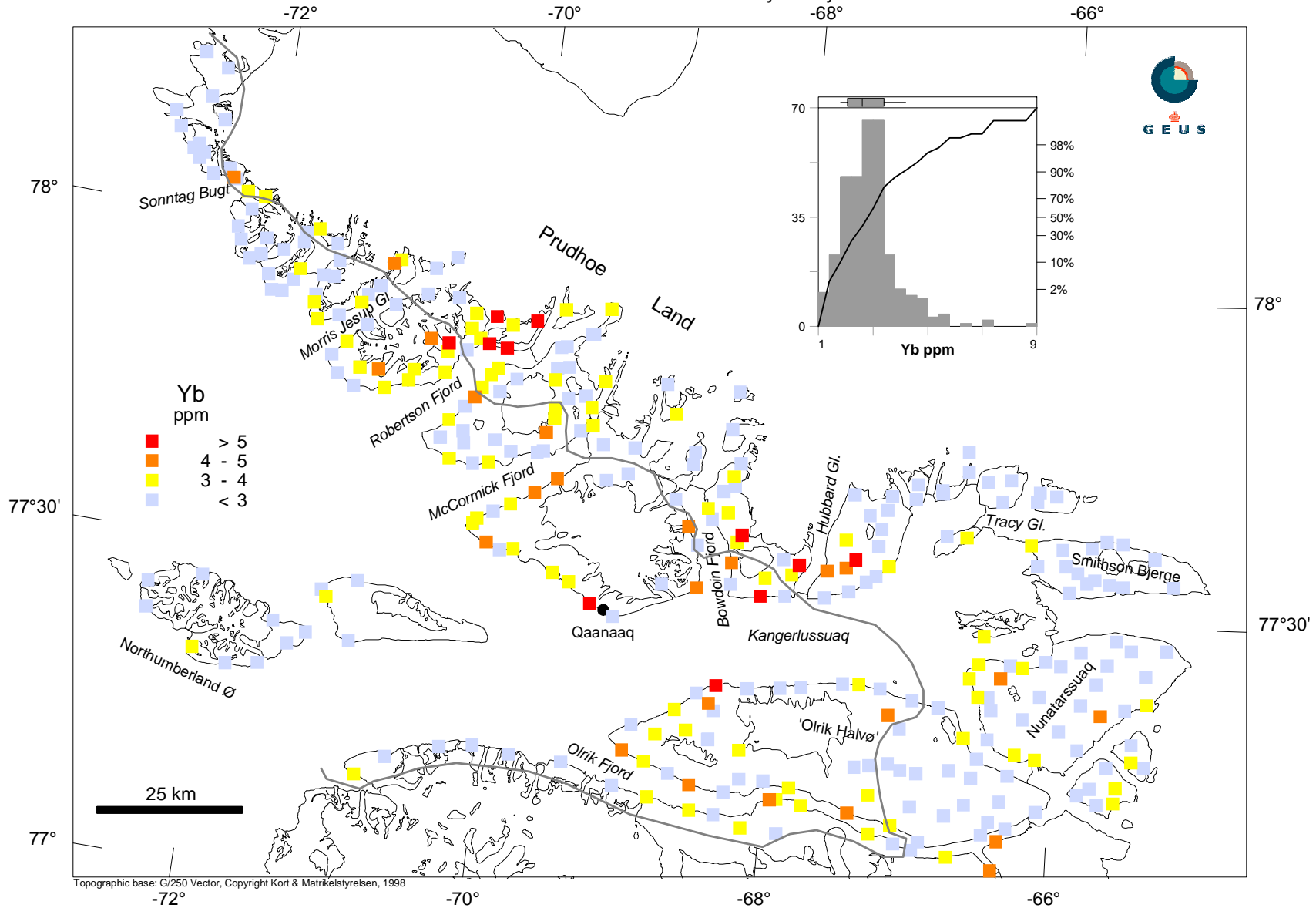


Map 43

Topographic base: G/250 Vector, Copyright Kort & Matrikelstyrelsen, 1998

# Stream sediment samples

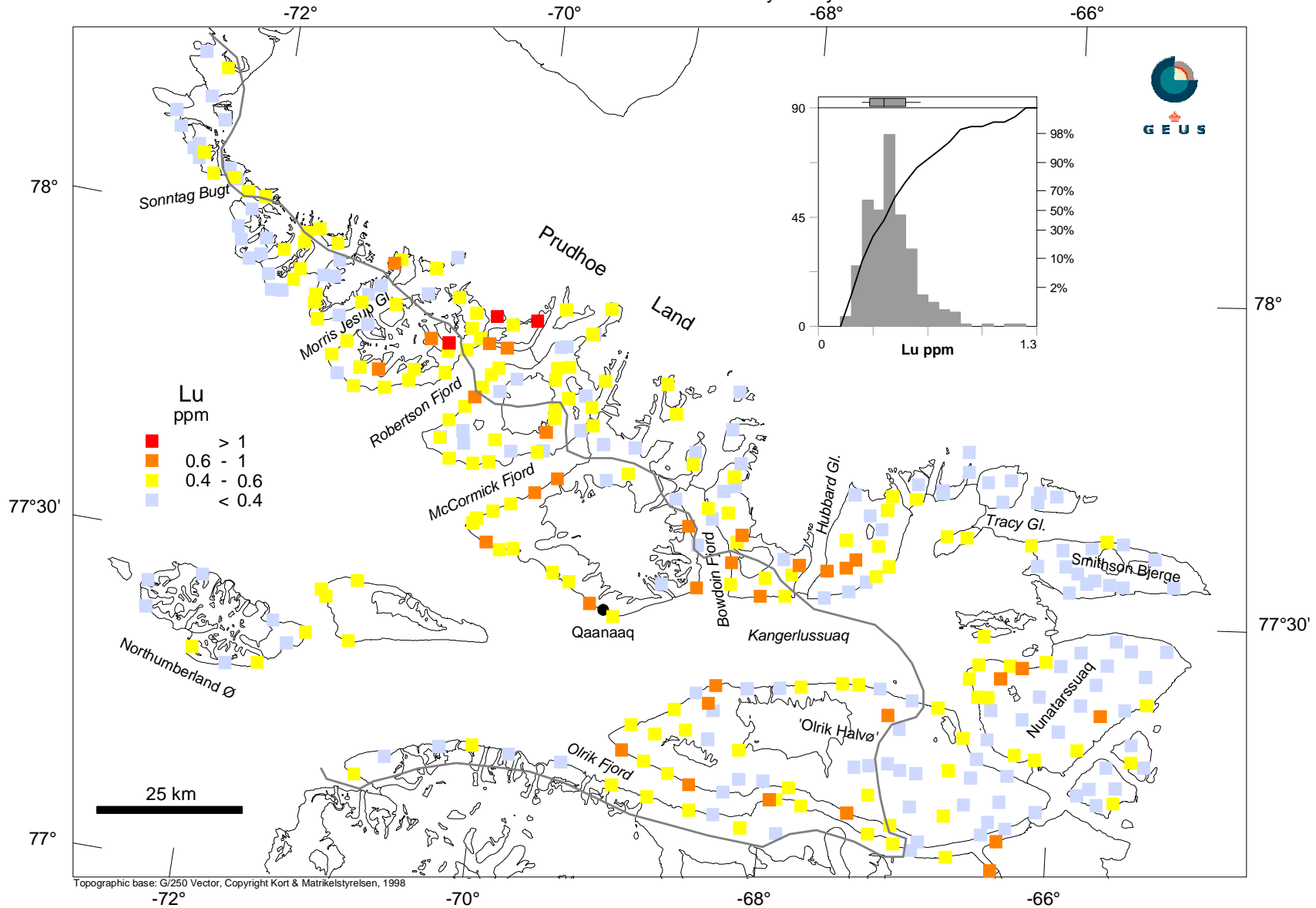
Grain size fraction < 0.1mm analysed by INAA



Topographic base: G/250 Vector, Copyright Kort & Matrikelstyrelsen, 1998

# Stream sediment samples

Grain size fraction < 0.1mm analysed by INAA

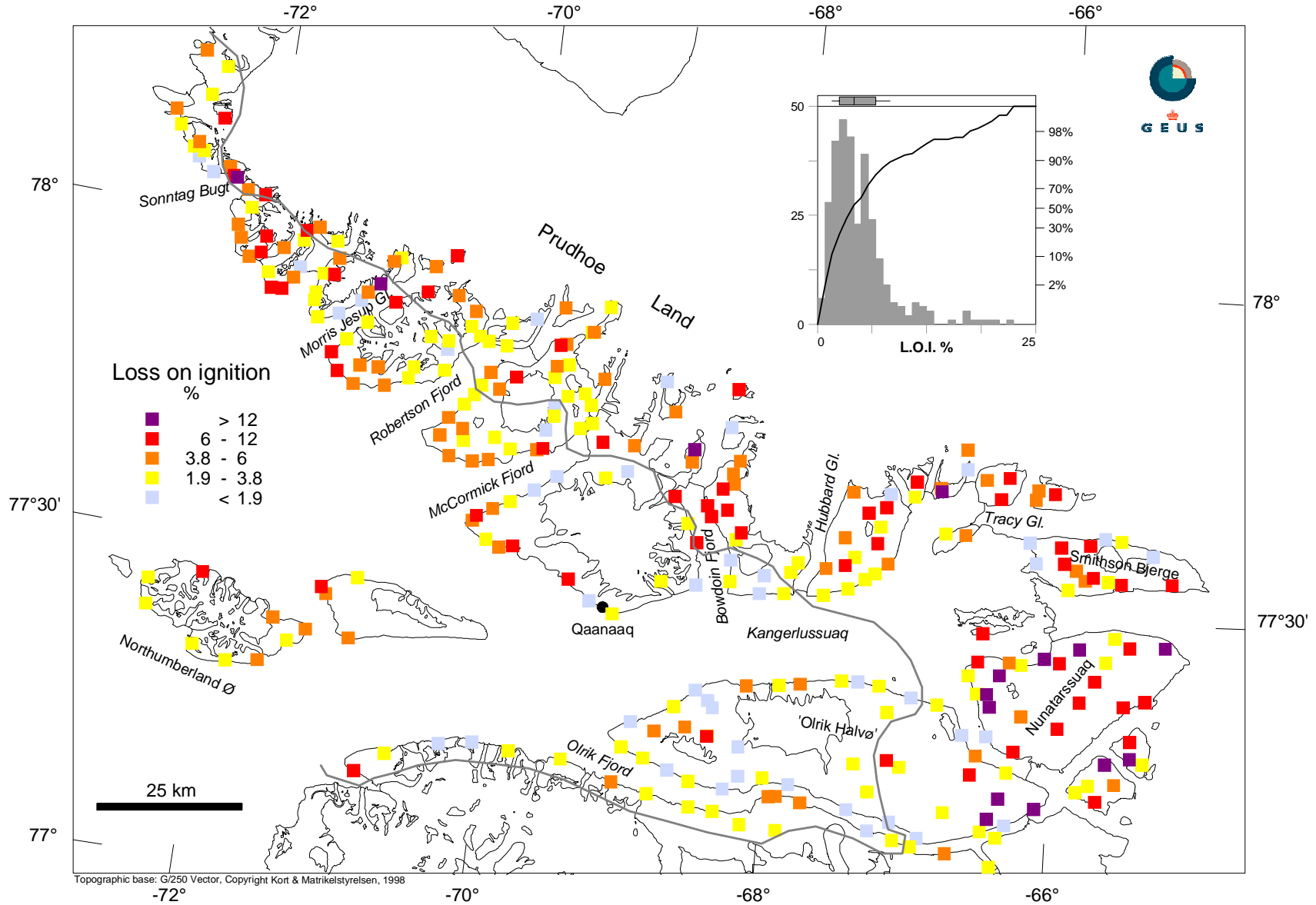


Map 45

Topographic base: G/250 Vector, Copyright Kort & Matrikelstyrelsen, 1998

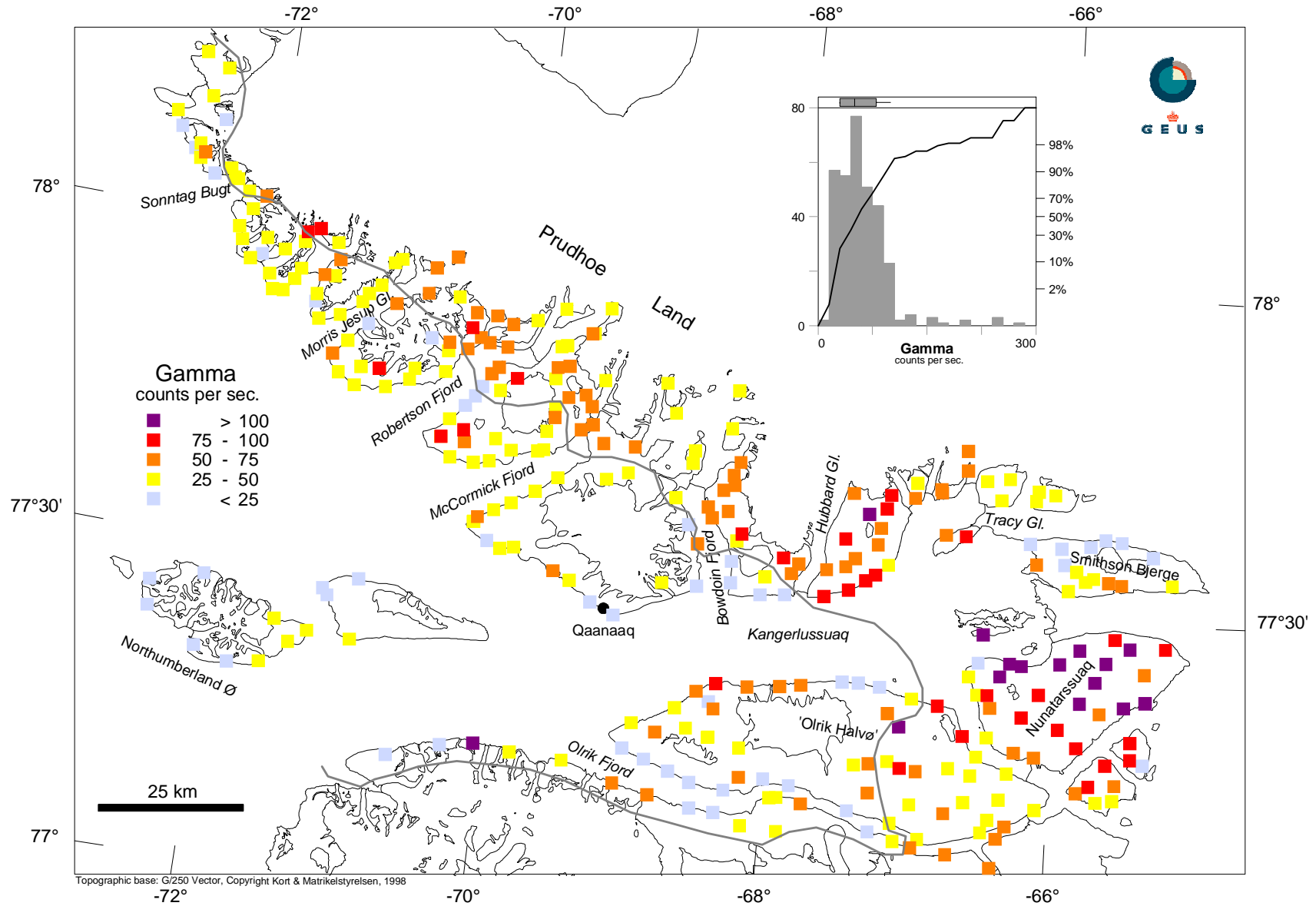
# Stream sediment samples

Grain size fraction < 0.1mm analysed by Fusion



# Stream sediment sample sites

Total gamma radiation measured by scintillometer



# Stream sediment samples

Geochemical classification relating to lithology

